Recent Advances on Visible Light Pyrrole-Derived Photoinitiators of Polymerization

Frédéric Dumur

Recent Advances on Visible Light Pyrrole-Derived Photoinitiators of Polymerization

Frédéric Dumur[a]*

[a] Aix Marseille Univ, CNRS, ICR, UMR 7273, F-13397 Marseille, France

frederic.dumur@univ-amu.fr

Abstract

Photopolymerization is the focus of intense research efforts due to the recent need to develop visible light photoinitiating systems activable under low light intensity and in the visible range. This effort is notably supported by the recent development of 3D/4D printing and light cured dental composite resins requiring new polymerization approaches. With aim at developing new formulations combining fast polymerization kinetics, high final monomer conversions, low energy consumption and activation in the visible range, pyrrole has been identified as an interesting scaffold for the design of various dyes. Indeed, numerous derivatives such as porphyrins, diketopyrrolopyrroles, chalcones, push-pull dyes can be prepared with pyrrole and related derivatives. As the main advantages, pyrrole is a five-membered ring heterocycle characterized by an easiness of chemical modification, low oxidation potential, high thermal and chemical stability that make pyrrole an interesting scaffold for the design of photoinitiators. More precisely, pyrrole has been used for the design of numerous Type II photoinitiators. In this review, an overview of the different dyes based on pyrrole and related derivatives, and reported to date is presented. Comparisons with benchmark photoinitiators will be established to evidence the interest of these new structures.

Keywords

Photoinitiator; pyrrole; photopolymerization; LED; low light intensity

1. Introduction

Photopolymerization is a polymerization technique which is facing a profound transformation, resulting from the progressive replacement of the historical UV technology by the more environmentally friendly visible light approach.[1–19] This intense research effort is supported by the wide range of applications using photopolymerization. Notably, photopolymerization is now commonly used in microelectronics, adhesives, coatings, dentistry, 3D and 4D printing.[20–29] Interest for developing visible light photoinitiating systems is supported by the numerous drawbacks related to the use of UV light. Notably, safety concerns can be mentioned as the primary cause of eviction of UV photopolymerization. Indeed, UV light can cause eye damages and skin cancers.[30–32] Ozone is also produced

during polymerization what constitutes another major drawback of the UV approach.[33] Parallel to this, expensive irradiation setups consuming a lot of energy have also to be used, entailing high running costs. In the present context of an improved control of the energy usage, energy saving has become increasingly important considering that the polymer industry is an energy-intensive industry. Interest for photopolymerization is also supported by the specificities of photopolymerization compared to the traditional thermal and solution phase polymerization. Notably, a spatial and a temporal control of the polymerization process can be obtained, meaning the polymerization occurs only for the surface exposed to light and during the light is switched on (See Figure 1).

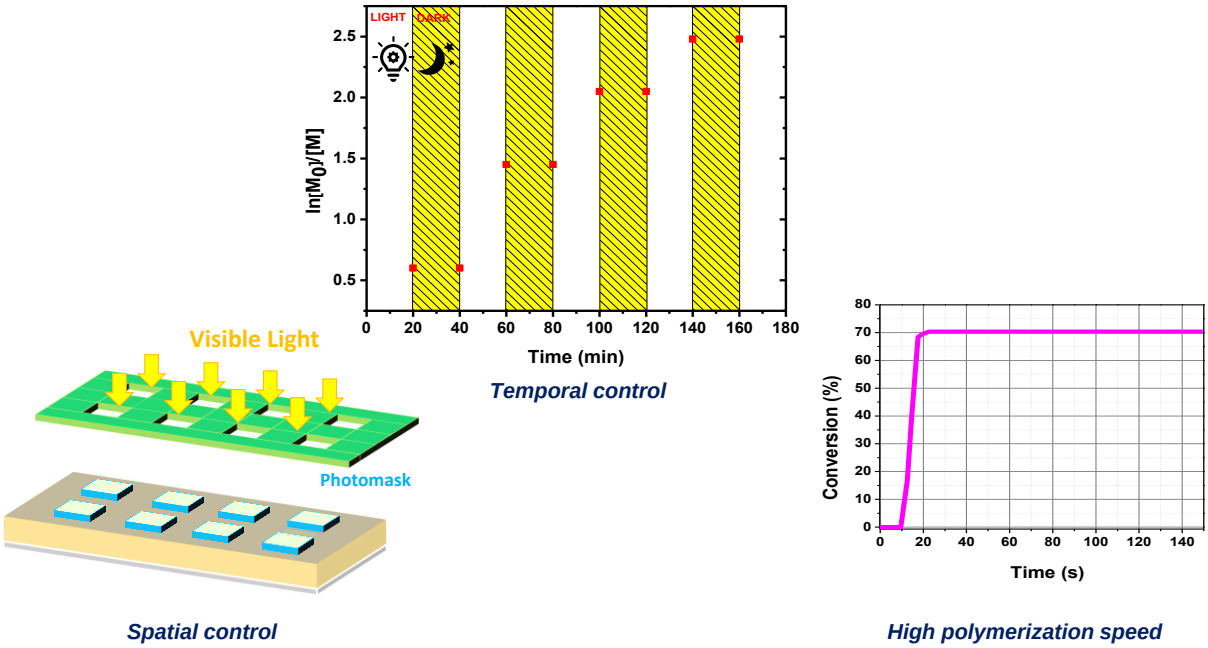

Figure 1. The different advantages of photopolymerization compared to the solution-phase polymerization.

Polymerization can also be carried out without solvent, avoiding the release of volatile organic compounds (VOCs).[33] Photopolymerization can also be carried out under low light intensity, enabling to use cheap, lightweight and compact light sources such as light-emitting diodes (LEDs).[34] Interestingly, these devices don't release heat during light irradiation so that heat-sensitive monomers can be photopolymerized under visible light. Interest for visible light is also supported by the higher light penetration that can be achieved in the visible range within the photocurable resin (from a few millimetres to a few centimetres), compared to that obtained in the UV range (only a few hundreds of micrometres) (See Figure 2).[35]

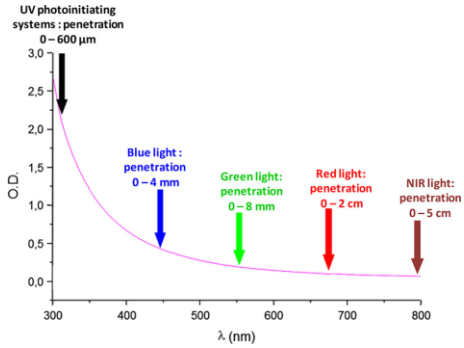

Figure 2. Light penetration in a polystyrene latex with an average diameter of 112 nm. Reprinted with permission from Bonardi et al.[35]

If, from a theoretical viewpoint, visible light photopolymerization is more appealing than UV photopolymerization, several drawbacks have to be mentioned and can't be denied. Notably, visible light photoinitiators are colored compounds, what can constitute a severe limitation for numerous applications. Indeed, due to their high molar extinction coefficients of these dyes, a color is often imposed to the final coating. Even if a few examples of photoinitiators capable to bleach have been reported in the literature, these examples remain scarce. Parallel to this, visible light photoinitiators are often less reactive than the UV ones. This is directly related to the less energetic irradiation wavelengths that are used in the visible range. Considering that a great deal of efforts remains to be done in order to develop photopolymerization systems with photobleaching properties, a wide range of structures have been examined ranging from pyrenes,[36–43] to 2,3-diphenylquinoxaline derivatives,[44,45] iodonium salts,[46–53] helicenes,[54,55] iridium complexes,[56–63] squaraines,[64–67] porphyrins,[68,69] metal organic framework (MOFs),[70–72] camphorquinones,[73,74] zinc complexes,[75] coumarins,[76–87] benzophenones,[88–95] diketopyrrolopyrroles,[96–98] phenothiazines,[99] curcumin,[100–103] carbazoles,[104–114] dithienophospholes,[115,116] acridones,[117,118] anthracene,[119] phenazines,[120] dihydro-anthraquinones,[121] iron complexes,[71,122–128] cyanines [129–134] polyoxometalates,[135,136] copper complexes,[137–152] conjugated polymers,[153] chromones and flavones,[154–156] perylenes,[157–160] chalcones,[28,161–173] Schiff bases,[174] cyclohexanones[175–178] naphthalimides,[46,179–194] truxene derivatives,[195] perovskites,[196,197] push-pull dyes,[122,198–211] thiophene derivatives,[212] triphenylamines,[213] thioxanthones,[214–226] and acridine-1,8-diones.[227–229] Even if only few of these photoinitiators exhibited photobleaching properties, besides, photopolymerization processes could be initiated from the near UV/visible range until the infrared region. With aim at developing new dyes with high photoinitiating ability, pyrrole-derived dyes are one of those. Pyrrole is a heterocyclic five-membered ring compound in which the involvement of the lone pair electrons of nitrogen to the aromaticity of pyrrole makes this heterocycle an excellent electron donating group when combined with the appropriate group. Pyrrole is extensively used in Organic Electronics for the design of semiconductors for organic field effect transistors,[230,231] as active layers for organic photovoltaics,[232–234], for the design of dyes with solvatochromic properties,[235] the design

of dyes with non-linear optical properties[236–239] or electrochromes.[240] Recently, pyrrole was investigated in the photopolymerization field and used as an elemental building block for the design of dyes of various structures. Notably, dyes absorbing from the near UV/visible range until the near infrared region could be prepared. As specificities, pyrrole is a five-membered heterocycle that is a relatively cheap building block. Pyrrole can also easily be oxidized so that pyrrole was extensively used as monomer for electropolymerization.[241,242] Easiness of oxidation is of crucial interest in order pyrrole-based photoinitiators to efficiently interact with additives. Pyrrole is also an excellent electron donor so that push-pull dyes could be designed with this heterocycle. [234,235,243–246] Overall, even if numerous families of dyes have been tested as photoinitiators, easiness of synthesis, easy oxidation of pyrrole and the facile tunability of the absorption properties of the pyrrole-based dyes could make pyrrole-based photoinitiators, dyes of higher reactivity than the aforementioned families. Difference of rate constant of interaction with the different additives, more appropriate excited state lifetimes could enable pyrrole-based dyes to outperform to the other dyes. However, potential toxicity of photoinitiators can also govern their future uses. Concerning pyrrole, an acute toxicity has notably been evidenced for numerous derivatives, what can constitute a severe limitation.[247–250] Besides, the search for new dyes exhibiting a high reactivity upon irradiation in the visible range is still very active, justifying that the toxicity issue is still considered as the primary factor to select a family of dyes. Face to these considerations, numerous pyrrole-based dyes were examined over the years. In this review, an overview of the different pyrrole-derived dyes is presented. In order to evidence the interest of these structures, comparisons with benchmark photoinitiators will be provided.

2. Pyrrole-derived dyes

2.1. Chalcones

Chalcones belong to the flavonoid family and these dyes can be abundantly found in edible plants, fruits, leaves, tea, spice, cereal grains and vegetables.[251–254] The first report mentioning the use of pyrrole-based photoinitiators in visible light photopolymerization was reported in 2020 by Nie and coworkers.[162] In this work, pyrrole was selected as a phenyl-free electron-donating group enabling to design a dye exhibiting a strong absorption in the 325-450 nm range with a maximum absorption located at 379 nm (ε = 26 335 $M^{-1}.cm^{-1}$). Based on the absorption of 1,3-*bis*(1-methyl-1*H*-pyrrol-2-yl)prop-2-en-1-one (BMO), polymerization processes could be initiated at 365, 385, 405 and 465 nm (See Figure 3). The design of phenyl-free constitutes an interesting approach, considering that aromatic compounds are facing numerous health and safety concerns. This point is of crucial importance, especially if photoinitiators are used for elaborating polymers used in food packaging or for biomedical applications.[255]

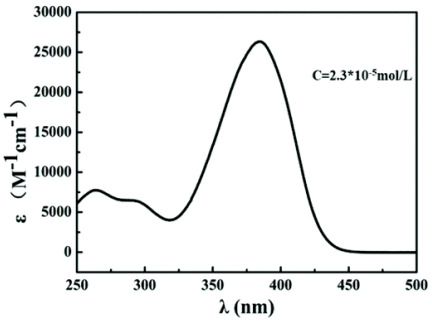

Figure 3. UV-visible absorption spectrum of BMO in acetonitrile. Reproduced from [162] with permission from The Royal Society of Chemistry.

To evidence the photoinitiating ability of BMO, comparisons were established with 2-isopropylthioxanthone (ITX) which is a benchmark photoinitiator (See Figure 4).[243–250]

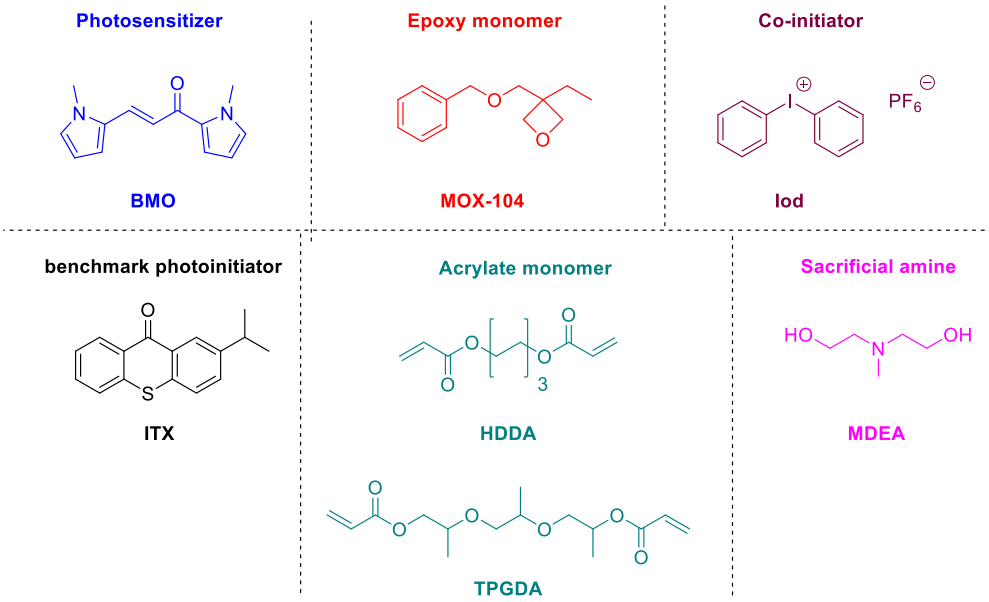

Figure 4. Chemical structures of BMO, the different monomers and additives.

Interestingly, when tested as sensitizer for the cationic polymerization (CP) of (3,4-epoxycyclohexane)methyl 3,4-epoxycyclohexylcarboxylate (EPOX) at 365 and 405 nm, similar monomer conversions were obtained with the two-component ITX/Iod (1%/3%, w/w) and BMO/Iod (1%/3%, w/w) systems (where Iod stands for diphenyliodonium hexafluorophosphate). Thus, upon irradiation at 365 nm for 600 s, a final monomer conversion of 60% could be obtained with the two systems. Only a slight improvement of the monomer conversion was detected at 405 nm. However, upon irradiation at longer wavelengths such as 385 or 465 nm, the two-component BMO/Iod (1%/3%, w/w) system could greatly outperform the reference system. The most significant enhancement was detected at 465 nm, an increase of 25% of the monomer conversion being evidenced for the BMO/Iod (1%/3%, w/w) system compared to the reference ITX/Iod system (See Figure 5).

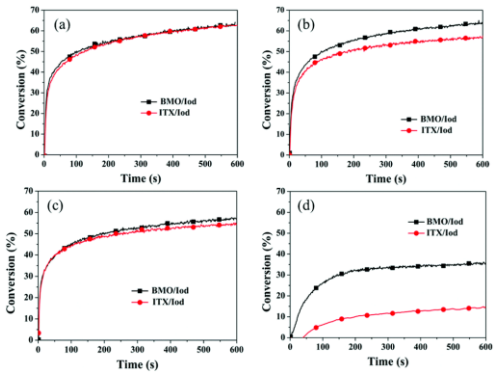

Figure 5. EPOX conversions obtained upon irradiation with a LED at a) 365 nm b) 385 nm c) 405 nm and d) 465 nm by using the two-component BMO/Iod (1%/3%, w/w) system and the reference system ITX/Iod (1%/3%, w/w). Reproduced from [162] with permission from The Royal Society of Chemistry.

Cationic polymerization of epoxides was not limited to EPOX and the copolymerization of two different monomers was also examined, as exemplified with the mixture of EPOX/ 3-benzyloxymethyl-3-ethyl-oxetane (MOX-104) (30%/70%, w/w). More interesting results were obtained during the free radical polymerization of acrylates. Notably, BMO proved to be an efficient hydrogen donor so that the FRP of 1,6-hexanediol diacrylate (HDDA) could be initiated simply using BMO. This ability to initiate a polymerization alone was assigned to the presence of tertiary amine groups in its structures.[256–259] Thus, during the FRP of HDDA and by using 1 wt% of BMO, a final monomer conversion of 68% could be obtained after 600 s of irradiation at 405 nm. Upon addition of an amine, namely *N*-methyldiethanolamine (MDEA), a final monomer conversion of 74% could be obtained with the two-component BMO/MDEA (1%/1% w/w) system after 300 s of irradiation at 405 nm. Conversely, when combined with Iod, the two-component BMO/Iod (1%/3% w/w) system could furnish a monomer conversion of 80%, outperforming that obtained with the two-component BMO/MDEA (1%/1% w/w) system. Finally, considering that BMO can both initiate the CP of epoxides and the FRP of acrylates, the preparation of interpenetrated polymer networks (IPN) was examined. This strategy is of crucial interest for addressing the oxygen inhibition issue. Indeed, the FRP of acrylates is highly sensitive to oxygen inhibition, resulting in low to moderate monomer conversion. By mean of a hybrid polymerization process, a synergetic effect can occur, enabling to advantageously combine fast polymerization speeds, low oxygen inhibition and high conversion rates. Thus, by increasing the EPOX content in the tripropylene glycol diacrylate (TPGDA)/EPOX monomer blend, the TPGDA conversion could increase up to 90% in the TPGDA/EPOX 10/90 blend while using the two-component BMO/Iod (1%/3%, w/w) system whereas the TPGDA conversion was limited to only 20% with the same photoinitiating system when TPGDA was polymerized alone in the same conditions (See Figure 6).

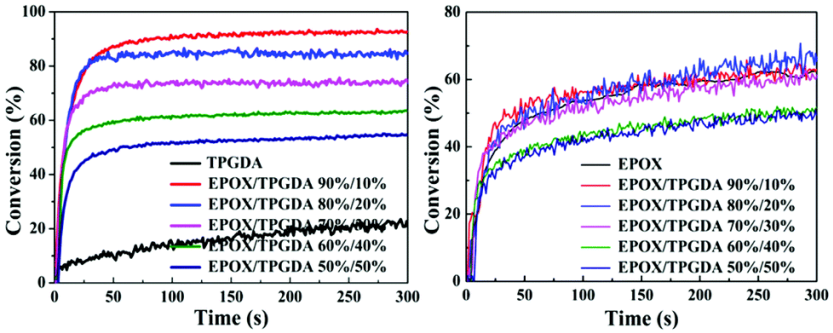

Figure 6. Hybrid polymerization of the TPGDA/EPOX blend, using the two-component BMO/Iod (1%/3%, w/w) photoinitiating system and upon irradiation at 405 nm. Reproduced from [162] with permission from The Royal Society of Chemistry.

To support the enhancement of the TPGDA conversion upon increase of the EPOX content, a rapid increase of the viscosity resulting from the photopolymerization of EPOX was proposed, reducing the oxygen permeation. As a result of this, oxygen inhibition adversely affecting the FRP of TPGDA could be efficiently overcome. Parallel to this, polymerization of acrylates is also well-known to be an exothermic reaction, what can be helpful for the CP of EPOX. Thus, an increase of the temperature up to 125°C during the concomitant polymerization of the TPGDA/EPOX 20/80 blend was observed. Logically, increase of the TPGDA content resulted in a decrease of the reaction temperature due to a pronounced oxygen inhibition. A temperature of only 74°C was obtained during the hybrid polymerization of the TPGDA/EPOX 80/20 blend.

In 2021, the same authors designed *bis*-chalcones, still using *N*-methylpyrrole as the electron donating group.[260] Three chalcones varying by the central cyclohexanones were designed, namely, 2,6-*bis*((1-methyl-1*H*-pyrrol-2-yl)methylene)cyclohexan-1-one (C6PY), 1-methyl-3,5-*bis*((1-methyl-1*H*-pyrrol-2-yl)methylene)piperidin-4-one (C6NPY) and 3,5-*bis*((1-methyl-1*H*-pyrrol-2-yl)methylene)tetrahydro-4*H*-thiopyran-4-one (C6SPY) (See Figure 7). Interestingly, modification of the substitution pattern of the central cyclohexanone did not significantly modify the optical properties of the three dyes, and absorption maxima located at 413, 415 and 412 nm for C6PY, C6NPY and C6SPY could be respectively determined in acetonitrile. Photolysis experiments also revealed the three dyes to rapidly photoisomerize in acetonitrile upon irradiation at 405 nm. Thus, after two seconds of irradiation at 405 nm, an equilibrium between Z/Z and Z/E isomers could be obtained. This behavior is not usual for chalcones and this phenomenon was previously reported by the same authors for another dye based on the *bis*-chalcone scaffold.[175] Monitoring of the photolysis experiments upon irradiation at 405 nm until 60 s revealed that almost no modification of the absorption spectra occurred, subsequent to the severe and initial decrease of the absorption intensity (See Figure 8).

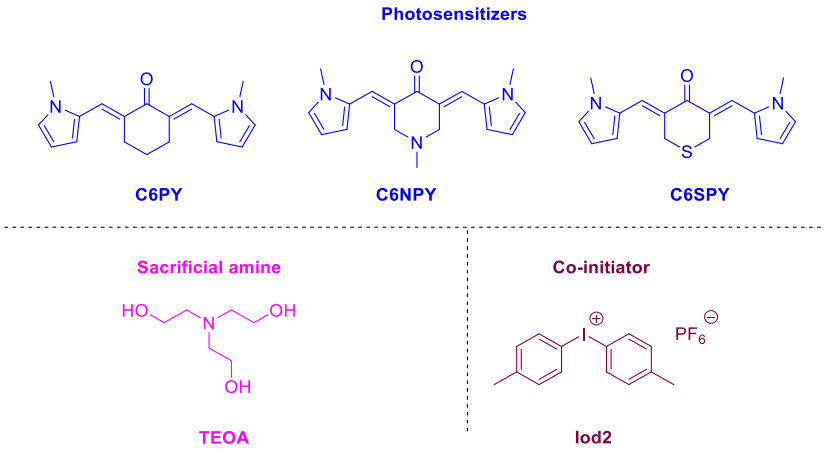

Figure 7. Chemical structures of C6PY, C6NPY C6SPY and different additives.

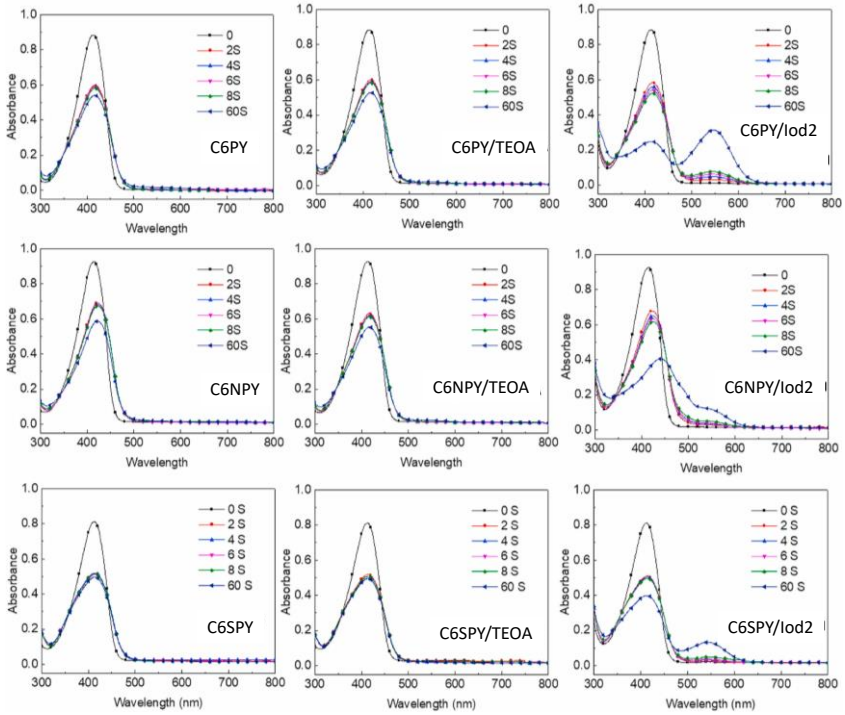

Figure 8. UV-visible absorption spectra of C6PY, C6NPY and C6SPY, top: alone; middle: dye/TEOA; bottom: dye/Iod2 in acetonitrile upon irradiation at 405 nm with a LED. Reproduced from [260] with permission from Elsevier.

Interestingly, a weak interaction of the three dyes with TEOA was demonstrated. Indeed, as shown in the Figure 8, the hydrogen donor had little effect on the photolysis rate of the different dyes. An almost similar behaviour was found for all dyes when combined with *bis*(4-methylphenyl)iodonium hexafluorophosphate (Iod2). It was thus concluded that TEOA and Iod2 were mostly interacting with the dyes, subsequent to their photoisomerizations. In the case of the dye/Iod2 combination, appearance of the new absorption band in the 500-600 nm range was observed, resulting from the reaction of the dyes with Bronsted acid released by the two-component dye/Iod2 system.[261] Examination of their photoinitiating ability during the FRP of TPGDA revealed the three dyes C6NPY, C6PY and C6SPY to be poor radical initiators alone, final monomer conversions of 14, 6 and 3% being determined after 600 s of

irradiation at 405 nm. When combined with Iod2, a significant enhancement of the monomer conversion was obtained, since conversions of 89, 75 and 55% were obtained with C6NPY, C6PY and C6SPY respectively after 600 s of irradiation with the two-component dye/Iod2 (0.1%/2% w/w) systems. By investigating the excited states of the three dyes, the authors revealed that the low photoinitiating ability of C6SPY could be assigned to its fast intersystem crossing (ISC) rate, which was determined as being 13 times faster than that of the fluorescence emission rate. Conversely, for C6PY and C6NPY, this difference was only reduced to 7 and 8 times for C6PY and C6NPY respectively. Therefore, the low photoinitiating ability of C6SPY was assigned to its fast intersystem crossing competing with the interaction of the dye with additives in the excited state.

Capitalizing on the ability of *bis*-chalcones to isomerize, the same group went a step further by developing 2,6-*bis*((1*H*-pyrrol-2-yl)methylene)cyclohexan-1-one (BPC), a dye unable to initiate any free radical polymerization in its *Z*,*E*-form but which is an efficient photoinitiator when thermally isomerized in its *E*,*E*-form (See Figure 9).[262] Using this approach, a thermally activable photoinitiator was proposed. More interestingly, the E,Z-form was determined as being thermodynamically stable at room temperature, even in the presence of TEOA and upon sunlight exposure due to the formation of intramolecular hydrogen bonds (N–H···O = C bonds), efficiently stabilizing the E,Z-form and preventing the E,Z-form to isomerize back to the E,E-form. Notably, after 14 days of sunlight exposure, almost no modification of the UV-visible absorption spectrum of E,Z-BPC in acetonitrile was detected. By mean of hydrogen bonds, the ability of the E,Z-form to abstract hydrogen of carbonyl was drastically reduced. Thermal analysis of the photoisomerization process revealed the E,Z → E,E isomerization to be extrememy slow at 40°C in acetonitrile. Conversely, at 60°C, a significant improvement of the isomerization kinetic was demonstrated in solution. Polymerization experiments carried out at 465 nm revealed the two-component *E*,*E*-BPC/TEOA (0.0625%/3% w/w) system to initiate the FRP of PEGDA even at room temperature whereas its *E*,*Z*-BPC/TEOA (0.0625%/3% w/w) analogue was totally inactive (See Figure 10a). Polymerization tests carried out by heating the resins at 40, 60, 80, 100 and 120°C for 15 min. prior to irradiation at 465 nm. Experiments revealed the *E*,*Z*-BPC/TEOA (0.0625%/3% w/w) system to furnish PEGDA conversions of 7, 29, 52, 60 and 70% respectively after 300 s of irradiation (See Figure 10b).

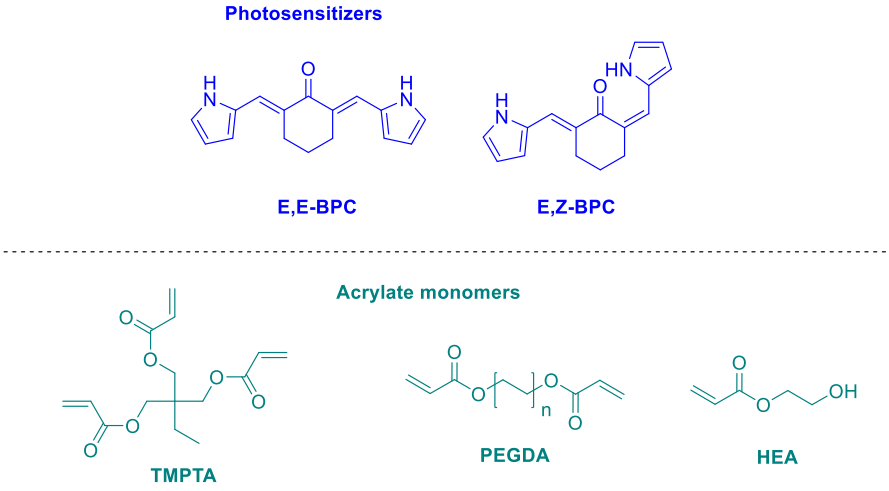

Figure 9. Chemical structures of BPC and different monomers.

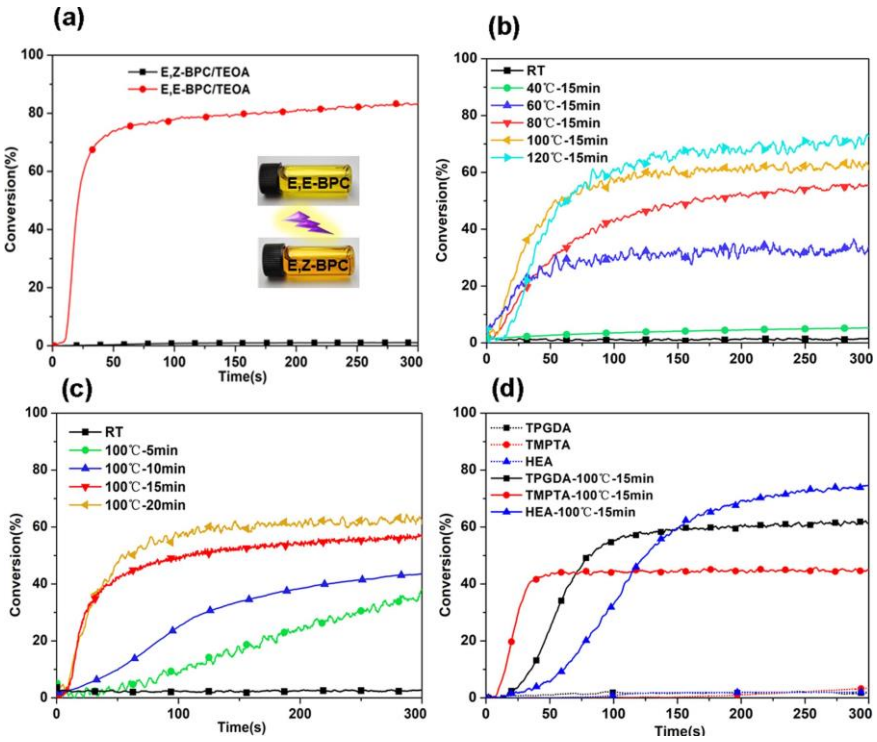

Figure 10. Polymerization profiles obtained upon irradiation at 465 nm. a) using *E,Z*-BPC/TEOA and *E,E*-BPC/TEOA for the FRP of PEGDA; b) using *E,Z*-BPC/TEOA/PEGDA for the FRP of PEGDA at different temperatures; c) using *E,Z*-BPC/TEOA heated for 5, 10, 15 and 20 min at 100°C for the FRP of PEGDA; d) using *E,Z*-BPC/TEOA for the FRP of various monomers with/without heating the resin for 15 min. at 100°C prior to irradiation. Reproduced from [260] with permission from Elsevier.

Investigation of the heating time at 100°C revealed an improvement of the PEGDA conversion upon elongation of the heating time. Thus, by using the two-component *E,Z*-BPC/TEOA (0.0625%/3% w/w) system and by heating the resins at 100°C for 5, 10, 15 and 20 min. prior to irradiation furnished 30, 40, 58 and 62% monomer conversions after 300 s of irradiation at 465 nm. It was thus concluded, based on the similarity of the monomer conversion obtained after 15 and 20 min. of heating (58 and 62% respectively), that the best

heating time was thus 15 min (See Figure 10c). Applicability of this process was expended to other monomers such as hydroxyethyl acrylate (HEA), tripropyleneglycol diacrylate (TPGDA) or trimethylolpropane triacrylate (TMPTA). Final monomer conversions of 43, 60 and 78% could be obtained using TMPTA, TPGDA or HEA as the monomers and *E*,*Z*-BPC/TEOA (0.0625%/3% w/w) as the photoinitiating system. Here again, the resins were heated at 100°C for 15 min. prior to polymerization at 465 nm.

It has to be noticed that BPC was also examined by the group of Lalevée and coworkers as photoinitiator for the CP of EPOX and the FRP of di(trimethylolpropane) tetraacrylates (TA).[164] Its photoinitiating ablity was notably compared to that of ketone 2, differing from BPC by the substitution of the central core (See Figure 11). Notably, in the case of ketone 2, *N*-ethyl-piperidinone was used as the central group. From the absorption viewpoint, if only a minor variation of the absorption maxima was found (416 nm for BPC vs. 405 nm for ketone 2), a two-fold enhancement of the molar extinction coefficient was found for ketone 2 compared to that of BPC (36 200 $M^{-1}.cm^{-1}$ vs. 18 800 $M^{-1}.cm^{-1}$). Considering the high molar extinction coefficients at 405 nm, polymerization tests could be carried out at this wavelength.

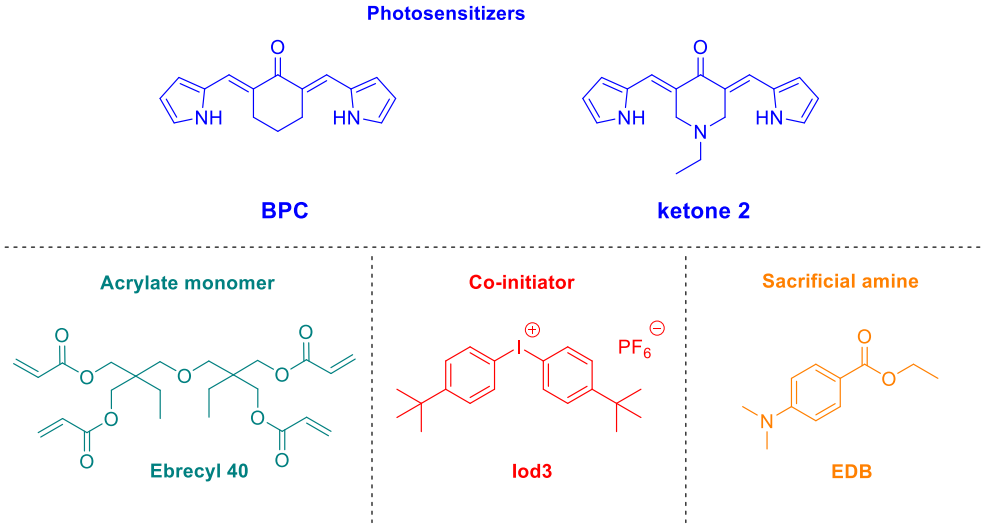

Figure 11. Chemical structure of BPC, ketone 2, EDB, Ebecryl 40 and Iod3.

As observed for the previous chalcones, photoinitiating ability of BPC and ketone 2 alone (0.1 % w) remained low, the conversion of Ebecryl 40 being lower than 20% upon irradiation at 405 nm. Polymerization tests done with the two-component BPC/Iod3 (0.1%/2%, w/w) (where Iod3 stands for *bis*(4-(*tert*-butyl)phenyl)iodonium hexafluorophosphate) and BPC/EDB (0.1%/2%, w/w) systems in thin films (25 µm) revealed the conversions of Ebecryl 40 to be low, peaking respectively at 55 and 40%. Finally, use of the three-component dye/EDB/Iod3 (0.1%/2%/2%, w/w/w) system enabled to get higher monomer conversions, reaching 85 and 64% using BPC and ketone 2 as the sensitizers, evidencing the necessity to use three-component photoinitiating systems. Here again, BPC proved to be an excellent dye for photoinitiation, outperforming ketone 2. This difference of monomer conversions could be rationalized by mean of steady state photolysis experiments. Thus, the photolysis done upon

irradiation at 405 nm in acetonitrile revealed for the two-component BPC/Iod3 (0.1%/2%, w/w) system a consumption of the dye of 78% after 10 min. whereas this value decreased to only 32% for the ketone 2/Iod3 system. The same analyses done for the two-component dye/EDB systems revealed a less favourable rate constant of interaction, the consumption of the dyes being reduced to 11 and 12% respectively after 10 min. of irradiation at 405 nm. The higher monomer conversion obtained with BPC is thus directly related to the higher photochemical reactivity of BPC with the iodonium salt compared to the amine. Fast interaction of BPC with Iod3 was confirmed by fluorescence quenching experiments. Determination of the electron transfer quantum yields revealed the BPC/Iod3 system to have a higher value (0.923) than that determined for the ketone 2/Iod3 system (0.899). Finally, high reactivity of the BPC/Iod3 combination was confirmed during the CP of EPOX. Thus, a conversion of 70% could be obtained with the BPC/Iod3 (0.1%/2%, w/w) system whereas a conversion of only 30% could be determined with the ketone 2-based photoinitiating system. Considering the high reactivity of the BPC-based three-component system, the access to composites was thus examined and polymers containing 20% weight percent of silica fillers were prepared. It has to be noticed that in these conditions, light penetration within the photocurable resins at 405 nm was only of 1.2 mm. Indeed, at present, photopolymerization of composites in the near UV/visible range is still a challenge, notably due to inner filter effects and the limited light penetration.[12,263] Besides, by laser write experiments, 3D patterns displaying an excellent spatial resolution could be obtained, upon irradiation at 405 nm. By optical microscopy, an excellent dispersion of the silica fillers within the polymer film could be demonstrated (See Figure 12).

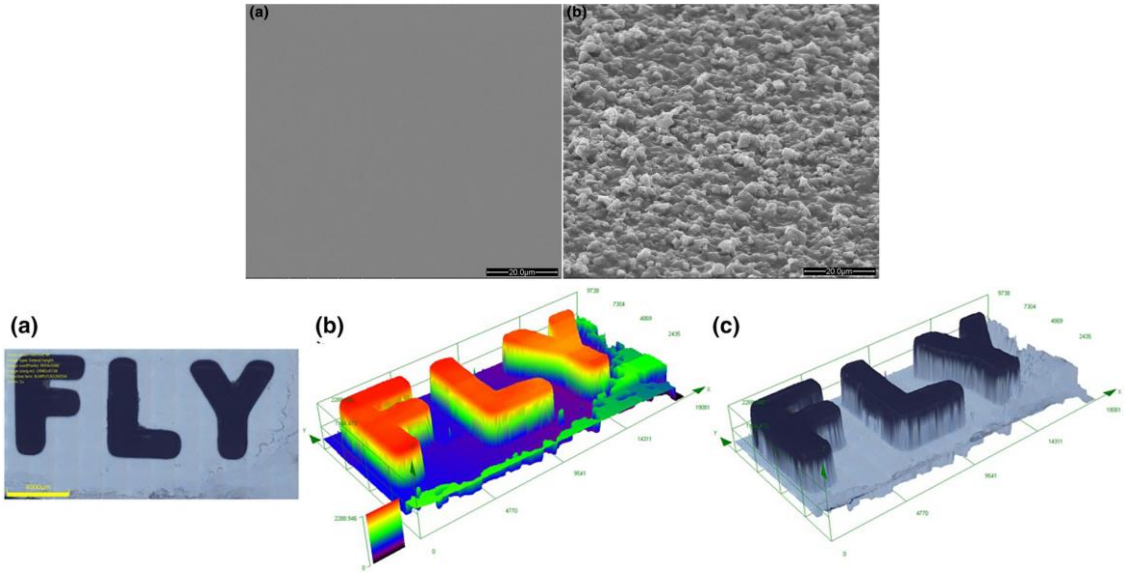

Figure 12. Top: SEM images of Ebecryl 40-based polymer with and without silica fillers. Bottom: images obtained by numerical optical microscopy of 3D patterns obtained by laser write experiments for resins containing 20% fillers, BPC/EDB/Iod3 (0.1%/2%/2%, w/w/w), 405 nm, 110 mW/cm². Reprinted by permission of John Wiley & Sons, Inc. Copyright © Ref. [164]

2.2. Penta-1,4-dien-3-ones

Bis-chalcones have been extensively studied as photoinitiators of polymerization.[167] From a structural viewpoint, *bis*-chalcones are extremely similar to penta-1,4-dien-3-ones (enones) so that this second family of dyes was logically examined in photopolymerization and the performances compared to that of *bis*-chalcones. Interest for penta-1,4-dien-3-ones as photoinitiators is recent, since the first reports mentioning their uses in photopolymerization have been reported in 2021. In this field, (1*E*,4*E*)-1,5-*bis*(1-methyl-1*H*-pyrrol-2-yl)penta-1,4-dien-3-one (C3PY) has been the most widely studied structure and different works have notably been reported by the group of Nie and coworkers (See Figure 13).[260]

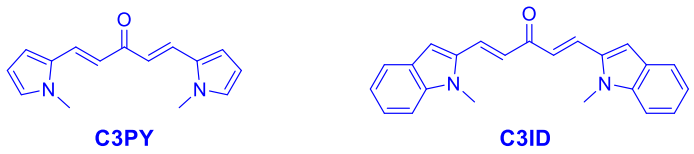

Figure 13. Chemical structure of C3PY and C3ID.

This dye is of crucial interest since a dramatic colour change of the final polymer was demonstrated, depending on the polymerization conditions. Due to its absorption maximum located at 414 nm, polymerization experiments were carried out at 405 nm. Noticeably, when used as a mono-component system or in combination with TEOA, colourless polymers could be obtained during the FRP of TPGDA or TMPTA. Conversely, when combined with Iod2, a deeply coloured polymer was obtained. Ability of C3PY to initiate alone a polymerization process was notably assigned to the coexistence of a ketone and two tertiary amines within this scaffold. Optimization of the polymerization conditions for TPGDA revealed 0.1 wt% to be the optimum concentration and a monomer conversion of 65% could be obtained after 600 s of irradiation at 405 nm with a LED. When combined with Iod2 or TEOA in two-component systems, conversions of 91 and 76% could be respectively obtained in the same conditions. This order of reactivity was confirmed during the FRP of TMPTA and final monomer conversions of 30, 39 and 50% could be obtained for C3PY (0.1% w), C3PY/TEOA (0.1%/3% w/w) and C3PY/Iod2 (0.1%/2% w/w) systems. To support the appearance of a red-violet colour for TPGDA-based polymers and a red-blue color for TMPTA-based polymers, appearance of two absorption bands at 513 and 637 nm were identified while using C3PY/Iod2 (0.1%/2% w/w) system. To support the appearance of an absorption band at 637 nm, the release of Bronsted acid during irradiation and the protonation of C3PY was proposed by the authors.[264] This hypothesis was verified in solution by addition of *para*-toluenesulfonic acid (PTSA) to an acetonitrile solution of C3PY. In that case, appearance of an absorption band at 600 nm could be clearly evidenced. By mean of nuclear magnetic resonance (NMR) studies, protonation on the ketone side and not formation of pyrrolium cation was clearly demonstrated. Finally, appearance of the absorption peak at 513 nm was assigned to the dimerization of $C3PY^{\bullet+}$, formation of the $C3PY^{\bullet+}$ radical cations resulting from the photoinduced electron transfer between C3PY and Iod2 in first step.

Considering the similarity of structures between C3PY, C6PY, C6NPY and C6SPY, comparisons of photoinitiating ability could be established.[260] Thus, during the FRP of

TPGDA, C3PY clearly outperformed the three other dyes, irrespective of the photoinitiating system used. Thus, a TPGDA conversion of 65% could be determined after 600 s of irradiation at 405 nm with C3PY alone whereas the best conversions obtained with *bis*-chalcones was limited to 14% for C6NPY in the same conditions. Similarly, C3PY could outperform C6NPY in two-component dye/TEOA (0.1%/3% w/w) systems, the conversion obtained with C3PY exceeding that of C6NPY by ca 23% (56% vs 33% after 600 s of irradiation). Finally, close monomer conversions could only be obtained using the two-component dye/Iod2 system. In that case, conversions of 92 and 89% could be respectively determined with C3PY and C6NPY. To support the higher monomer conversions obtained with C3PY compared to C6PY, C6NPY and C6SPY, the higher flexibility of the C3PY scaffold enabling a possible Z/E isomerization of one of the two double bonds and enabling to reduce the S_1-T_1 energy gap was suggested by the authors as a possible explanation.

Following these works, Nie and coworkers examined the possibility to replace the pyrrole moieties of C3PY by indole groups in C3ID (See Figure 13).[265] From the absorption viewpoint, the absorption spectrum of C3ID was slightly redshifted compared to that of C3PY (422 nm for C3ID vs. 414 nm for C3PY). For the two dyes, the absorption band was broad, extending from 300 until 500 nm. Under 405 nm LED irradiation, 65% and 80% TPGDA conversions could be obtained with C3PY and C3ID used alone. Upon addition of TEOA, only a minor improvement was obtained since monomer conversions of 77 and 84% could be obtained after 600 s of irradiation. Interestingly, photolysis experiments revealed C3PY and C3ID to give a fast photobleaching in solution, resulting from an efficient intramolecular hydrogen atom transfer (HAT) reaction due to the close co-existence of the ketone and the tertiary amine moieties. Addition of TEOA in acetonitrile solutions containing the dyes had only little influences on the photolysis rates, consistent the polymeriation results. Further investigation also revealed that an isomerization reaction was certainly occurring, the distance between the ketone group and the hydrogen donor being too important in the *E*,*E*-isomer in order the two groups to interact.[266] It was thus postulated the HAT reaction in the two dyes could only take place after isomerization. As shown in the Figure 14, the ketone and the *N*-methyl groups are highly adjacent only for the *E*,*Z*-conformations. Overall, the photochemical mechanism depicted in the Figure 15 was proposed. Thus, upon irradiation, a photoisomerization reaction occurs, enabling a HAT reaction to proceed. An unstable 1,6-biradical is thus formed, certainly undergoing a rapid radical recombination.[267] Considering that the intramolecular HAT reaction is faster for C3PY than for C3ID, higher monomer conversions could be obtained with C3ID compared to C3PY. Parallel to this, intermolecular HAT reactions of dyes with TEOA is faster than the intramolecular ones so that the polymerization rates were enhanced upon addition of TEOA.

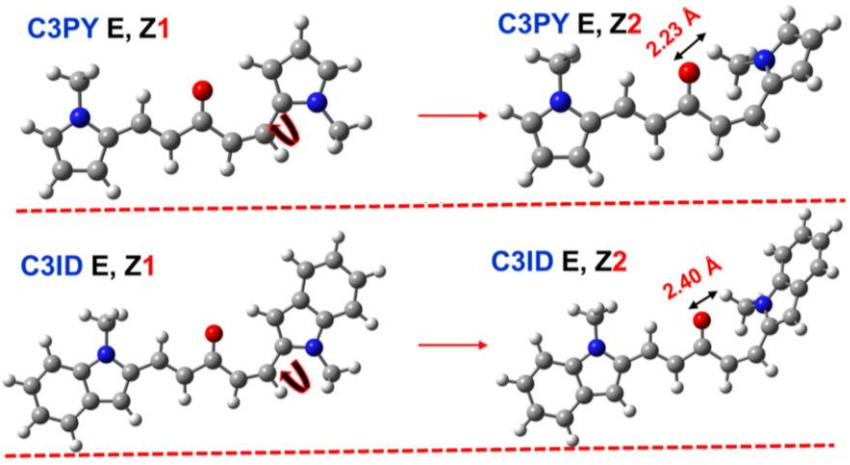

Figure 14. Optimized geometries of C3PY and C3ID for different conformations. Reproduced from Ref. [265] with permission from Elsevier.

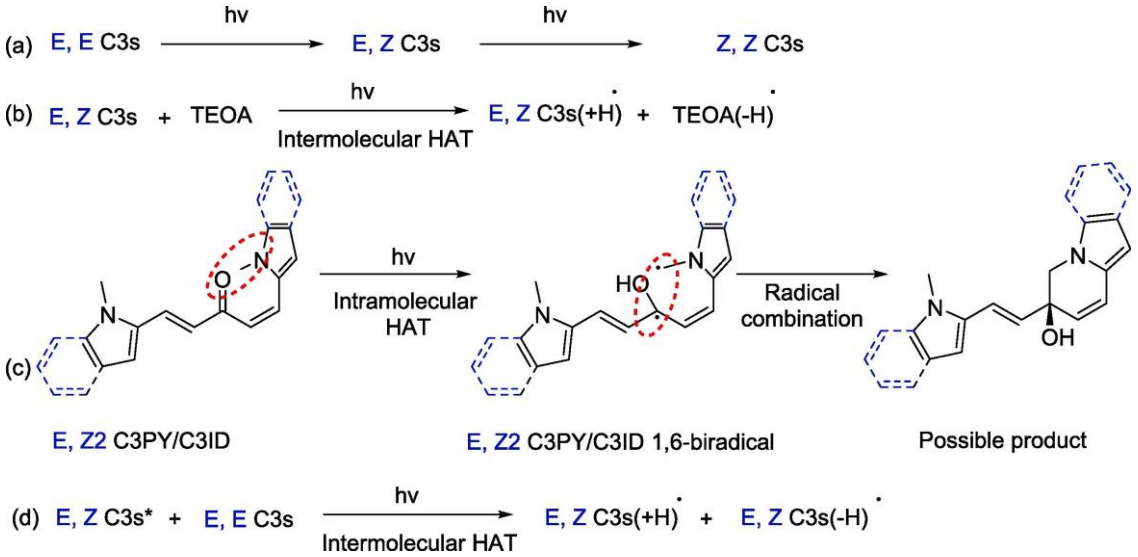

Figure 15. Photochemical transformations occurring for C3PY and C3ID with/without TEOA. Reproduced from Ref. [265] with permission from Elsevier.

2.3. Diketopyrrolopyrroles and 1,4-dihydropyrrolo[3,2-b]pyrroles

Pyrrole is an aromatic five-membered ring widely used for the design of dyes. In this field, diketopyrrolopyrrole (DKPP) corresponds to a dilactam form of pyrrole and this scaffold is at the origin of numerous organic dyes and pigments.[268–270] Among them, the most famous one is undoubtedly the well-known 'Ferrari Pigment'.[271,272] Diketopyrrolopyrrole has also been extensively used for the design of semi-conducting polymers used in organic field-effect transistors (OFETs) or as light-absorbing materials for organic solar cells.[273–277] Interestingly, DKPPs are characterized by a broad absorption so that these dyes were logically investigated as visible light photoinitiators of polymerization. The first report mentioning the use of diketopyrrolopyrroles as photosensitizers was reported in 2014 by the group of Lalevée and coworkers.[98] In this work, a comparison was established between 2,5-*bis*(2-

octyldodecyl)-3,6-di(thiophen-2-yl)-pyrrolo[3,4-*c*]pyrrole-1,4(2*H*,5*H*)-dione (DPPDT), a monomer used for the synthesis of a polymer, namely PDQT (See Figure 16).

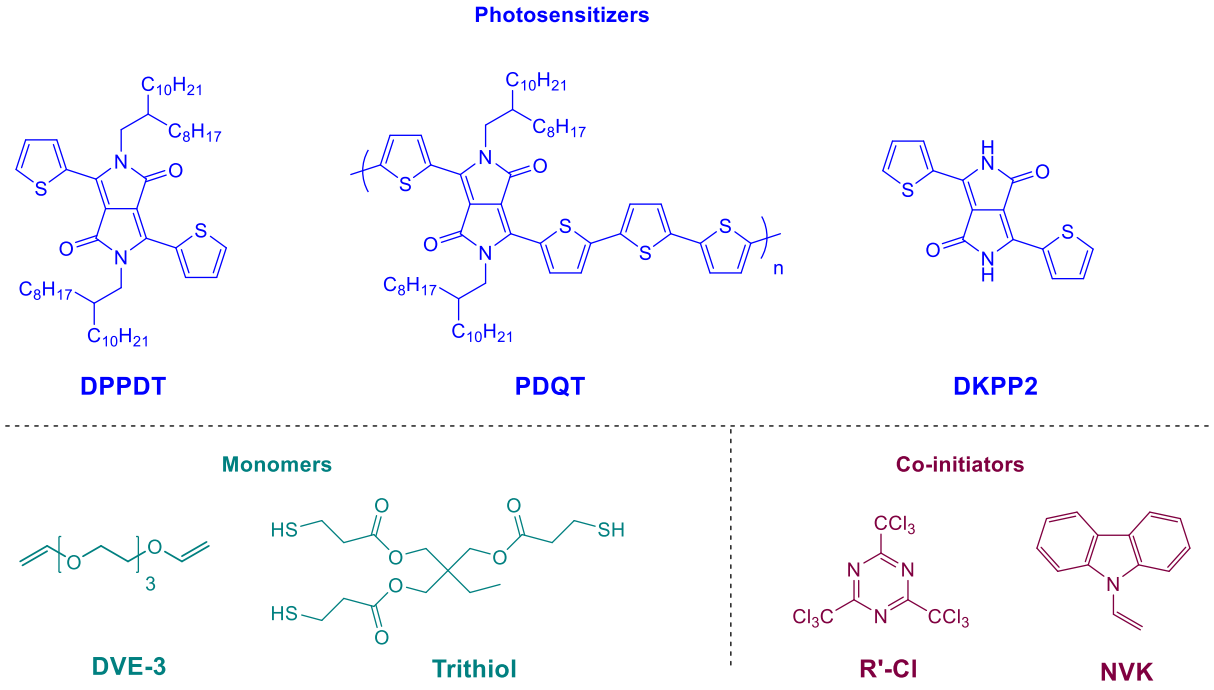

Figure 16. Chemical structures of DPPDT, PDQT, different monomers and additives.

From the absorption viewpoint, incorporation of DPPDT into a polymer drastically impacted the absorption properties (See Figure 17). Thus, the absorption maximum of DPPDT shifted from 548 nm for the monomer up to 781 nm when incorporated into PDQT, consistent with an elongation of the π-conjugation inside the polymer. Especially, the absorption spectrum of PDQT was broad, extending from 300 up to 1050 nm, making PDQT a panchromatic photoinitiator.

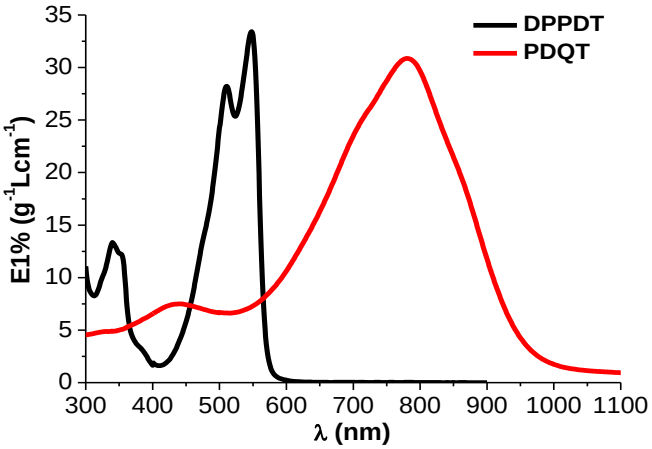

Figure 17. UV-visible absorption spectra of DPPDT and PDQT in tetrahydrofuran (THF). Reprinted with permission of Xiao et al. [98]

Based on their respective absorptions, polymerization tests were carried out for DPPDT at 473 and 532 nm with laser diodes or with a halogen lamp. Parallel to this, considering the strongly red-shifted absorption of PDQT, polymerization tests were also carried out at 808 nm.

Examination of the cationic polymerization of EPOX upon irradiation at 532 nm revealed the monomer conversion to be higher than that obtained at 473 nm (31% vs 21%) using the three-component DPPDT/Iod/NVK (0.5%/2%/3%, w/w/w) system. This is directly related to the higher molar extinction coefficient of DPPDT at 532 nm than 473 nm. Introduction of NVK into the photoinitiating system did not significantly improve the conversion since a value of 29% could already be obtained with the two-component DPPDT/Iod (0.5%/2%, w/w) system (See Table 1). Noticeably, the same conversion was obtained upon irradiation with a halogen lamp.

Table 1. EPOX conversions obtained under air upon exposure to different visible light sources for 800 s in the presence of DPPDT/Iod (0.5%/2%, w/w), DPPDT/Iod/NVK (0.5%/2%/3%, w/w/w), PDQT/Iod (0.5%/2%, w/w) or PDQT/Iod/NVK (0.5%/2%/3%, w/w/w).

	Halogen lamp	Laser diode at 473 nm	Laser diode at 532 nm	Laser diode at 808 nm
DPPDT/Iod	29%		29%	
DPPDT/Iod/NVK		21%	31%	
PDQT/Iod	np*			np
PDQT/Iod/NVK	np		np	np

* np: no photopolymerization.

While using tri(ethylene glycol)divinyl ether (DVE-3) as the monomer, a conversion as high as 96% could be obtained within 400 s in laminate with the two-component DPPDT/Iod (0.5%/2%, w/w) system upon irradiation at 532 nm. If a remarkable conversion was obtained in laminate, no conversion could be detected anymore under air, Ph-DVE-3$^{\bullet}$ radicals entirely reacting with oxygen and impeding the formation of Ph-DVE-3^{+}. Additionally, it also demonstrates the minor contribution of DPPDT$^{+\bullet}$ in the overall polymerization process. If DPPDT proved to be relatively performant, another situation was found for PDQT. Indeed, irrespective of the photoinitiating system or the irradiation wavelengths, no cationic polymerization could be initiated. This counter-performance was assigned to the low solubility of PDQT in resins, adversely affecting its photoinitiating ability. This issue was also evidenced for another DKPP derivative, namely DKPP2, in which no solubilizing chains have been introduced in its scaffold.[96] Using the three-component DKPP2/Iod/NVK system, a conversion of EPOX lower than 10% was obtained upon irradiation at 532 nm, whereas a 3-fold enhanced conversion could be obtained with the more soluble DPPDT (29% conversion) in the same conditions.

Surprisingly, low monomer conversions were obtained with DPPDT during the FRP of TMPTA upon irradiation with a halogen lamp in laminate. Thus, conversions of only 18% and 19% were respectively obtained using the two-component DPPDT/Iod (0.5%/2%, w/w) and PPDT/MDEA (0.5%/2%, w/w) systems during the FRP of this trifunctional monomer (See Table 2). While introducing R'-Cl in the two-component **DPPDT**/MDEA (0.5%/2%, w/w) system, the conversion increased up to 37%, corresponding to a two-fold enhancement of the

monomer conversion upon irradiation with a halogen lamp. Conversely, upon introduction of NVK in the two-component DPPDT/Iod (0.5%/2%, w/w) system, a lower monomer conversion was obtained (12% vs. 19%), whereas the highly reactive Ph-NVK• radicals are formed in these conditions. Noticeably, upon irradiation with a halogen lamp, only the three-component DPPDT/MDEA/R'-Cl (0.5%/2%/3%, w/w/w) system could furnish a TMPTA conversion comparable to that of the reference CQ/MDEA system (37% vs. 35% for the reference system) (See Table 2). Due to the lack of solubility of PDQT in TMPTA, no polymerization could be initiated, irrespective of the polymerization conditions.

Table 2. TMPTA conversions obtained in laminate upon exposure to different visible light sources for 800 s in the presence of DPPDT/MDEA (0.5%/2%, w/w), DPPDT/MDEA/R'-Cl (0.5%/2%/3%, w/w/w), DPPDT/Iod (0.5%/2%, w/w), DPPDT/Iod/NVK (0.5%/2%/3%, w/w/w), and PDQT/MDEA/R'-Cl (0.5%/2%/3%, w/w/w).

	Halogen lamp	Laser diode at 532 nm	Laser diode at 808 nm
DPPDT/MDEA	18%		
DPPDT/MDEA/R'-Cl	37%	38%	
DPPDT/Iod	19%		
DPPDT/Iod/NVK	12%	13%	
PDQT/MDEA/R'-Cl	np	np	np
CQ/MDEA	35%		

np: no photopolymerization

Finally, considering that DPPDT could initiate both the FRP of TMPTA and the CP of EPOX upon irradiation at 532 nm, interpenetrated polymer networks (IPN) could be obtained by the concomitant polymerization of EPOX and TMPTA. Noticeably, upon irradiation at 532 nm under air, a higher EPOX conversion than that obtained for TMPTA could be determined for a TMPTA/EPOX blend (50%/50% w/w). This is directly related to oxygen inhibition, adversely affecting the FRP of TMPTA under air (See Figure 18).

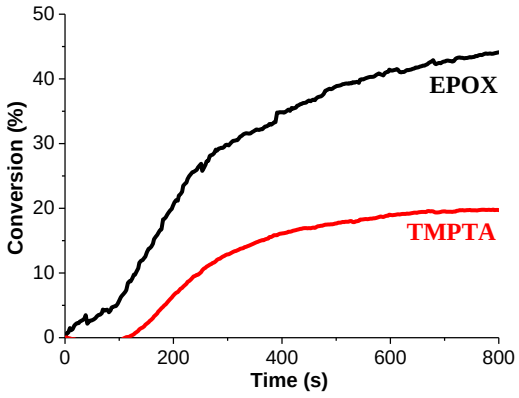

Figure 18. Photopolymerization profiles of a TMPTA/EPOX blend (50%/50%, w/w) in the presence of **DPPDT**/Iod/NVK (0.5%/2%/3%, w/w/w) under air upon the laser diode at 532 nm exposure. Reprinted with permission of Xiao et al. [98]

During the thiol–ene photopolymerization of a trithiol/DVE-3 blend (50%/ 50%, w/w) in laminate, a conversion of DVE-3 (around 99% after 400 s of irradiation) greatly higher than that determined for the thiol functions (around 42%) could be determined with the DPPDT/Iod (0.5%/2%, w/w) initiating system, attributable to the CP of DVE-3 competing with the thiol-ene polymerization process. Noticeably, the exceptional reactivity of the two-component DPPDT/Iod (0.5%/2%, w/w) initiating system could be demonstrated during the thiol-ene photopolymerization, ambient light being sufficient to initiate the polymerization process. By combining cyclic voltammetry, fluorescence quenching experiments, photolysis experiments in solution, and electron spin resonance spin trapping (ESR-ST) experiments, a full picture of the different species involved in the polymerization process could be determined (see equations r1-r10). Thus, $DPPDT^{\bullet+}$, $Ph–NVK^{+}$ and $Ph–DVE\text{-}3^{+}$ formed in equations r2, r8 and r5 were identified as the initiating species for the CP. On the opposite, $Ph^{\bullet}$, $Ph–NVK^{\bullet}$, $MDEA_{(-H)}{}^{\bullet}$ formed in equations (r3, r4, r6 and 10) can initiated the FRP of acrylates. Finally, thiyl radicals $RS^{\bullet}$ formed in r11-r13 can initiate the thiol-ene polymerization (See Scheme 1).

$$\mathbf{DPPDT} \rightarrow {}^{1}\mathbf{DPPDT}\ (h\nu) \quad \text{and} \quad {}^{1}\mathbf{DPPDT} \rightarrow {}^{3}\mathbf{DPPDT} \tag{r1}$$

$$^{1,3}\mathbf{DPPDT} + Ph_2I^{+} \rightarrow \mathbf{DPPDT}^{\bullet+} + Ph_2I^{\bullet} \tag{r2}$$

$$Ph_2I^{\bullet} \rightarrow Ph^{\bullet} + Ph\text{-}I \tag{r3}$$

$$Ph^{\bullet} + NVK\ (\text{or DVE-3}) \rightarrow Ph\text{-}NVK^{\bullet}\ (\text{or } Ph\text{-}DVE\text{-}3^{\bullet}) \tag{r4}$$

$$Ph\text{-}NVK^{\bullet}\ (Ph\text{-}DVE\text{-}3^{\bullet}) + Ph_2I^{+} \rightarrow Ph\text{-}NVK^{+}\ (Ph\text{-}DVE\text{-}3^{+}) + Ph^{\bullet} + Ph\text{-}I \tag{r5}$$

$$^{1,3}\mathbf{DPPDT} + MDEA \rightarrow \mathbf{DPPDT}^{\bullet-} + MDEA^{\bullet+} \rightarrow \mathbf{DPPDT}\text{-}H^{\bullet} + MDEA_{(-H)}{}^{\bullet} \tag{r6}$$

$$\mathbf{DPPDT}^{\bullet-} + R'\text{-}Cl \rightarrow \mathbf{DPPDT} + (R'\text{-}Cl)^{\bullet-} \tag{r7}$$

$$^{1,3}\mathbf{DPPDT} + R'\text{-}Cl \rightarrow \mathbf{DPPDT}^{\bullet+} + (R'\text{-}Cl)^{\bullet-} \tag{r8}$$

$$\mathbf{DPPDT}\text{-}H^{\bullet} + R'\text{-}Cl \rightarrow \mathbf{DPPDT} + H^{+} + (R'\text{-}Cl)^{\bullet-} \tag{r9}$$

$$(R'\text{-}Cl)^{\bullet-} \rightarrow R'^{\bullet} + Cl^{-} \tag{r10}$$

$$Ph^{\bullet} + RS\text{-}H \rightarrow Ph\text{-}H + RS^{\bullet} \tag{r11}$$

$$RS^{\bullet} + R'\text{-}CH{=}CH_2 \rightarrow R'\text{-}CH^{\bullet}\text{-}CH_2SR \tag{r12}$$

$$R'\text{-}CH^{\bullet}\text{-}CH_2SR + RSH \rightarrow R'\text{-}CH_2\text{-}CH_2SR + RS^{\bullet} \tag{r13}$$

Scheme 1. Chemical mechanisms occurring with the DPPDT/Iod; DPPDT/Iod/NVK; DPPDT/MDEA/R'-Cl photoinitiating systems, during FRP, CP and thiol-ene polymerizations.

Following this work, other diketopyrrolopyrroles were tested as photoinitiators, namely 2,5-*bis*(2-octyldodecyl)-3,6-di(furan-2-yl)pyrrolo[3,4-*c*]pyrrole-1,4(2*H*,5*H*)-dione (FuDPP) and 3,7-*bis*(4-bromophenyl)-1,5-*bis*(2-decyltetradecyl)pyrrolo[2,3-*f*]indole-2,6(1*H*,5*H*)-dione (M2), and their corresponding polymers i.e. PDBFBT and P2 (See Figure 19).[97]

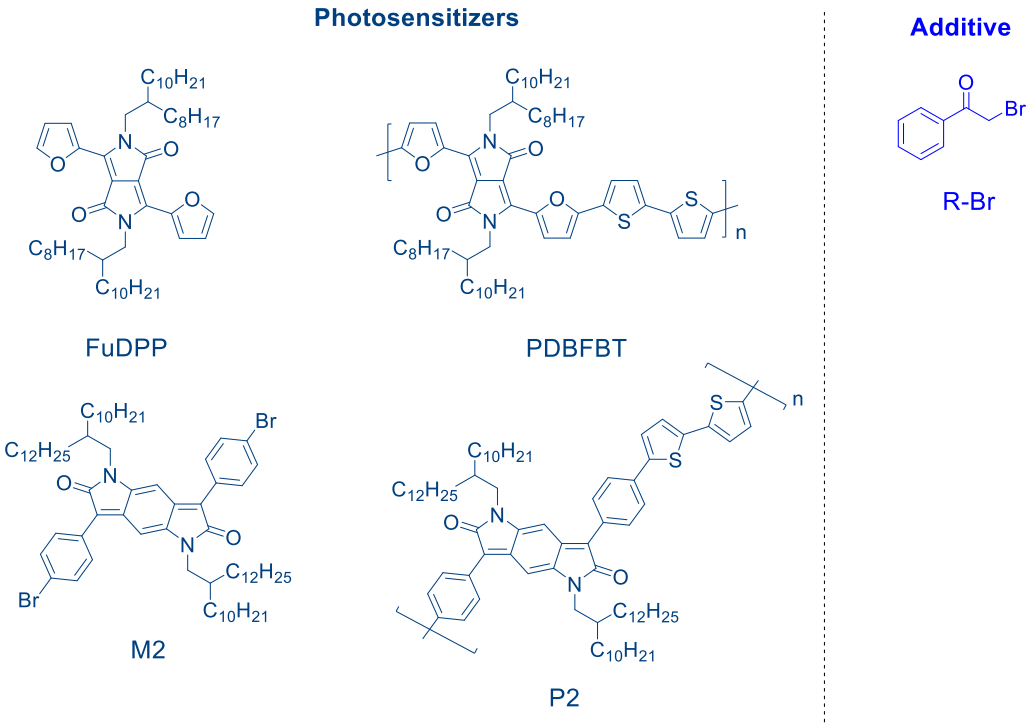

Figure 19. Chemical structures of FuDPP, M2 and the corresponding polymers PDBFBT and P2.

Examination of their UV-visible absorption spectra revealed the absorption of DPPDT to be redshifted compared to that of FuDPP (548 nm vs 537 nm). However, a higher molar extinction coefficient could be determined in an acetonitrile/toluene 50/50 mixture for FuDPP (42 800 $M^{-1}.cm^{-1}$ vs. 28 800 $M^{-1}.cm^{-1}$ for DPPDT) (See Figure 20). Conversely, for M2 whose structure strongly differs from that of FuDPP by the presence of an additional aromatic ring in the DKPP structure, a blueshift of the absorption of M2 could be determined compared to FuDPP, the absorption maximum peaking at 466 nm (ε = 41800 $M^{-1}.cm^{-1}$). As anticipated, absorption spectra of PDBFBT[278] and P2[279] which correspond respectively to the polymers of FuDPP and M2 were redshifted to 770 and 605 nm, consistent with a reduction of the HOMO-LUMO gaps upon polymerization (where HOMO stands for the highest Occupied Molecular Orbital and LUMO for the Lowest Unoccupied Molecular Orbital).

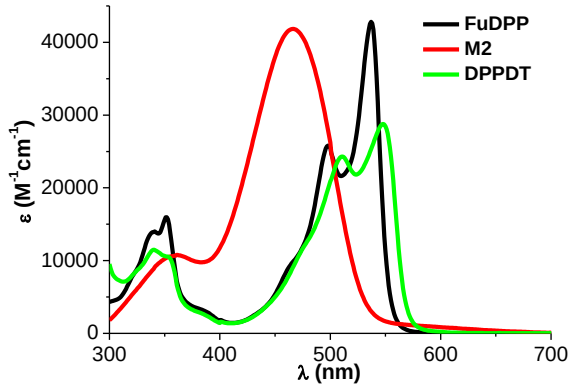

Figure 20. UV-visible absorption spectra of **FuDPP**, **M2** and **DPPDT** in acetonitrile/toluene (50%/50%, V/V). Reprinted with permission of Xiao et al. [97]

The four dyes, namely FuDPP, PDBTFBT, M2 and P2 were examined as photosensitizers for the cationic polymerization of EPOX under air, using two-component dye/Iod or three-component dye/Iod/NVK photoinitiating systems. Considering their broad absorptions, different visible lights sources were used, namely laser diodes emitting at 457, 473, 532, 635 and 808 nm. A halogen was also used. Monomer conversions obtained at the different irradiation wavelengths are given in Table 3. Compared to the previous DPPDT/Iod (0.5%/2%, w/w) system which furnished only a monomer conversion of 29% upon irradiation with a halogen lamp, this value increased up to 49% with the two-component FuDPP/Iod (0.5%/2%, w/w) system. A further improvement of the monomer conversion could even be obtained upon addition of NVK to the photoinitiating system. By using the three-component FuDPP/Iod/NVK (0.5%/2%/3%, w/w/w) system, a conversion of 55% could be obtained within 800 s of irradiation, still using a halogen lamp. The three-component FuDPP/Iod/NVK system also worked efficiently at 473 or 532 nm, furnishing conversions of 62% and 50% respectively. Surprisingly, M2 proved to be a poor candidate for photoinitiation, the efficiency of the three-component M2/Iod2/NVK (0.5%/2%/3%, w/w/w) remaining low (7% conversion). Finally, as previously observed for PDQT, no polymerization could be detected with the two DKKP-based polymers PDBFBT and P2 due to their low solubilities in resins. The different DKKP (FuDPP or M2) are of crucial interest for photoinitiation considering that the reference compound i.e. camphorquinone (CQ) is ineffective at the different wavelengths investigated.

Table 3. EPOX conversions obtained in air upon exposure to different visible light sources for 800 s in the presence of : FuDPP/Iod (0.5%/2%, w/w), FuDPP/Iod/NVK (0.5%/2%/3%, w/w/w), M2/Iod (0.5%/2%, w/w), M2/Iod/NVK (0.5%/2%/3%, w/w/w), related polymeric dyes based PISs; previously studied DPPDT/Iod2 (0.5%/2%, w/w) and DPPDT/Iod/NVK (0.5%/2%/3%, w/w/w).

PISs	Halogen lamp	Laser diode 457 nm	Laser diode 473 nm	Laser diode 532 nm	Laser diode 635 nm or 808 nm
FuDPP/Iod	49%				
FuDPP/Iod/NVK	55%		62%	50%	
M2/Iod	np*				
M2/Iod/NVK	7%	np	np		
DPPDT/Iod	29%			29%	
DPPDT/Iod/NVK			21%	31%	
PDBFBT (or P2, PDQT)/Iod/NVK	np				np

*np: no photopolymerization

Finally, photoinitiating ability of FuDPP was also examined during the FRP of TMPTA (See Table 4). Using the three-component FuDPP/Iod/NVK (0.5%/2%/3%, w/w/w), a conversion of 23% could be obtained at 532 nm, higher than that obtained with DPPDT (13%) in the same conditions. Noticeably, the three-component FuDPP/Iod/NVK (0.5%/2%/3%, w/w/w) system outperformed the reference CQ/Iod system, the reference system only furnishing a monomer conversion of 10% at 532 nm. Ability of FuDDP to react in reductive cycle was also investigated and for this purpose, the three-component FuDPP/MDEA/R-Br (0.5%/2%/3%, w/w/w) system (where R-Br stands for phenacyl bromide) was investigated.

Even if radicals could be still produced with this system, a lower efficiency could be however evidenced (5% conversion upon irradiation with a halogen lamp vs. 12% for the three-component FuDPP/Iod/NVK (0.5%/2%/3%, w/w/w) system., It was thus concluded that DKPP could react more efficiently in a photooxidative than in a photoreductive pathway.

Table 4. TMPTA conversions obtained in laminate upon exposure to different visible light sources for 400 s in the presence of FuDPP/Iod (0.5%/2%, w/w), FuDPP/Iod/NVK (0.5%/2%/3%, w/w/w), FuDPP/MDEA (0.5%/2%, w/w), FuDPP/MDEA/R-Br (0.5%/2%/3%, w/w/w)

PISs	Halogen lamp	Laser diode (473 nm)	Laser diode (532 nm)
FuDPP/Iod	12%		
FuDPP/Iod/NVK	13%	16%	23%
FuDPP/MDEA	15%		
FuDPP/MDEA/R-Br	5%	15%	15%
DPPDT/Iod	19%		
DPPDT/Iod/NVK	12%		13%
CQ/Iod			<10%

In 2017, a series of eleven diketopyrrolopyrroles was investigated, exhibiting unusual photobleaching properties (See Figure 21).[280] In this series, DKPP1-DKPP3 were designed with different dimethylamino co-initiators and different lengths of alkyl chains were used to connect co-initiators to the dye. For control experiments, DKPP4 was synthesized, only bearing an alkyl chain. To evidence the contribution of the thiophene unit in DKPP1-DKPP3, a second series of dyes i.e. DKPP5-DKPP7 substituted with peripheral aromatic rings was synthesized. Finally, a Type I photoinitiator i.e. DKPP11 derived from the well-known diphenyl(2,4,6-trimethylbenzoyl)phosphine oxide (TPO) was also designed, DKPP8-DKPP10 corresponding to intermediates giving access to DKPP11.[2,281–283] Examination of the UV-visible absorption spectra of DKPP1-DKPP4 revealed their absorptions to be strongly red-shifted compared to that DKPP5-DKPP7 (540 nm vs. 460 nm). This redshift was assigned to the higher electron-donating ability of the peripheral thiophene units in DKPP1-DKPP4 compared to the phenyl ring n DKPP5-DKPP7 (See Figure 22 and Table 5). The most redshifted absorption was found for DKPP11, peaking at 585 nm and exhibiting the longest π-conjugated system of the series. Noticeably, surprising results were obtained with these dyes. Thus, if DKKP1-DPP3, DKPP5-DKPP8 were designed to act as monocomponent systems, only a slow photobleaching of the acetonitrile solutions were detected during the photolysis experiments done upon irradiation at 520 nm, evidencing the inability of these dyes to act as monocomponent systems. Similarly, almost no photolysis was detected for DKPP11 in acetonitrile solutions, despites its specific design to react as a Type I photoinitiator. In fact, consumption of the eight dyes (DKPP1-DKPP3, DKPP5-DKPP8, DKPP11) was only observed in the presence of an iodonium salt. Within a few minutes, a complete bleaching of the different solutions could be evidenced. By decomposition of the iodonium salt, aryl radicals are formed, enabling to initiate the FRP of (meth)acrylates.

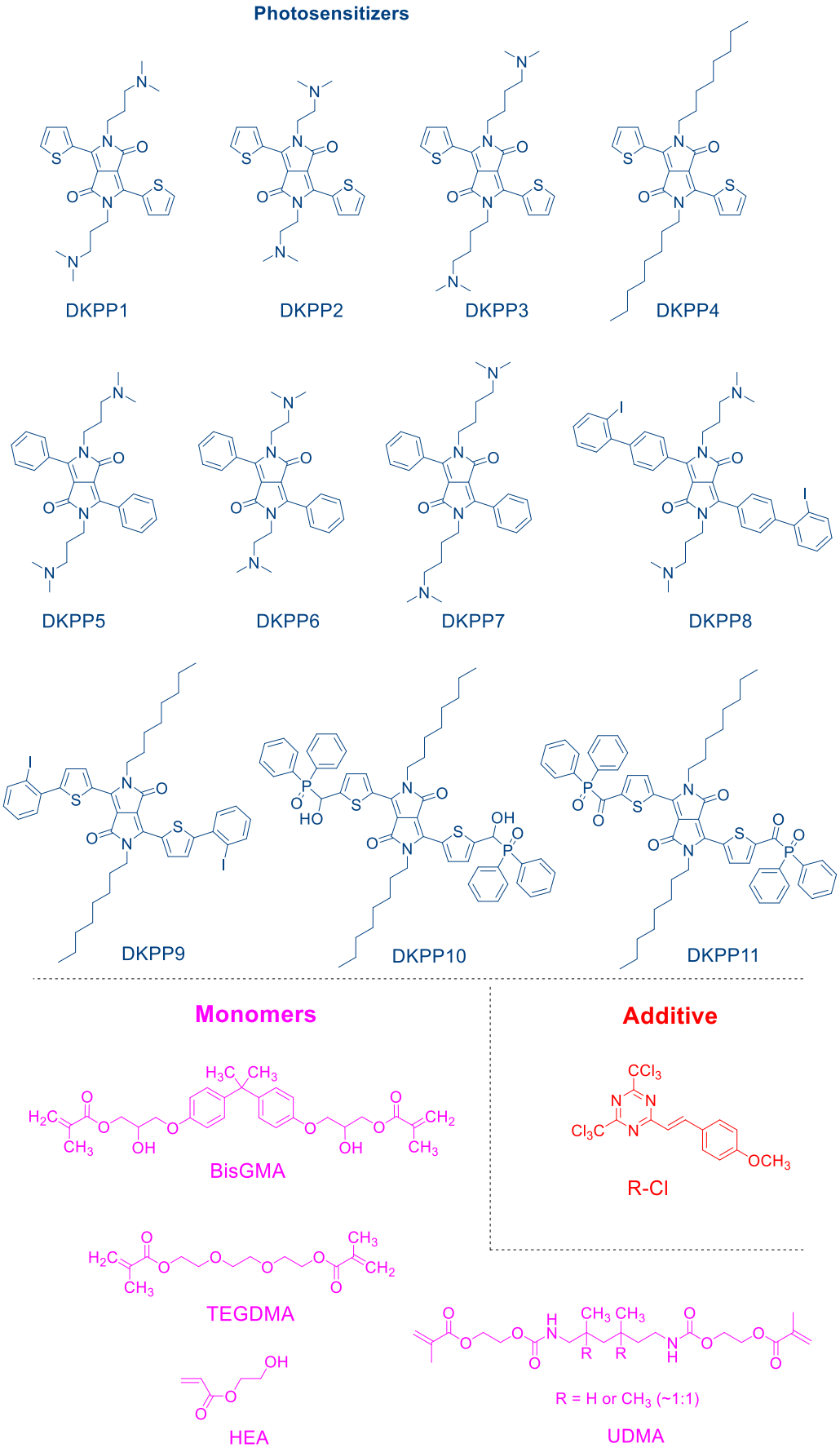

Figure 21. Chemical structures of DKKP1-DKPP11.

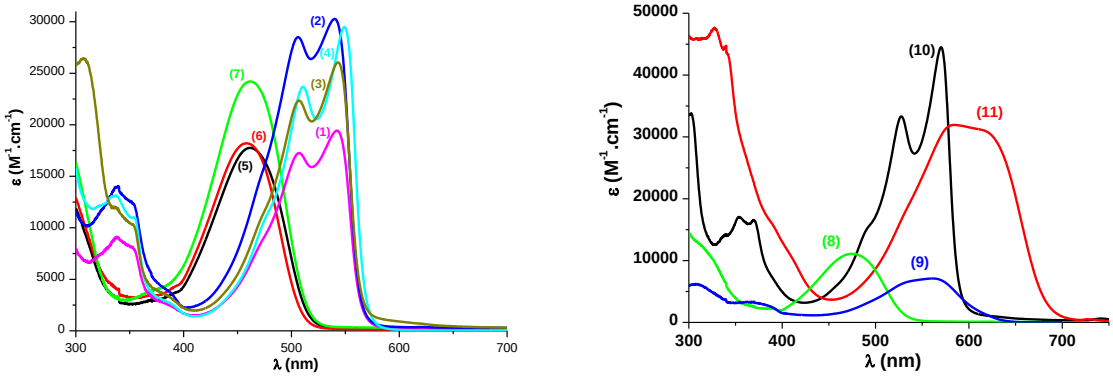

Figure 22. UV-visible spectra of the different diketopyrrolopyrrole in acetonitrile. Reprinted with permission of Bouzrati-Zerelli et al. [280]

Table 5. Light absorption properties of the investigated DKPP derivatives in acetonitrile and molar extinction coefficients of the different PIs at the investigated wavelengths.

	λ_{max} (nm)	ε_{max} ($M^{-1}.cm^{-1}$)	ε_{455nm} ($M^{-1}.cm^{-1}$)	ε_{470nm} ($M^{-1}.cm\text{-}^{1}$)	ε_{520nm} ($M^{-1}.cm^{-1}$)
DKPP1	540	19400	5100	8200	15900
DKPP2	540	30400	9100	14800	26500
DKPP3	540	26000	6700	10900	20400
DKPP4	550	29600	5700	9900	21000
DKPP5	460	17800	17400	17200	1000
DKPP6	460	18300	18200	17200	580
DKPP7	460	24300	23900	23600	1400
DKPP8	475	11200	9900	4200	3200
DKPP9	560	7300	1500	2060	5500
DKPP10	570	44600	5700	8200	14100
DKPP11	585	32100	3700	4500	29100

The different dyes were thus examined as photoinitiators for the FRP of methacrylates such as (2,2-*bis*-4-methacryloxy-2-hydroxy-propoxy-phenyl-propane (BisGMA), triethylene glycol dimethacrylate (TEGDMA), urethane dimethacrylate (UDMA) and 2-hydroxyethyl acrylate (HEA). Polymerization tests were carried out upon irradiation at 470 and 532 nm in thin and thick films while using three different photoinitiating systems, namely DKPP/Iod, DKPP/EDB and DKPP/R-Cl (where R-Cl stands for (4-methoxystyryl)-4,6-*bis*(trichloromethyl)-1,3,5-triazine. As anticipated, only low monomer conversions could be obtained with using DKPP1–DKPP3, DKPP5–DKPP8 and DKPP11 as monocomponent system, consistent with the photolysis experiments. Conversely, when combined with additives, good monomer conversions could be obtained both at 470 and 532 nm, but not with all dyes.

Thus, the monomer conversion determined during the FRP of BisGMA/TEGDMA blend (70/30 w/w) upon irradiation at 520 nm for 400 s in laminate increased from 18 to 30 and 50% while using DKPP1 as a monocomponent system (0.5 wt%), in the two-component DKPP1/Iod (0.5/2% w/w) system and the three-component DKPP1/Iod/EDB (0.5/2/2% w/w/w) system (See Table 6). Comparison with a reference system Eosin-Y/EDB (0.5/2% w/w) revealed the monomer conversion to be low, around 6%, demonstrating the remarkable efficiency of DKPP1 at 520 nm. Finally, monomer conversions of 50, 45, 45, 30 and 8% could be obtained upon irradiation at 470, 520, 532, 565 and 635 nm using the three-component DKPP1/Iod2/EDB (0.5%/2%/2% w/w/w) system. The low monomer conversion obtained at 635 nm is directly related to the low absorption of DKPP1 at this wavelength. Here again, the crucial role of the substitution was evidenced by comparing the monomer conversions obtained with DKPP2-DKPP8 and DKPP9-DKPP11 in three-component systems upon irradiation at 470 and 520 nm. Indeed, if monomer conversions varying from 46% for DKPP8 to 60% for DKPP5 and DKPP7, no polymerization could be detected for DKPP9-DKPP11. DKPP1 proved to be an exceptional photoinitiator since a BisGMA/TEGDMA conversion comparable to that obtained with camphorquinone (0.5 wt%) could be determined while using a photoinitiator content as low as 0.016 wt% in the three-component DKPP/Iod/EDB system. Interestingly, replacement of Iod by R-Cl in the three-component photoinitiating system enabled to greatly improve the monomer conversion. Thus, upon irradiation at 470 nm, the DKPP1/EDB/R-Cl (0.5%/2%/2% w/w/w) system furnished a conversion of 50% after 400 s of irradiation whereas the conversion achieved with the DKPP1/EDB/Iod2 (0.5%/2%/2% w/w/w) was limited to 40%.

Table 6. Final methacrylate function conversions (FC) (for a BisGMA/TEGDMA blend) obtained in laminate upon irradiation with two visible light sources and using different three-component DKPP/Iod/EDB (0.5/2/2% w/w/w) photoinitiating systems.

PIS	LED@470 nm	LED@520 nm
DKPP1/Iod/EDB	47 %	50 %
DKPP2/Iod/EDB		30 %
DKPP3/Iod/EDB		40 %
DKPP4/Iod/EDB		10 %
DKPP5/Iod/EDB	60 %	
DKPP6/Iod/EDB	57 %	
DKPP7/Iod/EDB	60 %	
DKPP8/Iod/EDB	46 %	n.p.
DKPP9/Iod/EDB	n.p.	n.p.
DKPP10/Iod/EDB		n.p.
DKPP11/Iod/EDB		n.p.

n.p. no polymerization.

Finally, good photobleaching properties could be evidenced with the different dyes, enabling to prepare colorless coatings (See Figure 23). This property is actively researched, especially for visible-light photoinitiating systems since the photosensitizer is often a strongly colored molecule that can impose the color to the final coating.

Figure 23. Photographs before and after irradiation of a 100 μm BisGMA/TEGDMA thick film. polymerized by using the three-component DKPP1/Iod/EDB (0.016%/2%/2% w/w/w) system upon irradiation with a LED at 477 nm. Reprinted with permission of Bouzrati-Zerelli et al. [280]

To support the polymerization reaction, a mechanism comparable to that proposed for the previous DKPP was established, based on the combination of different experiments (photolysis experiments, EPR, …) (See equations r19-r28 in Scheme 2).

$DKPP \rightarrow {}^1DKPP\ (h\nu)$ (r19)

${}^1DKPP + Ph_2I^+ \rightarrow DKPP^{\bullet+} + Ph_2I^\bullet$ (r20)

$Ph_2I^\bullet \rightarrow Ph^\bullet + Ph\text{-}I$ (r21)

${}^1DKPP + R\text{-}Cl \rightarrow DKPP^{\bullet+} + (R\text{-}Cl)^{\bullet-}$ (r22)

${}^1DKPP + EDB \rightarrow DKPP^{\bullet-} + EDB^{\bullet+} \rightarrow DKPP\text{-}H^\bullet + EDB_{(-H)}{}^\bullet$ (r23)

$DKPP^{\bullet+} + EDB \rightarrow DKPP + EDB^{\bullet+} \rightarrow DKPP + EDB_{(-H)}{}^\bullet + H^+$ (r24)

$DKPP^{\bullet-} + R\text{-}Cl \rightarrow DKPP + (R\text{-}Cl)^{\bullet-}$ (r25)

$DKPP\text{-}H^\bullet + R\text{-}Cl \rightarrow DKPP + H^+ + (R\text{-}Cl)^{\bullet-}$ (r26)

$(R\text{-}Cl)^{\bullet-} \rightarrow R^\bullet + Cl^-$ (r27)

$DKPP\text{-}H^\bullet + Ph_2I^+ \rightarrow DKPP + H^+ + Ph^\bullet + Ph\text{-}I$ (r28)

Scheme 2. Chemical mechanisms occurring in the DKPP/Iod (r19-r21); DKPP/amine/R-Cl (r22-r27) DKPP/Iod/amine (r20-r21, r23-r24, r28) photoinitiating systems.

Recently, another family of pyrrolopyrrole derivatives was examined as photoinitiators of polymerization, namely 1,4-dihydropyrrolo[3,2-*b*]pyrroles.[284] Interestingly, this structure comprising two fused pyrrole units could be prepared in one step,

by condensation of 4-bromoaniline, 4-nitrobenzaldehyde and butane-2,3-dione in acetic acid, in the presence of a catalytic amount of *para*-toluenesulfonic acid. 1,4-*Bis*(4-bromophenyl)-2,5-bis(4-nitrophenyl)-1,4-dihydropyrrolo[3,2-b]pyrrole (PyBN) could be obtained in pure form in 30% yield (See Scheme 3). It has to be noticed that if these structures have been synthesized for the first time in 1972, 1,4-dihydropyrrolo[3,2-*b*]pyrroles have never been examined as visible light photoinitiators prior to this work.[285–289] Based on its broad absorption extending from 350 up to 550 nm and its absorption maximum located at 462 nm, polymerization tests were carried out at 365, 395 and 470 nm. Noticeably, PyBN could even initiate the FRP of TMPTA alone, evidencing its ability to act as a monocomponent system. Thus, a conversion as high as 90% could be obtained upon irradiation at 365 and 395 nm after 250 s. Conversely, upon irradiation at 470 nm, no polymerization of TMPTA was detected. These results were confirmed with 1,4-*bis*(4-bromophenyl)-2,5-di-p-tolyl-1,4-dihydropyrrolo[3,2-*b*]pyrrole (PyBC) for which no polymerization was also detected at 470 nm.

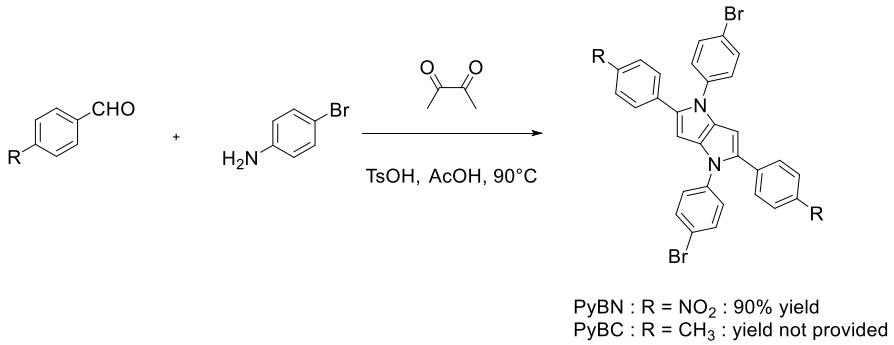

Scheme 3. Synthetic routes to PyBN and PyBC.

By combining nuclear magnetic resonance (NMR), electron paramagnetic resonance (EPR) and mass spectroscopy experiments, the conversion of the nitro groups of PyBN as carbonyl groups could be clearly evidenced. Thus, upon irradiation, nitro groups are converted as nitrite groups, enabling the generation of phenoxy radicals that can undergo a rearrangement to form carbonyl radicals (See Scheme 4).[290–293] Interestingly, comparisons of the photoinitiating ability of the two component PyBN/camphorquinone (CQ) (0.5%/1% w/w) and EDB/CQ (0.5%/1% w/w) system revealed the two systems to furnish similar monomer conversions at 470 nm for TMPTA, whereas no polymerization was detected for PyBN alone at this wavelength. PyBN can thus constitute an interesting substitute to EDB, enabling to generate efficient amine-free photoinitiating systems.

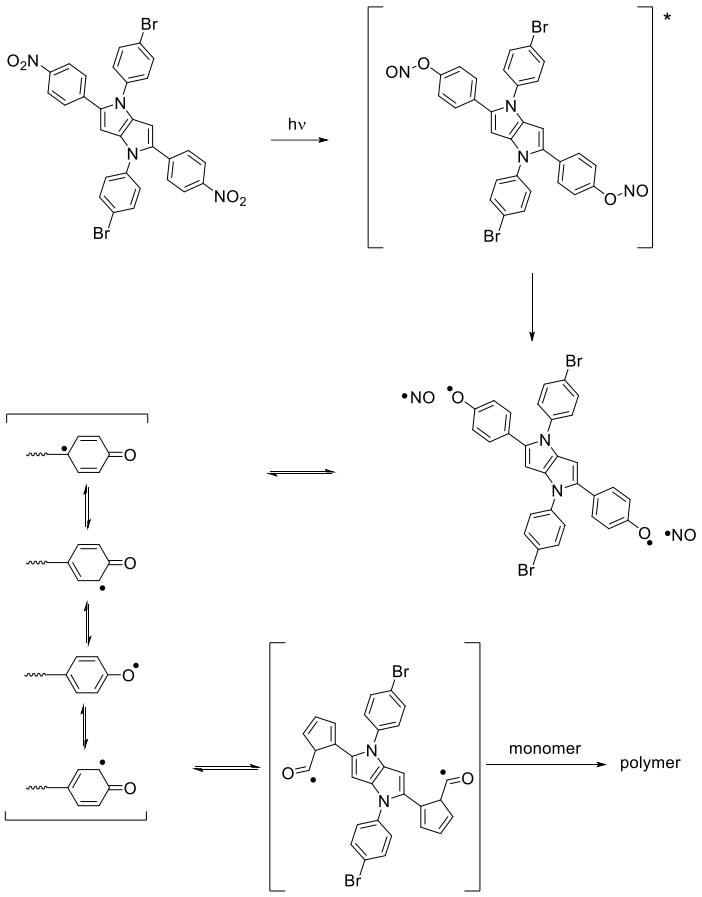

Scheme 4. photochemical mechanism involved in the polymerization of TMPTA with PyBN.

2.4. Porphyrins

Porphyrins are a class of aromatic heterocyclic compounds based on tetrapyrrole structures in which the four pyrrole rings are linked together by mean of methine carbon atoms.[294–296] As specificity, porphyrins strongly absorb in the visible range, making this family of dyes suitable candidates for photoinitiation. In this field, metal-based tetraphenylporphyrins are characterized by excellent light absorption properties for $\lambda > 400$ nm. The first report mentioning the use of porphyrins as photoinitiators was reported in 1994.[297] In this work, a living radical polymerization of methyl acrylate could be mediated by mean of a cobalt porphyrin i.e. cobalt(II) tetramesityl porphyrin (TMP)Co^{II}. Tetramesityl porphyrin (TMP)Co^{II} has been a popular porphyrin used for living radical polymerizations, as demonstrated by the numerous reports concerning this topic.[298–305] With aim at performing polymerization in water, water-soluble versions of (TMP)Co^{II} were developed, such as cobalt tetra(3,5-disulfonatomesityl)porphyrin (TMPS)Co^{II} or cobalt tetra(4-disulfonatomesityl)porphyrin (TMPS)Co^{II} (See Figure 24).[306] Another popular porphyrin is 5,10,15,20-tetraphenyl-21*H*,23*H*-porphyrin zinc (Zn(TPP)) which has been as a sensitizer for the photodecomposition of iodonium salts[307], or as a hydrophobic photoredox catalyst for the photoinduced electron/energy transfer-reversible addition-fragmentation chain transfer

(PET-RAFT) enabling to encapsulate the photocatalyst within hydrophobic nanoparticles.[308] The resulting nanoparticles soluble in water and containing Zn(TPP) showed promising properties in photodynamic therapy owing to their ability to generate singlet oxygen upon irradiation with visible light. More recently, Boyer and coworkers demonstrated that Zn(TPP) could activate the PET-RAFT polymerization of trithiocarbonates advantageously used for the polymerization of styrene, (meth)acrylates and (meth)acrylamides over a wide range of wavelengths (between 435 and 655 nm).[309] Following this work, boyer and coworkers used Chlorophyll a as an efficient photoredox catalyst to initiate an efficient photoinduced living radical polymerization process that could initiate a reversible addition-fragmentation chain transfer (RAFT) polymerization upon irradiation with blue or red LEDs.[310] Indeed, as shown in the Figure 25, Chlorophyll a exhibits two intense absorption bands at 461 nm and 635 nm, corresponding to the Soret and the Q-bands. Chlorophyll a is not the only biosourced porphyrin. Other examples of natural porphyrins such as hemoglobins, myoglobins and cytochromes can be cited as relevant examples.[311]

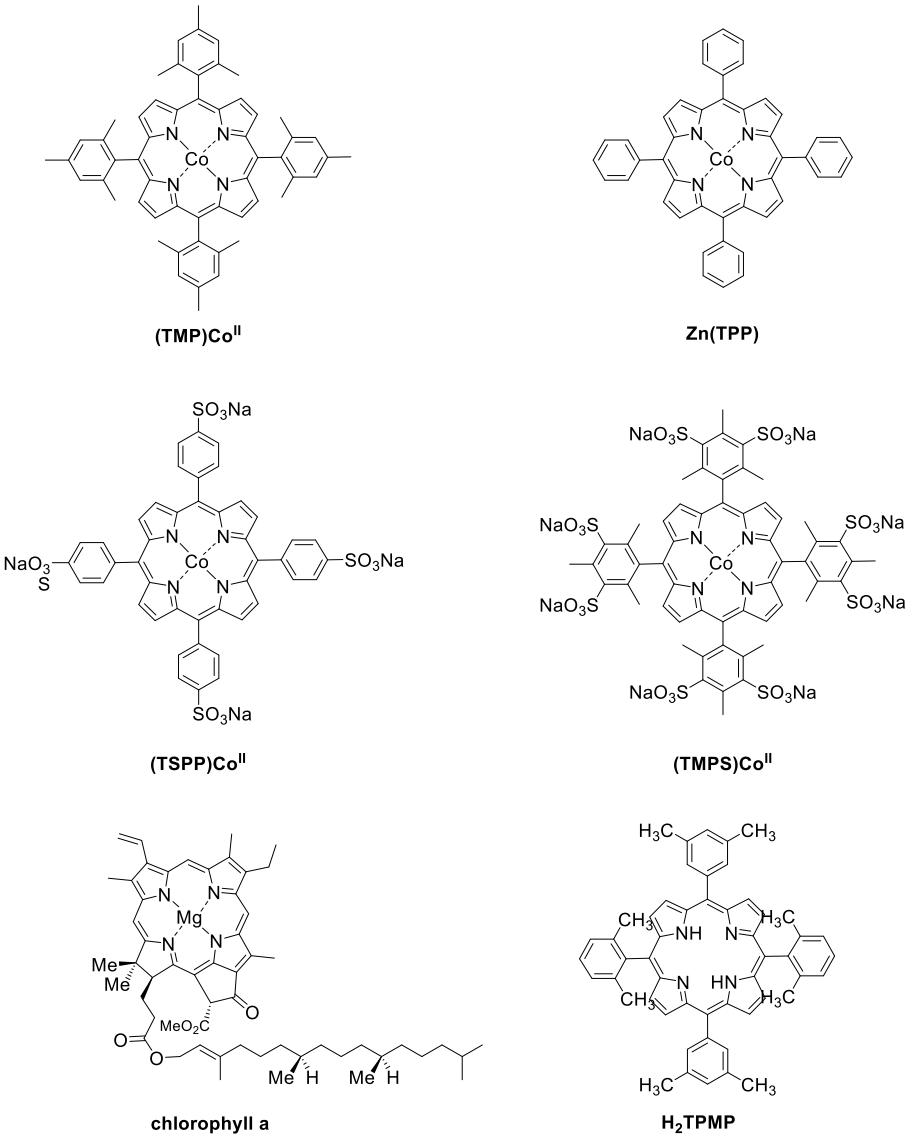

Figure 24. Chemical structures of various porphyrins.

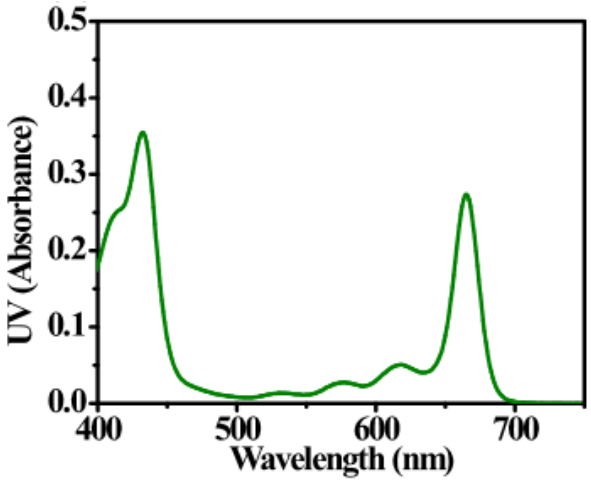

Figure 25. UV-visible absorption spectrum of Chlorophyll a in chloroform. Reproduced with permission from Shanmugam et al.[310] Copyright 2015 The Royal Society of Chemistry.

However, if the approach seems to be appealing, availability of Chlorophyll a remained limited since only 24 mg could be isolated in pure form from 100 g of spinach leaves. Additionnally, in order to be usable, Chlorophyll a has to be extracted for spinach leaves with the appropriate solvent and purified by column chromatography before use. Besides, the proof of concept that biosourced dyes could be used as photosensitizers was clearly demonstrated. If porphyrins were extensively used for the FRP of (meth)acrylates, the first investigations concerning the cationic polymerization of epoxides were only reported in 2017 by Lalevée and coworkers.[68] In this work, Zn(TPP) was jointly examined with 5,15-*bis*(2,6-dimethylphenyl)-10,20-*bis*(3,5-dimethylphenyl)porphyrin (H_2TPMP). As shown in the Figure 26, Zn(TPP) and H_2TPMP exhibited a broad absorption extending over the visible range. Interestingly, the two dyes had an intense absorption at 420 nm ε = 400 000 $M^{-1}.cm^{-1}$, corresponding to the Soret band.

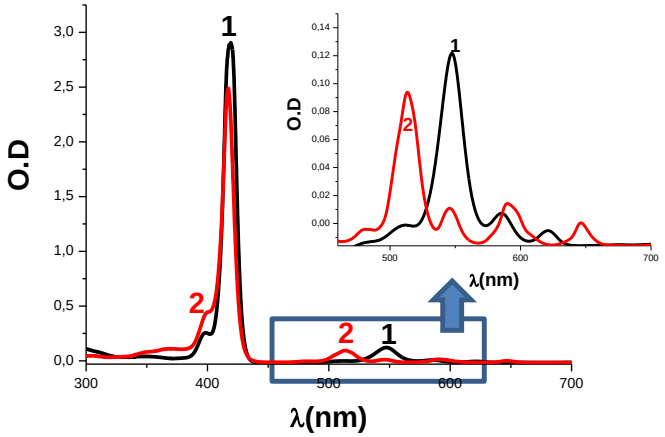

Figure 26. Absorption spectra of the investigated compounds in DCM: (1) Zn(TPP); (2) H_2TPMP. Reproduced with permission from Al Mousawi.[68] Copyright 2018 American Chemical Society

Based on the broad absorption of the two dyes, irradiations could be carried out at 405, 455, 477, and 530 nm. Interestingly, due to the presence of eight methyl groups, H_2TPMP exhibited a good solubility in EPOX. Examination of the CP of EPOX at 405 nm revealed the two-component Zn(TPP)/Iod (0.5%/1% w/w) system to furnish an EPOX conversion of 53% after 800 s. Reduction of the photoinitiator content to 0.3% gave almost similar monomer conversion (47%). Interestingly, reasonable monomer conversions were obtained at 455 and 530 nm (39 and 33% conversions respectively). An opposite situation was found for H_2TPMP. Indeed, irrespective of the irradiation wavelengths, no polymerization could be detected (See Table 7). Considering that Zn(TPP) and H_2TPMP exhibit similar absorption properties, it therefore evidences the crucial role of the metal center in Zn(TPP). Examination of the photochemical mechanism by ESR experiments revealed $Zn(TPP)^{\bullet+}$ to be the initiating species during the CP of EPOX. Indeed, ESR spectrum of $Zn(TPP)^{\bullet+}$ consisted in a broad line pattern at g = 2.0027 in full accordance with results previously reported in the literature. Overall, the mechanism depicted in equations r29 and r30 was proposed (See Scheme 5).[312]

$$Zn(TPP) \rightarrow {}^{*}Zn(TPP) \quad (h\nu) \qquad \text{(r29)}$$

$$^{*}Zn(TPP) + Ph_2I^{+} \rightarrow Zn(TPP)^{\bullet+} + Ph_2I^{\bullet} \rightarrow Zn(TPP)^{\bullet+} + Ph^{\bullet} + PhI \qquad \text{(r30)}$$

Scheme 5. Photochemical mechanism involving Zn(TPP)

Table 7. Final epoxy function conversion (FC) for the EPOX after 800s of irradiation at different irradiation wavelengths.

	Epoxy function conversion (FC) %	
	Zn(TPP)/Iod (thickness=25 μm) under air	H_2TPMP/Iod (thickness=25 μm) under air
LED@405nm	53% (0.5%/1% w/w); 47% (0.3%/1% w/w)	n.p. (0.5%/1% w/w)
LED@455nm	39% (0.3%/1% w/w)	n.p. (0.5%/1% w/w)
LED@530nm	33% (0.3%/1% w/w)	n.p. (0.5%/1% w/w)

n.p.: no polymerization

In 2020, the possibility to initiate polymerization processes by mean of a dual photochemical/photothermal approach was examined upon excitation in the near-infrared (NIR) region.[69] Indeed, near infrared (NIR) dyes are well-known to release heat upon photoexcitation, what can be advantageously used to initiate the decomposition of a thermal photoinitiator. It can thus provide a second and additional source of radicals that can be generated in situ, in complement to those formed by the photochemical mechanism, improving the overall monomer conversion. Light-triggered heat release of NIR dyes is well-established in the literature and used for numerous biomedical applications such as phototherapy or drug delivery.[313–315] In the context of photopolymerization, a series of six metalloporphyrins, namely Fe-Porph_1, Cu-Porph_2, Zn-Porph_2, Pd-Porph_2, Fe-Porph_2

and Zn-Porph_4 varying by the central metal cations was examined (See Figure 27). Besides, if six porphyrins were prepared, only three of them could be examined during the polymerization experiments, namely Fe-Porph_1, Zn-Porph_2 and Zn-Porph_4, the other porphyrins being not soluble in resins. Interestingly, if the different dyes exhibited a low absorption at 785 nm (Q band), polymerization experiments could however be carried out at this wavelength (See Figure 28).

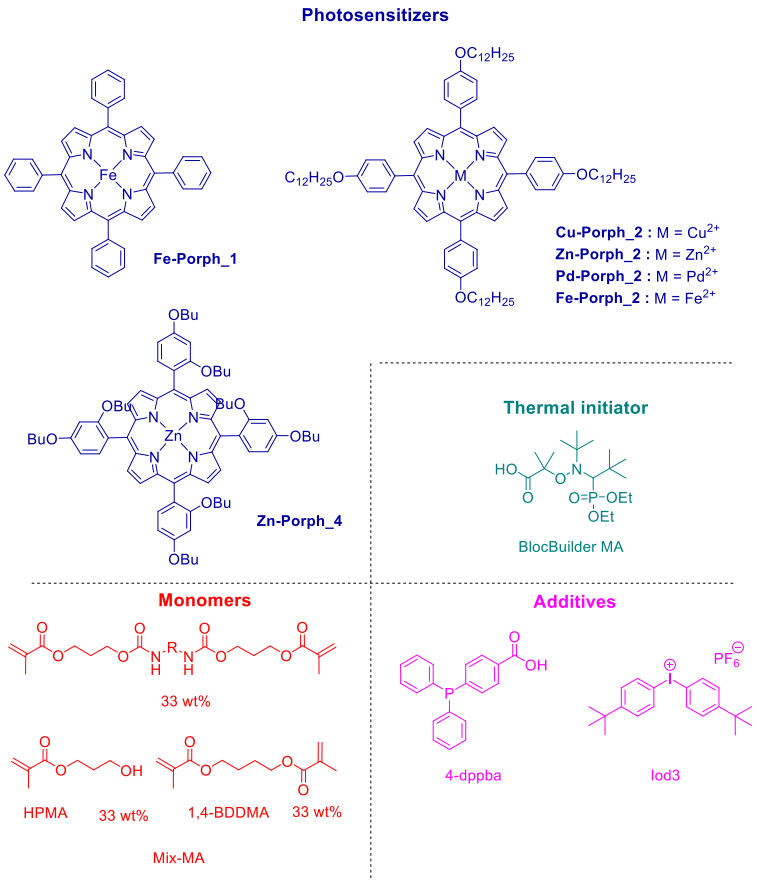

Figure 27. Chemical structures of porphyrins examined as heaters for photothermal effects.

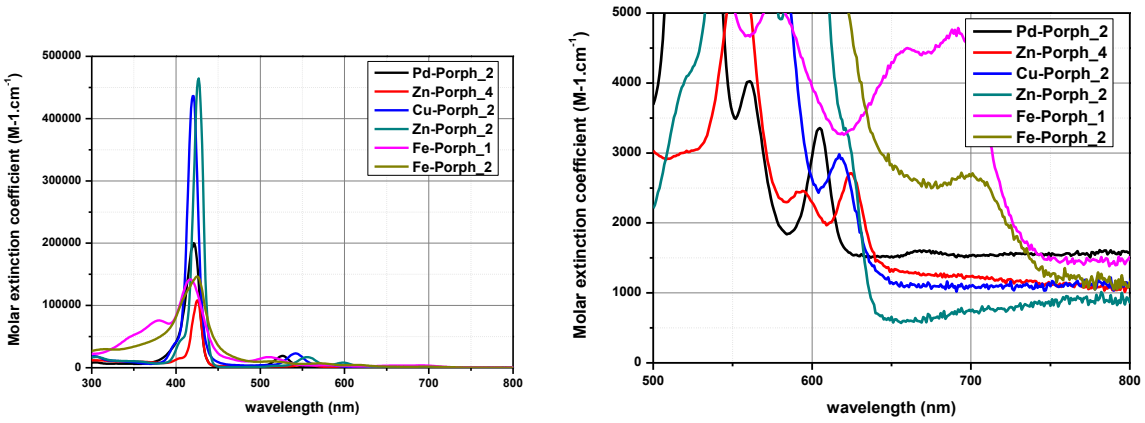

Figure 28. UV-visible absorption spectra of Fe-Porph_1, Cu-Porph_2, Zn-Porph_2, Pd-Porph_2, Fe-Porph_2 and Zn-Porph_4 in chloroform (top) expansion of the UV-visible absorption spectra of the same porphyrins in the 500-800 nm region. Reproduced with permission of Ref. [69].

Indeed, molar extinction coefficients higher than 1000 $L.mol^{-1}.cm^{-1}$ could be determined for Fe-Porph_1, Zn-Porph_2 and Zn-Porph_4, sufficient to initiate polymerization processes. As thermal initiator, a thermosensitive alkoxyamine i.e. 2-((*tert*-butyl(1-(diethoxyphosphoryl)-2,2-dimethylpropyl)amino)oxy)-2-methylpropanoic acid (blocbuilder® MA) was selected. This molecule is notably characterized by a low decomposition temperature ranging between 50 and 70 °C.[316] When tested in four-component dye/Iod3/2-dppba/blockbuilder® MA (0.1%/3%/2%/2% w/w/w/w) systems (where 4-dppba stands for 4-(diphenylphosphino)benzoic acid), long inhibition times could be determined during the FRP of a mixture of Mix-MA (Mix-Ma is a resin composed of three different monomers in a 33/33/33 (wt%/wt%/wt%) ratio, composed of HPMA (2-hydroxypropyl) methacrylate, 1,4-BDDMA (1,4-butanediol dimethacrylate) and UDMA (a urethane dimethacrylate)) upon irradiation at 785 nm, evidencing a strong oxygen inhibition despite the presence of 4-dppba (See Figure 29).

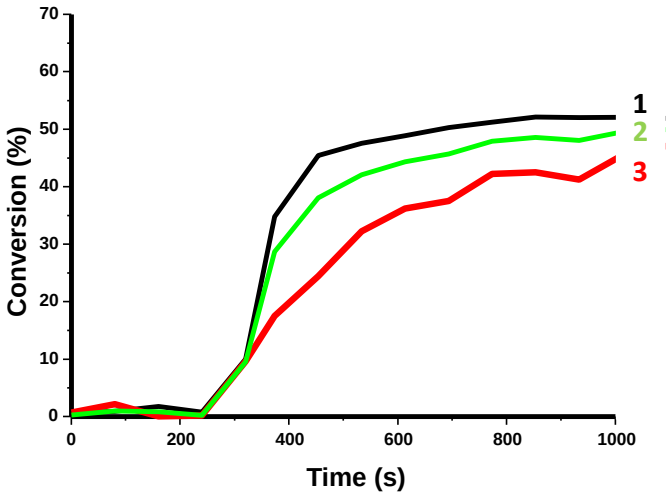

Figure 29. Photopolymerization profiles for Mix-MA in air (methacrylate function conversion vs. irradiation time) upon irradiation at 785 nm using four-component photoinitiating dye/Iod3/2-dppba/blockbuilder® MA (0.1%/3%/2%/2% w/w/w/w) systems using (1) Fe-Porph_1, (2) Zn-Porph_2 and (3) Zn-Porph_4, thickness = 1.4 mm. Reproduced with permission of Ref. [69].

Indeed, 2-dppba is a phosphine extensively used in photopolymerization due to its ability to reduce oxygen inhibition.[317,318] In the present case, an inhibition time of ca 200 s was however determined. After 1000 s of irradiation, a final monomer conversion of 55% could be obtained with Fe-Porph_1, higher than that obtained with Zn-Porph_4 (50%). Comparison of the monomer conversions obtained with/without blockbuilder® MA revealed a significant enhancement of the monomer conversion in the presence of the thermal initiator, increasing from 30% up to 50%. It thus clearly shows the contribution of the photothermal effect in the overall conversion. To support the enhancement of the monomer conversion in the presence of the thermal initiator, the mechanism depicted in equations r31-r37 was proposed. In fact, initiating radicals can be formed due to the concomitant presence of two mechanisms. First, the purely photochemical pathway enabled by photodecomposition of the iodonium salt to

generate aryl radicals (r32). Parallel to this, excitation of the NIR dye resulted in the release of heat (conversion of the NIR light into heat) within the photocurable resin, promoting the thermal decomposition of blockbuilder® MA. In fact, control experiments done with the NIR light source alone revealed the irradiation source to be unable to initiate the decomposition of blockbuilder® MA, demonstrating that the presence of the NIR dye was compulsory in order to convert light into heat. Owing to the non-radiative deactivation channels, the energy absorbed by dyes upon photoexcitation with the appropriate wavelength of light is released as heat. Parallel to this, polymerization of acrylates is also well-known to be exothermic, facilitating the elevation of temperature. Consequently, when the temperature is sufficient, the thermal initiator can decompose, furnishing an additional source of radicals (See equations r33-r34). Contribution of blockbuilder® MA in the polymerization process can notably be clearly detected at ca. 300 s of irradiation, a significant modification of the slopes being detected on the polymerization profile (See Figure 29). If 4-dppba enabled to reduce the oxidized photosensitizer, it also contributed to reduce oxygen inhibition by converting the non-initiating peroxy radicals (ROO•) as reactive alkoxy radicals (RO•) (see equations r35-r37, see Scheme 6).[319]

dye → *dye (hν)	(r31)
*dye + Ar_2I^+ → $dye^{•+}$ + Ar• + ArI	(r32)
*dye → dye + Δ	(r33)
Blocbuilder + Δ → free radicals	(r34)
ROO• + PAr_3 → ROO-P•Ar_3	(r35)
ROO-P•Ar_3 → RO• + O=PAr_3	(r36)
$dye^{•+}$ + PAr_3 → dye + $PAr_3^{•+}$	(r37)

Scheme 6. The different equations involved in the polymerization process.

Overall, efficiency of the dual photochemical/photothermally induced polymerization of Mix-MA at 785 nm is summarized in the Figure 30.

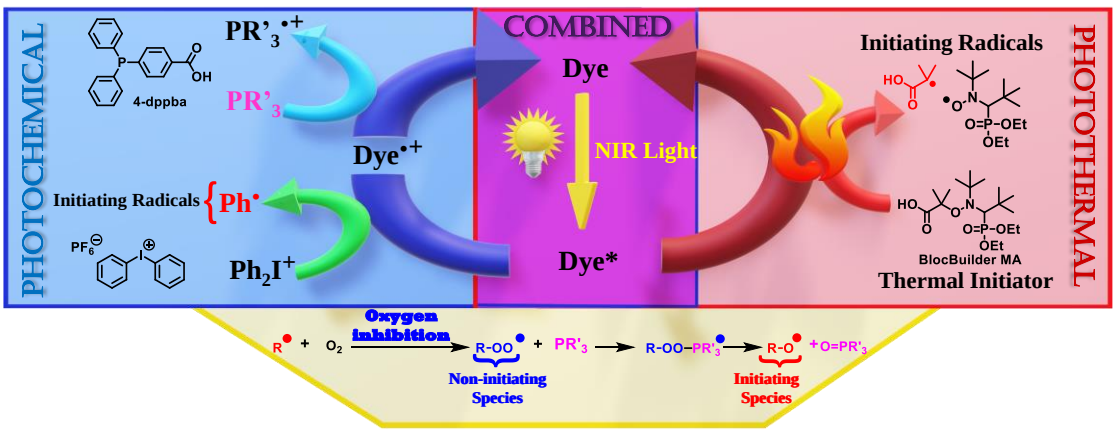

Figure 30. The dual photochemical and photothermal mechanism of polymerization. Reproduced with permission of Ref. [69].

2.5. Push-pull dyes

Push-pull dyes have been extensively used as photoinitiators of polymerization due to their easiness of synthesis, the facile tuneability of their absorption maxima and the excellent control of the molar extinction coefficient by mean of the π-conjugation length.[122,198–211] Typically, push-pull dyes are composed of an electron donor connected to an electron acceptor by mean of a conjugated spacer.[320,321] In 2020, pyrrole-based push-pull dyes were examined as photoinitiators capable to induce sunlight photopolymerization with three-component systems.[208] Sunlight-induced photopolymerization constitutes an appealing approach as Sun is a free and unlimited light source on Earth that could help to reduce energy consumption. Besides, if appealing, characteristics of sunlight are different from that of LEDs. Thus, Sun exhibits a much broader emission spectrum than those of LEDs. Light intensity of Sun is also lower than that of LEDs so that photoinitiators adapted for LED irradiations can be totally inefficient under sunlight.[322–324] In fact, sunlight is adapted for panchromatic photoinitiators. At present, availability of photoinitiators activable under sunlight remains scarce.[325–328] In 2020, Lalevée and coworkers examined a series of three pyrrole-based push-pull dyes and compared their photoinitiating abilities to that of thiophene-based analogues (See Figure 31). [208]

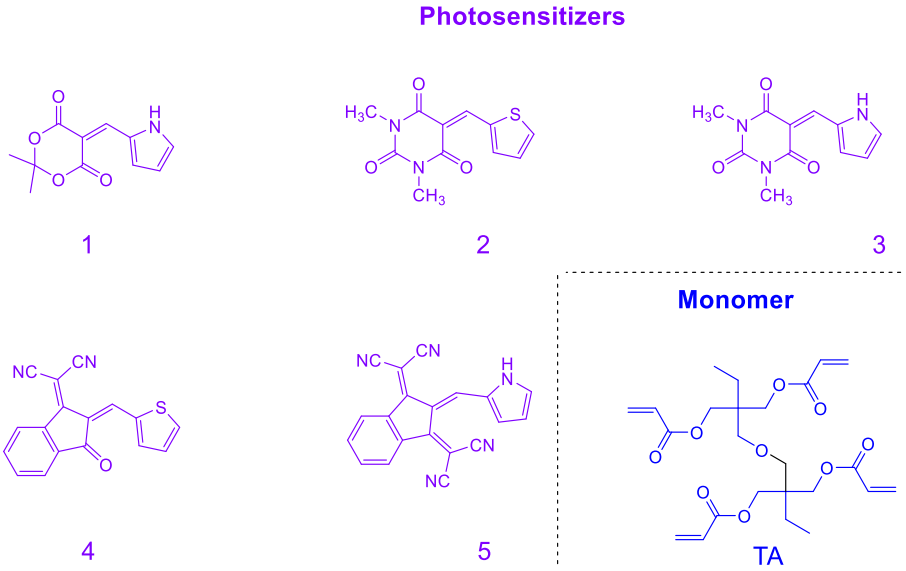

Figure 31. Chemical structures of push-pull dyes based on pyrrole.

Due to the fact that Meldrum acid is a weak electron acceptor, absorption maximum of dyes 1 remained located in the near UV-visible absorption range. Conversely, by using stronger electron acceptors, absorption maximum ranging from 404 nm for dye 3 to 473 nm

for dye 5. Interestingly, comparison of dye 2 and dye 3 that possess the same electron acceptor revealed pyrrole to be a stronger electron donor than thiophene. Indeed, absorption maxima located at 368 and 404 nm were respectively determined for dye 2 and dye 3 (See Table 8).

Table 8. Light absorption properties of the different push-pull dyes in acetonitrile: maximum absorption wavelengths λ_{max}; molar extinction coefficients at λ_{max} and extinction coefficients at the emission wavelength of the LED@405 nm.

	λ_{max} (nm)	ε_{max} ($M^{-1}.cm^{-1}$)	$\varepsilon_{@405nm}$ ($M^{-1}.cm^{-1}$)
Dye 1	391	50990	17680
Dye 2	368	27740	4010
Dye 3	404	55460	55350
Dye 4	430	28310	21820
Dye 5	473	10490	5990

Photopolymerization experiments of TA using three-component dye/Iod3/EDB (0.1%/2%/2% w/w/w) photoinitiating systems (PISs) upon irradiation with a LED at 405 nm revealed the monomer conversion to be extremely high for all pyrrole-based push-pull dyes. Thus, conversion ranging between 96% for dye 1 and dye 3 up to 98% for dye 5 could be determined after 400 s of irradiation at 405 nm. Interestingly, the thiophene-based dye i.e. dye 2 exhibits a significantly reduced photoinitiating ability than its pyrrole-based analogue (dye 3) since a reduction of the monomer conversion by ca. 23% could be determined for dye 2 (See Table 9). Low photoinitiating ability of the thiophene-based dye was confirmed with dye 4, furnishing a lower monomer conversion than all pyrrole-based dyes. Upon sunlight irradiation, an order of reactivity similar to that obtained with the LED emitting at 405 nm was found. Within 30 s, conversions as high 99, 95 and 92% for dye 1, 3 and 5 were determined, still using the same three-component system. Considering that these monomer conversions have been obtained during the winter during a cloudy day, it therefore demonstrated the full potential of pyrrole-based push-pull dyes as photoinitiators for sunlight irradiation during a sunny summer day. Due to the high reactivity of the dye 5-based three-component photoinitiating system, direct laser write experiments were carried out at 405 nm. As shown in the Figure 32a, 3D patterns exhibiting a remarkable spatial resolution with smooth surfaces could be obtained using TA as the monomer. Photocomposites could also be prepared by incorporating silica into the photocurable resin. By introducing 20% weight of silica fillers, 3D profiles with an excellent spatial resolution could also be obtained. Besides, due to a more limited light penetration within the resin, thinner 3D patterns were however obtained (See Figure 32b). The success access to photocomposites evidenced the remarkable photoinitiating abilities of pyrrole-based dyes and silica fillers-based photocomposites can be regarded as useful materials usable in additive manufacturing/vat photopolymerization.

Table 9. Summary of the monomer conversion determined at 405 nm and under sunlight for TA using three-component photoinitiating systems.

No.	Push-pull dyes	Conversion at 405 LED	Conversion at sunlight
1	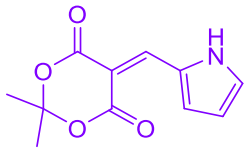	~96%	~99%
2	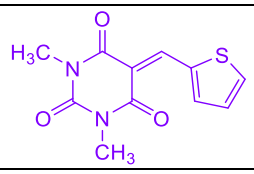	~73%	-
3	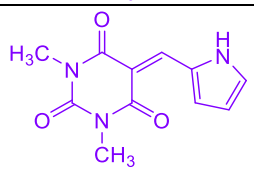	~96%	~95%
4	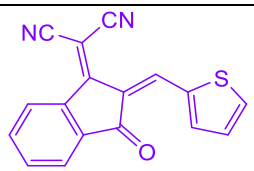	~85%	-
5	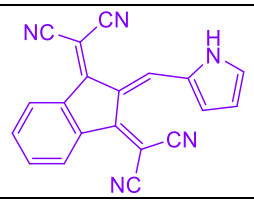	~98%	~92%

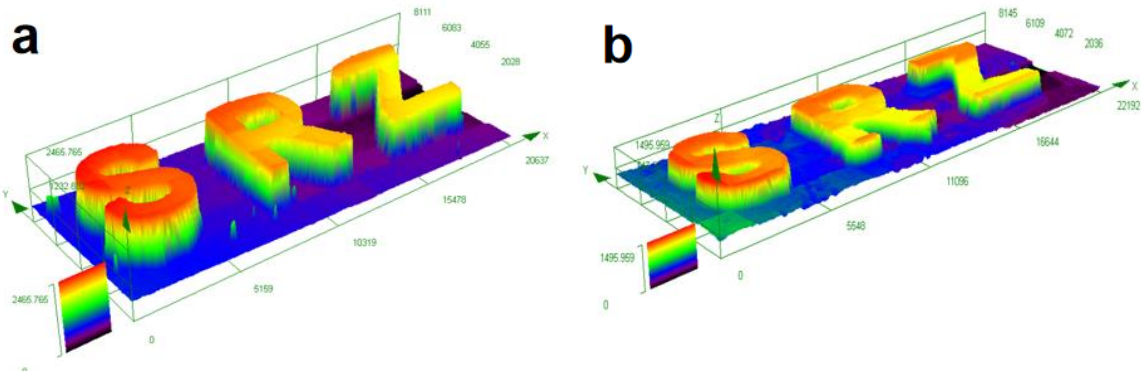

Figure 32. 3D patterns obtained by direct laser write experiments in TA. Characterization of the 3D patterns by numerical optical microscopy in the presence of: (a) dye 5/Iod3/EDB (0.1%/2%/2% in TA, w/w/w); (b) dye 5/Iod3/EDB/silica (0.1%/2%/2%/20% in TA, w/w/w/w). Reproduced with permission of Ref. [208]

2.6. 1,3,5-Triaryl-2-pyrazoline sulfonium salt photoacid generators

Photoacid generators (PAGs) are an important class of photoinitiators enabling to produce cationic reactive species upon absorption of light by the dye. In this field, sulfonium salts have been extensively studied due to their remarkable thermal stability in the dark and their remarkable ability to release Bronsted acids upon irradiation.[329–331] In 2021, four 1,5-diphenyl-3-aromatic heterocyclyl-2-pyrazoline based sulfonium salts were prepared by Wan and coworkers.[332] To examine the influence of the substitution pattern, a comparison between sulfonium salts varying by the pendant heterocycles was carried out, namely, thiophene, pyrrole and furane. In the case of thiophene-based sulfonium salts, isomers of positions were designed and synthesized, namely PAG-αS and PAG-βS (See Figure 33). For comparison, a benchmark PAG was used, namely diphenyl(4-(phenylthio)phenyl)sulfonium hexafluorophosphate (PAG-6992M).

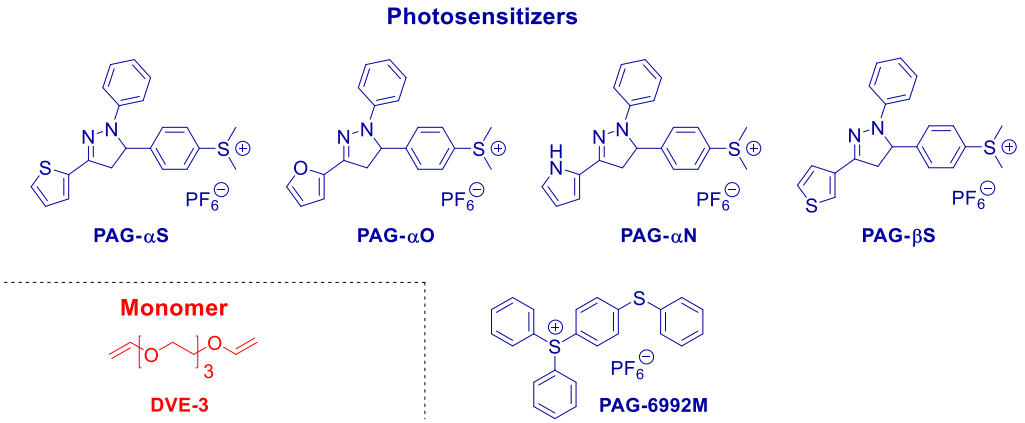

Figure 33. Chemical structures of sulfonium salts comprising different heterocycles.

Examination of the UV-visible absorption spectra of PAG-αS, PAG-αO, PAG-αN and PAG-βS revealed the absorption maxima of PAG-βS (λ_{max} = 333 nm), PAG-αN (λ_{max} = 339 nm), PAG-αO (λ_{max} = 344 nm) to be located in the same region. Conversely, a significant redshift was found for PAG-αS (λ_{max} = 364 nm) comprising a thiophene unit as substituent (See Figure 34). Noticeably, if PAG-βS, PAG-αN and PAG-αO showed almost similar molar extinction coefficients, a significant reduction of the molar extinction coefficient was found for PAG-αS (ε_{max}= 15 700 $M^{-1}.cm^{-1}$ vs. 17 500-17 900 $M^{-1}.cm^{-1}$ for PAG-βS, PAG-αN and PAG-αO).

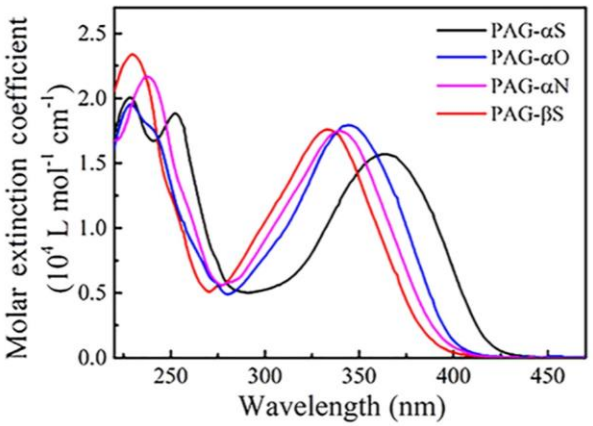

Figure 34. UV-visible absorption spectra of PAGs in acetonitrile. Reproduced with permission of Ref. [332]

Determination of the quantum yields of photoacid generation (Φ_{H^+}) for all sulfonium salts upon irradiation with a LED@385 nm revealed PAG-βS to furnish the highest quantum yield (0.72 vs 0.54, 0.66 and 0.69 for PAG-αS, PAG-αO, PAG-αN respectively). A molecular structure dependence of the photoacid generation quantum yields could thus be established. Notably, difference of photoacid generation ability was assigned to the photoinduced electron transfer (PET) efficiency from the π-conjugated systems towards the dimethylsulfonium moieties. By changing the irradiation wavelength from 365 to 385, 395, 405 and 425 nm, a severe reduction of the photoacid generation ability was determined. This is directly related to a reduction of the photon energy at longer wavelengths, rendering the cleavage of the S-C bond less efficient.

Examination of the photoinitiating ability of the different PAGs at five different wavelengths revealed the EPOX conversion to be highest at 385 nm, except for PAG-αO for which the conversion was higher at 395 nm (See Table 10). These results were confirmed during the CP of DVE-3 (See Table 11). While comparing the four PAGs, PAG-βS could furnish monomer conversions on par with that of the benchmark photoinitiator i.e. PAG-6992 M. PAG-βS proved also to be the most efficient PAG of the series, irrespective of the irradiation wavelength.

Table 10. EPOX conversions obtained with different PAGs (1 wt%) at different irradiation wavelengths.

	365 nm	385 nm	395 nm	405 nm	425 nm
PAG-αS	50.76	57.37	52.43	60.81	50.91
PAG-αO	52.23	58.82	64.04	58.57	38.26
PAG-αN	49.25	55.90	55.64	48.89	43.75
PAG-βS	59.00	62.09	59.94	48.89	38.55
PAG-6992 M	59.31	43.63	-	-	-

Table 11. DVE-3 conversions obtained with different PAGs (1 wt%) at different irradiation wavelengths.

	365 nm	385 nm	395 nm	405 nm	425 nm
PAG-αS	85.17	85.25			90.08
PAG-αO	89.38	94.74			77.89
PAG-αN	86.88	90.56			66.97
PAG-βS	93.03	96.79			61.79
PAG-6992 M	87.62	60.03			-

A summary of the different optical properties and the polymerization results is presented in the Table 12.

Table 12. Chemical structures, optical characteristics and summary of the polymerization results.

Dye	Chemical structure	Maximum absorption wavelength (nm)	Photoinitiating systems	Monomers	Light source	Monomer conversion	Ref.
2.1. chalcones							
BMO	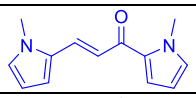	379	BMO/Iod (1%/3%, w/w)	EPOX	365 nm	60%	[162]
BMO	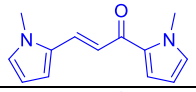	379	BMO/Iod (1%/3%, w/w)	HDDA	405 nm	80%	[162]
BMO	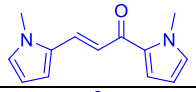	379	BMO/MDEA (1%/1% w/w)	HDDA	405 nm	74%	[162]
C6PY	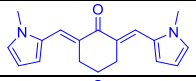	413	C6PY/Iod2 (0.1%/2% w/w)	TPGDA	405 nm	75%	[260]
C6NPY	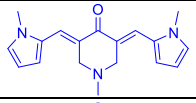	415	C6NPY/Iod2 (0.1%/2% w/w)	TPGDA	405 nm	89%	[260]
C6SPY	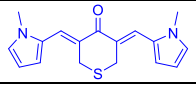	412	C6SPY/Iod2 (0.1%/2% w/w)	TPGDA	405 nm	55%	[260]
BPC	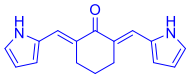	416	BPC/TEOA (0.0625%/3% w/w)	PEGDA	465 nm	70% at 120°C	[262]
BPC	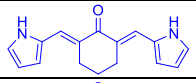	416	BPC/Iod3 (0.1%/2%, w/w)	Ebecryl 40	405 nm	55%	[262]
BPC	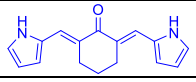	416	BPC/EDB (0.1%/2%, w/w)	Ebecryl 40	405 nm	40%	[262]
BPC	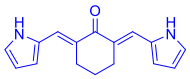	416	BPC/EDB/Iod3 (0.1%/2%/2%, w/w/w)	Ebecryl 40	405 nm	85%	[262]
BPC	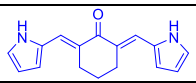	416	BPC/Iod3 (0.1%/2%, w/w)	EPOX	405 nm	70%	[262]
2.2. Penta-1,4-dien-3-ones							

C3PY	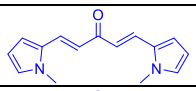	414	C3PY/TEOA (0.1%/3% w/w)	TMPTA	405 nm	39%	[265]
C3PY	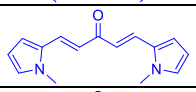	414	C3PY/Iod2 (0.1%/2% w/w)	TMPTA	405 nm	50%	[265]
C3PY	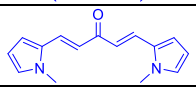	414	C3PY/TEOA (0.1%/3% w/w)	TPGDA	405 nm	91%	[265]
C3PY	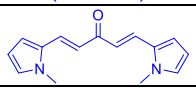	414	C3PY/Iod2 (0.1%/2% w/w)	TPGDA	405 nm	76%	[265]
C3ID	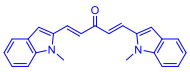	422	C3ID/TEOA (0.1%/3% w/w)	TPGDA	405 nm	84%	[265]
2.3. Diketopyrrolopyrroles and 1,4-dihydropyrrolo[3,2-b]pyrroles							
DPPDT	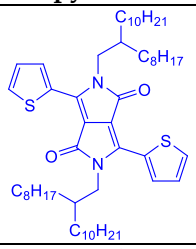	548	DPPDT/Iod (0.5%/2%, w/w)	EPOX	532 nm	29%	[98]
DPPDT	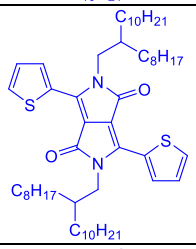	548	DPPDT/Iod/ NVK (0.5%/2%/3%, w/w/w)	EPOX	532 nm	31%	[98]
DPPDT	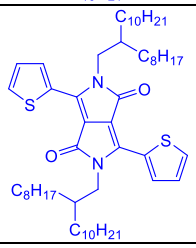	548	DPPDT/Iod (0.5%/2%, w/w)	DVE-3	532 nm	96%	[98]
DPPDT	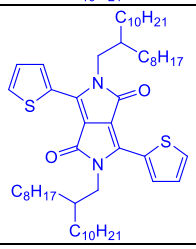	548	DPPDT/Iod/ NVK (0.5%/2%/3%, w/w/w)	TMPTA	532 nm	13%	[98]
DPPDT	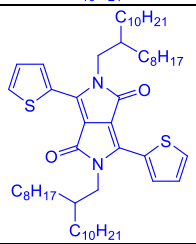	548	DPPDT/MDEA /R′-Cl (0.5%/2%/3%, w/w/w)	TMPTA	532 nm	38%	[98]
PDQT	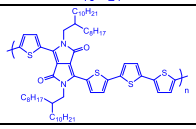	781	PDQT/Iod (0.5%/2%, w/w)	EPOX	532 nm	no polymerization	[98]

PDQT	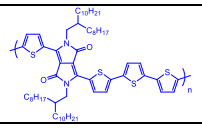	781	PDQT/Iod/NVK (0.5%/2%/3%, w/w/w)	EPOX	532 nm	no polymerization	[98]
DKPP2	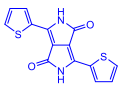	525	DKPP2/Iod/NVK (0.5%/2%/3%, w/w/w)	EPOX	532 nm	10%	[96]
FuDPP	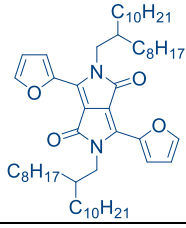	548	FuDPP/Iod/NVK (0.5%/2%/3%, w/w/w)	EPOX	532 nm	50%	[97]
FuDPP	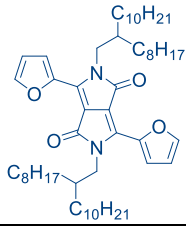	548	FuDPP/Iod/NVK (0.5%/2%/3%, w/w/w)	TMPTA	532 nm	23%	[97]
FuDPP	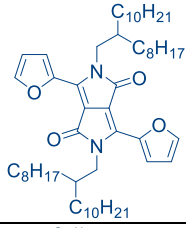	548	FuDPP/MDEA/R-Br (0.5%/2%/3%, w/w/w)	TMPTA	532 nm	15%	[97]
M2	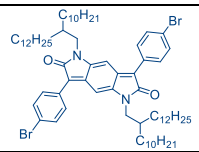	466	M2/Iod/NVK (0.5%/2%/3%, w/w/w)	EPOX	halogen lamp	7%	[97]
DKPP1	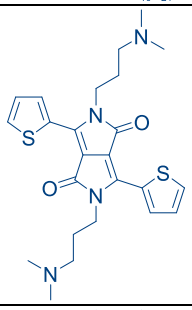	540	DKPP1/Iod/EDB (0.5/2/2% w/w/w)	BisGMA/TEGDMA	520 nm	50%	[280]
DKPP2	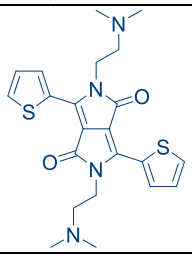	540	DKPP2/Iod/EDB (0.5/2/2% w/w/w)	BisGMA/TEGDMA	520 nm	30%	[280]

DKPP3	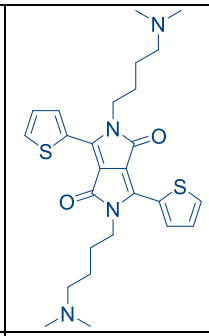	540	DKPP3/Iod/EDB (0.5/2/2% w/w/w)	BisGMA/TEGDMA	520 nm	40%	[280]
DKPP4	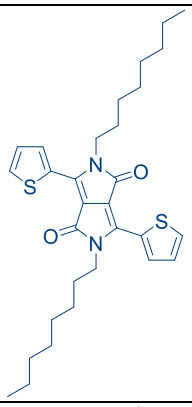	550	DKPP4/Iod/EDB (0.5/2/2% w/w/w)	BisGMA/TEGDMA	520 nm	10%	[280]
DKPP5	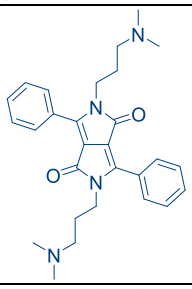	460	DKPP5/Iod/EDB (0.5/2/2% w/w/w)	BisGMA/TEGDMA	470 nm	60%	[280]
DKPP6	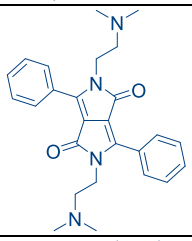	460	DKPP6/Iod/EDB (0.5/2/2% w/w/w)	BisGMA/TEGDMA	470 nm	57%	[280]
DKPP7	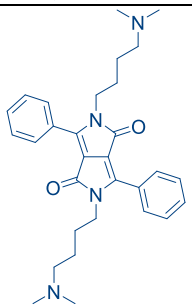	460	DKPP7/Iod/EDB (0.5/2/2% w/w/w)	BisGMA/TEGDMA	470 nm	60%	[280]
DKPP8	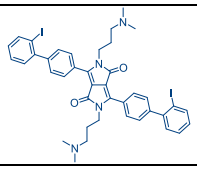	475	DKPP8/Iod/EDB (0.5/2/2% w/w/w)	BisGMA/TEGDMA	470 nm	46%	[280]

DKPP9	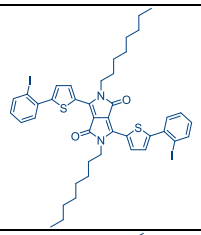	560	DKPP9/Iod/EDB (0.5/2/2% w/w/w)	BisGMA/TEGDMA	520 nm	no polymerization	[280]
DKPP10	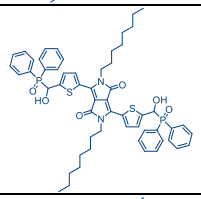	570	DKPP10/Iod/EDB (0.5/2/2% w/w/w)	BisGMA/TEGDMA	520 nm	no polymerization	[280]
DKPP11		585	DKPP11/Iod/EDB (0.5/2/2% w/w/w)	BisGMA/TEGDMA	520 nm	no polymerization	[280]
PyBN	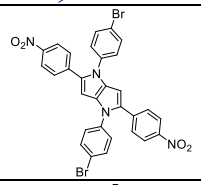	350-550	PyBN (0.5 %w)	TMPTA	365 nm	> 90%	[284]
PyBN	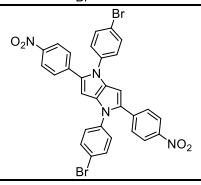	350-550	PyBN (0.5 %w)	TMPTA	395 nm	> 90%	[284]
2.4. Porphyrins							
Zn(TPP)	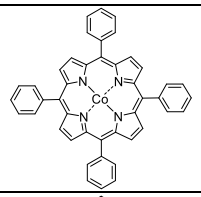	420	Zn(TPP)/Iod (0.5%/1% w/w)	EPOX	405 nm	53%	[68]
Zn(TPP)	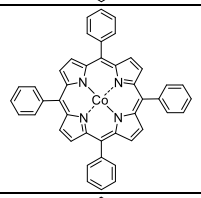	420	Zn(TPP)/Iod (0.3%/1% w/w)	EPOX	405 nm	47%	[68]
Zn(TPP)	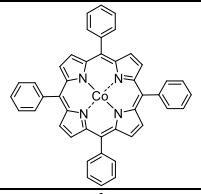	420	Zn(TPP)/Iod (0.3%/1% w/w)	EPOX	455 nm	39%	[68]
Zn(TPP)	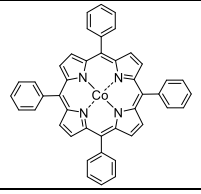	420	Zn(TPP)/Iod (0.3%/1% w/w)	EPOX	530 nm	33%	[68]

Fe-Porph_1	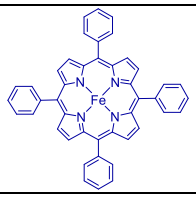	420	dye/Iod3/2-dppba/blockbuilder® MA (0.1%/3%/2%/2% w/w/w/w)	Mix-MA	785 nm	55%	[69]
Zn-Porph_2	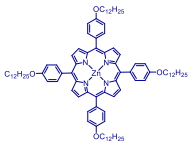	420	dye/Iod3/2-dppba/blockbuilder® MA (0.1%/3%/2%/2% w/w/w/w)	Mix-MA	785 nm	52%	[69]
Zn-Porph_4	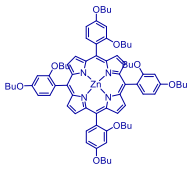	420	dye/Iod3/2-dppba/blockbuilder® MA (0.1%/3%/2%/2% w/w/w/w)	Mix-MA	785 nm	50%	[69]
2.5. Push-pull dyes							
1	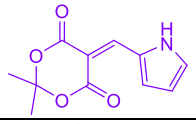	391	dye/Iod3/EDB (0.1%/2%/2% w/w/w)	TA	405 nm	96%	[208]
2	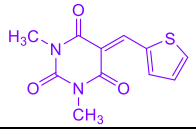	368	dye/Iod3/EDB (0.1%/2%/2% w/w/w)	TA	405 nm	73%	[208]
3	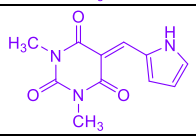	404	dye/Iod3/EDB (0.1%/2%/2% w/w/w)	TA	405 nm	96%	[208]
4	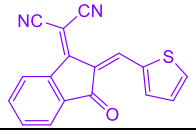	430	dye/Iod3/EDB (0.1%/2%/2% w/w/w)	TA	405 nm	85%	[208]
5	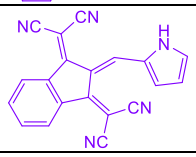	473	dye/Iod3/EDB (0.1%/2%/2% w/w/w)	TA	405 nm	98%	[208]
2.6. 1,3,5-Triaryl-2-pyrazoline sulfonium salt							
PAG-αS	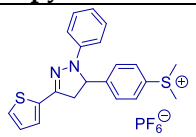	364	PAGs (1 wt%)	EPOX	405 nm	60.81	[332]
PAG-αO	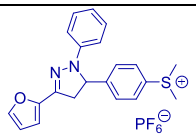	344	PAGs (1 wt%)	EPOX	405 nm	58.57	[332]
PAG-αN	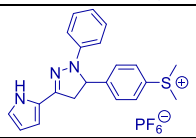	339	PAGs (1 wt%)	EPOX	405 nm	48.89	[332]
PAG-βS	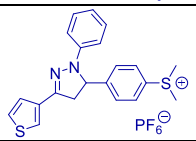	333	PAGs (1 wt%)	EPOX	405 nm	48.89	[332]

PAG-6992M	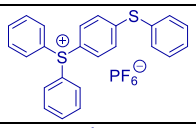	-	PAGs (1 wt%)	EPOX	405 nm	-	[332]
PAG-αS	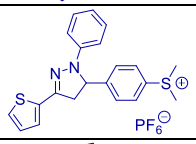	364	PAGs (1 wt%)	DVE-3	385 nm	85.25	[332]
PAG-αO	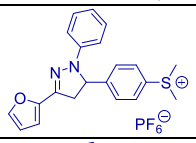	344	PAGs (1 wt%)	DVE-3	385 nm	94.74	[332]
PAG-αN	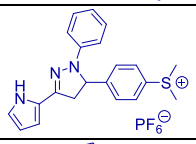	339	PAGs (1 wt%)	DVE-3	385 nm	90.56	[332]
PAG-βS	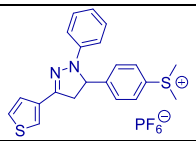	333	PAGs (1 wt%)	DVE-3	385 nm	96.79	[332]
PAG-6992M	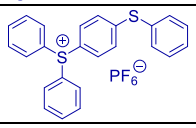	-	PAGs (1 wt%)	DVE-3	385 nm	60.03	[332]

Conclusion

To conclude, pyrrole is a versatile scaffold for the design of numerous dyes. Over the years, six different families of dyes have been prepared, namely, chalcones, enones, diketopyrrolopyrroles, 1,4-dihydropyrrolo[3,2-*b*]pyrroles, porphyrins, push-pull dyes and photoacid generators. As the most interesting results, photoinitiating systems capable to bleach have been prepared with diketopyrrolopyrroles. In the case of push-pull dyes, sunlight-induced polymerization could be performed, even during a cloudy day, demonstrating all the potential of pyrrole-based push-pull dyes. Besides, if remarkable polymerization results have been obtained with the different families of dyes, a great deal of efforts remains to be done with aim at simplifying the photocurable resins. Notably, no pyrrole-based Type I photoinitiators have been reported to date. In this field, the most accessible structures are undoubtedly oxime esters, which exhibit a good stability while combining an easiness of synthesis. Indeed, oxime esters can be simply obtained by esterification of the corresponding oximes with various acid chlorides in the presence of a base.[86,111,113,333–337] By developing such structures, it could pave the way towards a major simplification of the photocurable resins. The design of water-soluble dyes is also another challenge. Indeed, polymerization in water could give access to polymers prepared in greener polymerization conditions.

Acknowledgments

Aix Marseille University and the Centre National de la Recherche Scientifique (CNRS) are acknowledged for financial supports.

Conflicts of Interest

The authors declare no conflict of interest.

References

[1] J. Lalevée, H. Mokbel, J.-P. Fouassier, Recent Developments of Versatile Photoinitiating Systems for Cationic Ring Opening Polymerization Operating at Any Wavelengths and under Low Light Intensity Sources, Molecules. 20 (2015) 7201–7221. https://doi.org/10.3390/molecules20047201.

[2] M.A. Tehfe, F. Louradour, J. Lalevée, J.-P. Fouassier, Photopolymerization Reactions: On the Way to a Green and Sustainable Chemistry, Applied Sciences. 3 (2013) 490–514. https://doi.org/10.3390/app3020490.

[3] P. Xiao, J. Zhang, F. Dumur, M.A. Tehfe, F. Morlet-Savary, B. Graff, D. Gigmes, J.P. Fouassier, J. Lalevée, Visible light sensitive photoinitiating systems: Recent progress in cationic and radical photopolymerization reactions under soft conditions, Progress in Polymer Science. 41 (2015) 32–66. https://doi.org/10.1016/j.progpolymsci.2014.09.001.

[4] K. Sun, P. Xiao, F. Dumur, J. Lalevée, Organic dye-based photoinitiating systems for visible-light-induced photopolymerization, Journal of Polymer Science. 59 (2021) 1338–1389. https://doi.org/10.1002/pol.20210225.

[5] J. Lalevée, S. Telitel, P. Xiao, M. Lepeltier, F. Dumur, F. Morlet-Savary, D. Gigmes, J.-P. Fouassier, Metal and metal-free photocatalysts: mechanistic approach and application as photoinitiators of photopolymerization, Beilstein J. Org. Chem. 10 (2014) 863–876. https://doi.org/10.3762/bjoc.10.83.

[6] P. Xiao, F. Dumur, B. Graff, J.P. Fouassier, D. Gigmes, J. Lalevée, Cationic and Thiol–Ene Photopolymerization upon Red Lights Using Anthraquinone Derivatives as Photoinitiators, Macromolecules. 46 (2013) 6744–6750. https://doi.org/10.1021/ma401513b.

[7] M.-A. Tehfe, D. Gigmes, F. Dumur, D. Bertin, F. Morlet-Savary, B. Graff, J. Lalevée, J.-P. Fouassier, Cationic photosensitive formulations based on silyl radical chemistry for green and red diode laser exposure, Polym. Chem. 3 (2012) 1899–1902. https://doi.org/10.1039/C1PY00460C.

[8] P. Garra, C. Dietlin, F. Morlet-Savary, F. Dumur, D. Gigmes, J.-P. Fouassier, J. Lalevée, Redox two-component initiated free radical and cationic polymerizations: Concepts, reactions and applications, Progress in Polymer Science. 94 (2019) 33–56. https://doi.org/10.1016/j.progpolymsci.2019.04.003.

[9] Y. Zhang, Y. Xu, A. Simon-Masseron, J. Lalevée, Radical photoinitiation with LEDs and applications in the 3D printing of composites, Chem. Soc. Rev. 50 (2021) 3824–3841. https://doi.org/10.1039/D0CS01411G.

[10] F. Dumur, Recent Advances on Visible Light Metal-Based Photocatalysts for Polymerization under Low Light Intensity, Catalysts. 9 (2019). https://doi.org/10.3390/catal9090736.
[11] C. Pigot, G. Noirbent, D. Brunel, F. Dumur, Recent advances on push–pull organic dyes as visible light photoinitiators of polymerization, European Polymer Journal. 133 (2020) 109797. https://doi.org/10.1016/j.eurpolymj.2020.109797.
[12] P. Garra, C. Dietlin, F. Morlet-Savary, F. Dumur, D. Gigmes, J.-P. Fouassier, J. Lalevée, Photopolymerization processes of thick films and in shadow areas: a review for the access to composites, Polym. Chem. 8 (2017) 7088–7101. https://doi.org/10.1039/C7PY01778B.
[13] W. Tomal, J. Ortyl, Water-Soluble Photoinitiators in Biomedical Applications, Polymers. 12 (2020) 1073. https://doi.org/10.3390/polym12051073.
[14] N. Corrigan, J. Yeow, P. Judzewitsch, J. Xu, C. Boyer, Seeing the Light: Advancing Materials Chemistry through Photopolymerization, Angewandte Chemie International Edition. 58 (2019) 5170–5189. https://doi.org/10.1002/anie.201805473.
[15] A. Banerji, K. Jin, K. Liu, M.K. Mahanthappa, C.J. Ellison, Cross-Linked Nonwoven Fibers by Room-Temperature Cure Blowing and in Situ Photopolymerization, Macromolecules. 52 (2019) 6662–6672. https://doi.org/10.1021/acs.macromol.9b01002.
[16] G. Yilmaz, Y. Yagci, Light-induced step-growth polymerization, Progress in Polymer Science. 100 (2020) 101178. https://doi.org/10.1016/j.progpolymsci.2019.101178.
[17] M. Layani, X. Wang, S. Magdassi, Novel Materials for 3D Printing by Photopolymerization, Advanced Materials. 30 (2018) 1706344. https://doi.org/10.1002/adma.201706344.
[18] C. Dietlin, S. Schweizer, P. Xiao, J. Zhang, F. Morlet-Savary, B. Graff, J.-P. Fouassier, J. Lalevée, Photopolymerization upon LEDs: new photoinitiating systems and strategies, Polym. Chem. 6 (2015) 3895–3912. https://doi.org/10.1039/C5PY00258C.
[19] S. Shanmugam, J. Xu, C. Boyer, Photocontrolled Living Polymerization Systems with Reversible Deactivations through Electron and Energy Transfer, Macromolecular Rapid Communications. 38 (2017) 1700143. https://doi.org/10.1002/marc.201700143.
[20] F. Jasinski, P.B. Zetterlund, A.M. Braun, A. Chemtob, Photopolymerization in dispersed systems, Progress in Polymer Science. 84 (2018) 47–88. https://doi.org/10.1016/j.progpolymsci.2018.06.006.
[21] C. Noè, M. Hakkarainen, M. Sangermano, Cationic UV-Curing of Epoxidized Biobased Resins, Polymers. 13 (2021) 89. https://doi.org/10.3390/polym13010089.
[22] Y. Yuan, C. Li, R. Zhang, R. Liu, J. Liu, Low volume shrinkage photopolymerization system using hydrogen-bond-based monomers, Progress in Organic Coatings. 137 (2019) 105308. https://doi.org/10.1016/j.porgcoat.2019.105308.
[23] I.V. Khudyakov, J.C. Legg, M.B. Purvis, B.J. Overton, Kinetics of Photopolymerization of Acrylates with Functionality of 1−6, Ind. Eng. Chem. Res. 38 (1999) 3353–3359. https://doi.org/10.1021/ie990306i.
[24] S.H. Dickens, J.W. Stansbury, K.M. Choi, C.J.E. Floyd, Photopolymerization Kinetics of Methacrylate Dental Resins, Macromolecules. 36 (2003) 6043–6053. https://doi.org/10.1021/ma021675k.
[25] A. Maffezzoli, A.D. Pietra, S. Rengo, L. Nicolais, G. Valletta, Photopolymerization of dental composite matrices, Biomaterials. 15 (1994) 1221–1228. https://doi.org/10.1016/0142-9612(94)90273-9.

[26] T. Dikova, J. Maximov, V. Todorov, G. Georgiev, V. Panov, Optimization of Photopolymerization Process of Dental Composites, Processes. 9 (2021) 779. https://doi.org/10.3390/pr9050779.
[27] A. Andreu, P.-C. Su, J.-H. Kim, C.S. Ng, S. Kim, I. Kim, J. Lee, J. Noh, A.S. Subramanian, Y.-J. Yoon, 4D printing materials for vat photopolymerization, Additive Manufacturing. 44 (2021) 102024. https://doi.org/10.1016/j.addma.2021.102024.
[28] H. Chen, G. Noirbent, Y. Zhang, K. Sun, S. Liu, D. Brunel, D. Gigmes, B. Graff, F. Morlet-Savary, P. Xiao, F. Dumur, J. Lalevée, Photopolymerization and 3D/4D applications using newly developed dyes: Search around the natural chalcone scaffold in photoinitiating systems, Dyes and Pigments. 188 (2021) 109213. https://doi.org/10.1016/j.dyepig.2021.109213.
[29] A. Bagheri, J. Jin, Photopolymerization in 3D Printing, ACS Appl. Polym. Mater. 1 (2019) 593–611. https://doi.org/10.1021/acsapm.8b00165.
[30] B.K. Armstrong, A. Kricker, The epidemiology of UV induced skin cancer, Journal of Photochemistry and Photobiology B: Biology. 63 (2001) 8–18. https://doi.org/10.1016/S1011-1344(01)00198-1.
[31] F.R. de Gruijl, Skin cancer and solar UV radiation, European Journal of Cancer. 35 (1999) 2003–2009. https://doi.org/10.1016/S0959-8049(99)00283-X.
[32] D.L. Narayanan, R.N. Saladi, J.L. Fox, Review: Ultraviolet radiation and skin cancer, International Journal of Dermatology. 49 (2010) 978–986. https://doi.org/10.1111/j.1365-4632.2010.04474.x.
[33] J. Shao, Y. Huang, Q. Fan, Visible light initiating systems for photopolymerization: status, development and challenges, Polym. Chem. 5 (2014) 4195–4210. https://doi.org/10.1039/C4PY00072B.
[34] F. Petko, A. Świeży, J. Ortyl, Photoinitiating systems and kinetics of frontal photopolymerization processes – the prospects for efficient preparation of composites and thick 3D structures, Polym. Chem. 12 (2021) 4593–4612. https://doi.org/10.1039/D1PY00596K.
[35] A.H. Bonardi, F. Dumur, T.M. Grant, G. Noirbent, D. Gigmes, B.H. Lessard, J.-P. Fouassier, J. Lalevée, High Performance Near-Infrared (NIR) Photoinitiating Systems Operating under Low Light Intensity and in the Presence of Oxygen, Macromolecules. 51 (2018) 1314–1324. https://doi.org/10.1021/acs.macromol.8b00051.
[36] M.-A. Tehfe, F. Dumur, E. Contal, B. Graff, F. Morlet-Savary, D. Gigmes, J.-P. Fouassier, J. Lalevée, New insights into radical and cationic polymerizations upon visible light exposure: role of novel photoinitiator systems based on the pyrene chromophore, Polym. Chem. 4 (2013) 1625–1634. https://doi.org/10.1039/C2PY20950K.
[37] S. Telitel, F. Dumur, T. Faury, B. Graff, M.-A. Tehfe, D. Gigmes, J.-P. Fouassier, J. Lalevée, New core-pyrene π structure organophotocatalysts usable as highly efficient photoinitiators, Beilstein J. Org. Chem. 9 (2013) 877–890. https://doi.org/10.3762/bjoc.9.101.
[38] N. Uchida, H. Nakano, T. Igarashi, T. Sakurai, Nonsalt 1-(arylmethyloxy)pyrene photoinitiators capable of initiating cationic polymerization, Journal of Applied Polymer Science. 131 (2014). https://doi.org/10.1002/app.40510.
[39] A. Mishra, S. Daswal, 1-(Bromoacetyl)pyrene, a novel photoinitiator for the copolymerization of styrene and methylmethacrylate, Radiation Physics and Chemistry. 75 (2006) 1093–1100. https://doi.org/10.1016/j.radphyschem.2006.01.013.

[40] M.-A. Tehfe, F. Dumur, B. Graff, F. Morlet-Savary, D. Gigmes, J.-P. Fouassier, J. Lalevée, Design of new Type I and Type II photoinitiators possessing highly coupled pyrene–ketone moieties, Polym. Chem. 4 (2013) 2313–2324. https://doi.org/10.1039/C3PY21079K.
[41] F. Dumur, Recent advances on pyrene-based photoinitiators of polymerization, European Polymer Journal. 126 (2020) 109564. https://doi.org/10.1016/j.eurpolymj.2020.109564.
[42] M.-A. Tehfe, F. Dumur, N. Vilà, B. Graff, C.R. Mayer, J.P. Fouassier, D. Gigmes, J. Lalevée, A Multicolor Photoinitiator for Cationic Polymerization and Interpenetrated Polymer Network Synthesis: 2,7-Di-tert-butyldimethyldihydropyrene, Macromolecular Rapid Communications. 34 (2013) 1104–1109. https://doi.org/10.1002/marc.201300302.
[43] S. Telitel, F. Dumur, D. Gigmes, B. Graff, J.P. Fouassier, J. Lalevée, New functionalized aromatic ketones as photoinitiating systems for near visible and visible light induced polymerizations, Polymer. 54 (2013) 2857–2864. https://doi.org/10.1016/j.polymer.2013.03.062.
[44] B. Corakci, S.O. Hacioglu, L. Toppare, U. Bulut, Long wavelength photosensitizers in photoinitiated cationic polymerization: The effect of quinoxaline derivatives on photopolymerization, Polymer. 54 (2013) 3182–3187. https://doi.org/10.1016/j.polymer.2013.04.008.
[45] P. Xiao, F. Dumur, D. Thirion, S. Fagour, A. Vacher, X. Sallenave, F. Morlet-Savary, B. Graff, J.P. Fouassier, D. Gigmes, J. Lalevée, Multicolor Photoinitiators for Radical and Cationic Polymerization: Monofunctional vs Polyfunctional Thiophene Derivatives, Macromolecules. 46 (2013) 6786–6793. https://doi.org/10.1021/ma401389t.
[46] N. Zivic, M. Bouzrati-Zerrelli, S. Villotte, F. Morlet-Savary, C. Dietlin, F. Dumur, D. Gigmes, J.P. Fouassier, J. Lalevée, A novel naphthalimide scaffold based iodonium salt as a one-component photoacid/photoinitiator for cationic and radical polymerization under LED exposure, Polym. Chem. 7 (2016) 5873–5879. https://doi.org/10.1039/C6PY01306F.
[47] H. Mokbel, J. Toufaily, T. Hamieh, F. Dumur, D. Campolo, D. Gigmes, J.P. Fouassier, J. Ortyl, J. Lalevée, Specific cationic photoinitiators for near UV and visible LEDs: Iodonium versus ferrocenium structures, Journal of Applied Polymer Science. 132 (2015). https://doi.org/10.1002/app.42759.
[48] S. Villotte, D. Gigmes, F. Dumur, J. Lalevée, Design of Iodonium Salts for UV or Near-UV LEDs for Photoacid Generator and Polymerization Purposes, Molecules. 25 (2020) 149. https://doi.org/10.3390/molecules25010149.
[49] M.A. Tasdelen, V. Kumbaraci, S. Jockusch, N.J. Turro, N. Talinli, Y. Yagci, Photoacid Generation by Stepwise Two-Photon Absorption: Photoinitiated Cationic Polymerization of Cyclohexene Oxide by Using Benzodioxinone in the Presence of Iodonium Salt, Macromolecules. 41 (2008) 295–297. https://doi.org/10.1021/ma7023649.
[50] J.V. Crivello, J.H.W. Lam, Diaryliodonium Salts. A New Class of Photoinitiators for Cationic Polymerization, Macromolecules. 10 (1977) 1307–1315. https://doi.org/10.1021/ma60060a028.
[51] Y. He, W. Zhou, F. Wu, M. Li, E. Wang, Photoreaction and photopolymerization studies on squaraine dyes/iodonium salts combination, Journal of Photochemistry and Photobiology A: Chemistry. 162 (2004) 463–471. https://doi.org/10.1016/S1010-6030(03)00390-3.

[52] L.I. Jun, L.I. Miaozhen, S. Huaihai, Y. Yongyuan, W. Erjian, Photopolymerization Initiated by Dimethylaminochalcone/Diphenyliodonium Salt Combination System Sensitive to Visible Light, Chinese J. Polym. Sci. 11 (1993) 163–170.
[53] N. Zivic, P.K. Kuroishi, F. Dumur, D. Gigmes, A.P. Dove, H. Sardon, Recent Advances and Challenges in the Design of Organic Photoacid and Photobase Generators for Polymerizations, Angewandte Chemie International Edition. 58 (2019) 10410–10422. https://doi.org/10.1002/anie.201810118.
[54] A.A. Mousawi, F. Dumur, P. Garra, J. Toufaily, T. Hamieh, F. Goubard, T.-T. Bui, B. Graff, D. Gigmes, J.P. Fouassier, J. Lalevée, Azahelicenes as visible light photoinitiators for cationic and radical polymerization: Preparation of photoluminescent polymers and use in high performance LED projector 3D printing resins, Journal of Polymer Science Part A: Polymer Chemistry. 55 (2017) 1189–1199. https://doi.org/10.1002/pola.28476.
[55] A. Al Mousawi, M. Schmitt, F. Dumur, J. Ouyang, L. Favereau, V. Dorcet, N. Vanthuyne, P. Garra, J. Toufaily, T. Hamieh, B. Graff, J.P. Fouassier, D. Gigmes, J. Crassous, J. Lalevée, Visible Light Chiral Photoinitiator for Radical Polymerization and Synthesis of Polymeric Films with Strong Chiroptical Activity, Macromolecules. 51 (2018) 5628–5637. https://doi.org/10.1021/acs.macromol.8b01085.
[56] J. Lalevée, M. Peter, F. Dumur, D. Gigmes, N. Blanchard, M.-A. Tehfe, F. Morlet-Savary, J.P. Fouassier, Subtle Ligand Effects in Oxidative Photocatalysis with Iridium Complexes: Application to Photopolymerization, Chemistry – A European Journal. 17 (2011) 15027–15031. https://doi.org/10.1002/chem.201101445.
[57] J. Lalevée, M.-A. Tehfe, F. Dumur, D. Gigmes, N. Blanchard, F. Morlet-Savary, J.P. Fouassier, Iridium Photocatalysts in Free Radical Photopolymerization under Visible Lights, ACS Macro Lett. 1 (2012) 286–290. https://doi.org/10.1021/mz2001753.
[58] J. Lalevée, F. Dumur, C.R. Mayer, D. Gigmes, G. Nasr, M.-A. Tehfe, S. Telitel, F. Morlet-Savary, B. Graff, J.P. Fouassier, Photopolymerization of N-Vinylcarbazole Using Visible-Light Harvesting Iridium Complexes as Photoinitiators, Macromolecules. 45 (2012) 4134–4141. https://doi.org/10.1021/ma3005229.
[59] M.-A. Tehfe, M. Lepeltier, F. Dumur, D. Gigmes, J.-P. Fouassier, J. Lalevée, Structural Effects in the Iridium Complex Series: Photoredox Catalysis and Photoinitiation of Polymerization Reactions under Visible Lights, Macromolecular Chemistry and Physics. 218 (2017) 1700192. https://doi.org/10.1002/macp.201700192.
[60] S. Telitel, F. Dumur, S. Telitel, O. Soppera, M. Lepeltier, Y. Guillaneuf, J. Poly, F. Morlet-Savary, P. Fioux, J.-P. Fouassier, D. Gigmes, J. Lalevée, Photoredox catalysis using a new iridium complex as an efficient toolbox for radical, cationic and controlled polymerizations under soft blue to green lights, Polym. Chem. 6 (2014) 613–624. https://doi.org/10.1039/C4PY01358A.
[61] S. Telitel, F. Dumur, M. Lepeltier, D. Gigmes, J.-P. Fouassier, J. Lalevée, Photoredox process induced polymerization reactions: Iridium complexes for panchromatic photoinitiating systems, Comptes Rendus Chimie. 19 (2016) 71–78. https://doi.org/10.1016/j.crci.2015.06.016.
[62] F. Dumur, D. Bertin, D. Gigmes, Iridium (III) complexes as promising emitters for solid–state Light–Emitting Electrochemical Cells (LECs), International Journal of Nanotechnology. 9 (2012) 377–395. https://doi.org/10.1504/IJNT.2012.045343.
[63] F. Dumur, G. Nasr, G. Wantz, C.R. Mayer, E. Dumas, A. Guerlin, F. Miomandre, G. Clavier, D. Bertin, D. Gigmes, Cationic iridium complex for the design of soft salt-

based phosphorescent OLEDs and color-tunable light-emitting electrochemical cells, Organic Electronics. 12 (2011) 1683–1694. https://doi.org/10.1016/j.orgel.2011.06.014.
[64] N. Giacoletto, M. Ibrahim-Ouali, F. Dumur, Recent advances on squaraine-based photoinitiators of polymerization, European Polymer Journal. 150 (2021) 110427. https://doi.org/10.1016/j.eurpolymj.2021.110427.
[65] P. Xiao, F. Dumur, T.T. Bui, F. Goubard, B. Graff, F. Morlet-Savary, J.P. Fouassier, D. Gigmes, J. Lalevée, Panchromatic Photopolymerizable Cationic Films Using Indoline and Squaraine Dye Based Photoinitiating Systems, ACS Macro Lett. 2 (2013) 736–740. https://doi.org/10.1021/mz400316y.
[66] V. Launay, A. Caron, G. Noirbent, D. Gigmes, F. Dumur, J. Lalevée, NIR Organic Dyes as Innovative Tools for Reprocessing/Recycling of Plastics: Benefits of the Photothermal Activation in the Near-Infrared Range, Advanced Functional Materials. 31 (2021) 2006324. https://doi.org/10.1002/adfm.202006324.
[67] A. Bonardi, F. Bonardi, G. Noirbent, F. Dumur, C. Dietlin, D. Gigmes, J.-P. Fouassier, J. Lalevée, Different NIR dye scaffolds for polymerization reactions under NIR light, Polym. Chem. 10 (2019) 6505–6514. https://doi.org/10.1039/C9PY01447K.
[68] A. Al Mousawi, C. Poriel, F. Dumur, J. Toufaily, T. Hamieh, J.P. Fouassier, J. Lalevée, Zinc Tetraphenylporphyrin as High Performance Visible Light Photoinitiator of Cationic Photosensitive Resins for LED Projector 3D Printing Applications, Macromolecules. 50 (2017) 746–753. https://doi.org/10.1021/acs.macromol.6b02596.
[69] G. Noirbent, Y. Xu, A.-H. Bonardi, D. Gigmes, J. Lalevée, F. Dumur, Metalated porphyrins as versatile visible light and NIR photoinitiators of polymerization, European Polymer Journal. 139 (2020) 110019. https://doi.org/10.1016/j.eurpolymj.2020.110019.
[70] C. Brahmi, M. Benltifa, C. Vaulot, L. Michelin, F. Dumur, F. Millange, M. Frigoli, A. Airoudj, F. Morlet-Savary, L. Bousselmi, J. Lalevée, New hybrid MOF/polymer composites for the photodegradation of organic dyes, European Polymer Journal. 154 (2021) 110560. https://doi.org/10.1016/j.eurpolymj.2021.110560.
[71] J. Zhang, F. Dumur, P. Horcajada, C. Livage, P. Xiao, J.P. Fouassier, D. Gigmes, J. Lalevée, Iron-Based Metal-Organic Frameworks (MOF) as Photocatalysts for Radical and Cationic Polymerizations under Near UV and Visible LEDs (385–405 nm), Macromolecular Chemistry and Physics. 217 (2016) 2534–2540. https://doi.org/10.1002/macp.201600352.
[72] C. Brahmi, M. Benltifa, C. Vaulot, L. Michelin, F. Dumur, E. Gkaniatsou, C. Sicard, A. Airoudj, F. Morlet-Savary, L. Bousselmi, J. Lalevée, New Hybrid Fe-based MOFs/Polymer Composites for the Photodegradation of Organic Dyes, ChemistrySelect. 6 (2021) 8120–8132. https://doi.org/10.1002/slct.202102194.
[73] E.A. Kamoun, A. Winkel, M. Eisenburger, H. Menzel, Carboxylated camphorquinone as visible-light photoinitiator for biomedical application: Synthesis, characterization, and application, Arabian Journal of Chemistry. 9 (2016) 745–754. https://doi.org/10.1016/j.arabjc.2014.03.008.
[74] A. Santini, I.T. Gallegos, C.M. Felix, Photoinitiators in Dentistry: A Review, Prim Dent J. 2 (2013) 30–33. https://doi.org/10.1308/205016814809859563.
[75] M.-A. Tehfe, F. Dumur, S. Telitel, D. Gigmes, E. Contal, D. Bertin, F. Morlet-Savary, B. Graff, J.-P. Fouassier, J. Lalevée, Zinc-based metal complexes as new photocatalysts in polymerization initiating systems, European Polymer Journal. 49 (2013) 1040–1049. https://doi.org/10.1016/j.eurpolymj.2013.01.023.

[76] M. Abdallah, A. Hijazi, B. Graff, J.-P. Fouassier, G. Rodeghiero, A. Gualandi, F. Dumur, P.G. Cozzi, J. Lalevée, Coumarin derivatives as versatile photoinitiators for 3D printing, polymerization in water and photocomposite synthesis, Polym. Chem. 10 (2019) 872–884. https://doi.org/10.1039/C8PY01708E.
[77] M. Abdallah, F. Dumur, A. Hijazi, G. Rodeghiero, A. Gualandi, P.G. Cozzi, J. Lalevée, Keto-coumarin scaffold for photoinitiators for 3D printing and photocomposites, Journal of Polymer Science. 58 (2020) 1115–1129. https://doi.org/10.1002/pol.20190290.
[78] M. Abdallah, A. Hijazi, F. Dumur, J. Lalevée, Coumarins as Powerful Photosensitizers for the Cationic Polymerization of Epoxy-Silicones under Near-UV and Visible Light and Applications for 3D Printing Technology, Molecules. 25 (2020) 2063. https://doi.org/10.3390/molecules25092063.
[79] M. Abdallah, A. Hijazi, P.G. Cozzi, A. Gualandi, F. Dumur, J. Lalevée, Boron Compounds as Additives for the Cationic Polymerization Using Coumarin Derivatives in Epoxy Silicones, Macromolecular Chemistry and Physics. 222 (2021) 2000404. https://doi.org/10.1002/macp.202000404.
[80] Q. Chen, Q. Yang, P. Gao, B. Chi, J. Nie, Y. He, Photopolymerization of Coumarin-Containing Reversible Photoresponsive Materials Based on Wavelength Selectivity, Ind. Eng. Chem. Res. 58 (2019) 2970–2975. https://doi.org/10.1021/acs.iecr.8b05164.
[81] Z. Li, X. Zou, G. Zhu, X. Liu, R. Liu, Coumarin-Based Oxime Esters: Photobleachable and Versatile Unimolecular Initiators for Acrylate and Thiol-Based Click Photopolymerization under Visible Light-Emitting Diode Light Irradiation, ACS Appl. Mater. Interfaces. 10 (2018) 16113–16123. https://doi.org/10.1021/acsami.8b01767.
[82] M. Rahal, H. Mokbel, B. Graff, J. Toufaily, T. Hamieh, F. Dumur, J. Lalevée, Mono vs. Difunctional Coumarin as Photoinitiators in Photocomposite Synthesis and 3D Printing, Catalysts. 10 (2020) 1202. https://doi.org/10.3390/catal10101202.
[83] M. Rajeshirke, M.C. Sreenath, S. Chitrambalam, I.H. Joe, N. Sekar, Enhancement of NLO Properties in OBO Fluorophores Derived from Carbazole–Coumarin Chalcones Containing Carboxylic Acid at the N-Alykl Terminal End, J. Phys. Chem. C. 122 (2018) 14313–14325. https://doi.org/10.1021/acs.jpcc.8b02937.
[84] M. Rahal, B. Graff, J. Toufaily, T. Hamieh, F. Dumur, J. Lalevée, Design of keto-coumarin based photoinitiator for Free Radical Photopolymerization: Towards 3D printing and photocomposites applications, European Polymer Journal. 154 (2021) 110559. https://doi.org/10.1016/j.eurpolymj.2021.110559.
[85] M. Rahal, B. Graff, J. Toufaily, T. Hamieh, G. Noirbent, D. Gigmes, F. Dumur, J. Lalevée, 3-Carboxylic Acid and Formyl-Derived Coumarins as Photoinitiators in Photo-Oxidation or Photo-Reduction Processes for Photopolymerization upon Visible Light: Photocomposite Synthesis and 3D Printing Applications, Molecules. 26 (2021). https://doi.org/10.3390/molecules26061753.
[86] F. Hammoud, N. Giacoletto, G. Noirbent, B. Graff, A. Hijazi, M. Nechab, D. Gigmes, F. Dumur, J. Lalevée, Substituent effects on the photoinitiation ability of coumarin-based oxime-ester photoinitiators for free radical photopolymerization, Mater. Chem. Front. 5 (2021) 8361–8370. https://doi.org/10.1039/D1QM01310F.
[87] F. Dumur, Recent advances on coumarin-based photoinitiators of polymerization, European Polymer Journal. 163 (2022) 110962. https://doi.org/10.1016/j.eurpolymj.2021.110962.
[88] S. Liu, H. Chen, Y. Zhang, K. Sun, Y. Xu, F. Morlet-Savary, B. Graff, G. Noirbent, C. Pigot, D. Brunel, M. Nechab, D. Gigmes, P. Xiao, F. Dumur, J. Lalevée,

Monocomponent Photoinitiators based on Benzophenone-Carbazole Structure for LED Photoinitiating Systems and Application on 3D Printing, Polymers. 12 (2020) 1394. https://doi.org/10.3390/polym12061394.
[89] P. Xiao, F. Dumur, B. Graff, D. Gigmes, J.P. Fouassier, J. Lalevée, Variations on the Benzophenone Skeleton: Novel High Performance Blue Light Sensitive Photoinitiating Systems, Macromolecules. 46 (2013) 7661–7667. https://doi.org/10.1021/ma401766v.
[90] J. Zhang, M. Frigoli, F. Dumur, P. Xiao, L. Ronchi, B. Graff, F. Morlet-Savary, J.P. Fouassier, D. Gigmes, J. Lalevée, Design of Novel Photoinitiators for Radical and Cationic Photopolymerizations under Near UV and Visible LEDs (385, 395, and 405 nm)., Macromolecules. 47 (2014) 2811–2819. https://doi.org/10.1021/ma500612x.
[91] S. Liu, D. Brunel, G. Noirbent, A. Mau, H. Chen, F. Morlet-Savary, B. Graff, D. Gigmes, P. Xiao, F. Dumur, J. Lalevée, New multifunctional benzophenone-based photoinitiators with high migration stability and their applications in 3D printing, Mater. Chem. Front. 5 (2021) 1982–1994. https://doi.org/10.1039/D0QM00885K.
[92] S. Liu, D. Brunel, K. Sun, Y. Zhang, H. Chen, P. Xiao, F. Dumur, J. Lalevée, Novel Photoinitiators Based on Benzophenone-Triphenylamine Hybrid Structure for LED Photopolymerization, Macromolecular Rapid Communications. 41 (2020) 2000460. https://doi.org/10.1002/marc.202000460.
[93] S. Liu, D. Brunel, K. Sun, Y. Xu, F. Morlet-Savary, B. Graff, P. Xiao, F. Dumur, J. Lalevée, A monocomponent bifunctional benzophenone–carbazole type II photoinitiator for LED photoinitiating systems, Polym. Chem. 11 (2020) 3551–3556. https://doi.org/10.1039/D0PY00644K.
[94] M.-A. Tehfe, F. Dumur, B. Graff, F. Morlet-Savary, J.-P. Fouassier, D. Gigmes, J. Lalevée, Trifunctional Photoinitiators Based on a Triazine Skeleton for Visible Light Source and UV LED Induced Polymerizations, Macromolecules. 45 (2012) 8639–8647. https://doi.org/10.1021/ma301931p.
[95] J.-T. Lin, J. Lalevee, Efficacy Modeling of New Multi-Functional Benzophenone-Based System for Free-Radical/Cationic Hybrid Photopolymerization Using 405 nm LED, (2021). https://doi.org/10.20944/preprints202106.0502.v1.
[96] J. Zhang, N. Zivic, F. Dumur, C. Guo, Y. Li, P. Xiao, B. Graff, D. Gigmes, J.P. Fouassier, J. Lalevée, Panchromatic photoinitiators for radical, cationic and thiol-ene polymerization reactions: A search in the diketopyrrolopyrrole or indigo dye series, Materials Today Communications. 4 (2015) 101–108. https://doi.org/10.1016/j.mtcomm.2015.06.007.
[97] P. Xiao, W. Hong, Y. Li, F. Dumur, B. Graff, J.P. Fouassier, D. Gigmes, J. Lalevée, Diketopyrrolopyrrole dyes: Structure/reactivity/efficiency relationship in photoinitiating systems upon visible lights, Polymer. 55 (2014) 746–751. https://doi.org/10.1016/j.polymer.2014.01.003.
[98] P. Xiao, W. Hong, Y. Li, F. Dumur, B. Graff, J.P. Fouassier, D. Gigmes, J. Lalevée, Green light sensitive diketopyrrolopyrrole derivatives used in versatile photoinitiating systems for photopolymerizations, Polym. Chem. 5 (2014) 2293–2300. https://doi.org/10.1039/C3PY01599H.
[99] F. Dumur, Recent advances on visible light Phenothiazine-based photoinitiators of polymerization, European Polymer Journal. 165 (2022) 110999. https://doi.org/10.1016/j.eurpolymj.2022.110999.
[100] J. Zhao, J. Lalevée, H. Lu, R. MacQueen, S.H. Kable, T.W. Schmidt, M.H. Stenzel, P. Xiao, A new role of curcumin: as a multicolor photoinitiator for polymer fabrication

under household UV to red LED bulbs, Polym. Chem. 6 (2015) 5053–5061. https://doi.org/10.1039/C5PY00661A.
[101] J.V. Crivello, U. Bulut, Curcumin: A naturally occurring long-wavelength photosensitizer for diaryliodonium salts, Journal of Polymer Science Part A: Polymer Chemistry. 43 (2005) 5217–5231. https://doi.org/10.1002/pola.21017.
[102] W. Han, H. Fu, T. Xue, T. Liu, Y. Wang, T. Wang, Facilely prepared blue-green light sensitive curcuminoids with excellent bleaching properties as high performance photosensitizers in cationic and free radical photopolymerization, Polym. Chem. 9 (2018) 1787–1798. https://doi.org/10.1039/C8PY00166A.
[103] A. Mishra, S. Daswal, Curcumin, A Novel Natural Photoinitiator for the Copolymerization of Styrene and Methylmethacrylate, Null. 42 (2005) 1667–1678. https://doi.org/10.1080/10601320500246974.
[104] J. Zhang, D. Campolo, F. Dumur, P. Xiao, D. Gigmes, J.P. Fouassier, J. Lalevée, The carbazole-bound ferrocenium salt as a specific cationic photoinitiator upon near-UV and visible LEDs (365–405 nm), Polym. Bull. 73 (2016) 493–507. https://doi.org/10.1007/s00289-015-1506-1.
[105] A. Al Mousawi, F. Dumur, P. Garra, J. Toufaily, T. Hamieh, B. Graff, D. Gigmes, J.P. Fouassier, J. Lalevée, Carbazole Scaffold Based Photoinitiator/Photoredox Catalysts: Toward New High Performance Photoinitiating Systems and Application in LED Projector 3D Printing Resins, Macromolecules. 50 (2017) 2747–2758. https://doi.org/10.1021/acs.macromol.7b00210.
[106] A. Al Mousawi, D.M. Lara, G. Noirbent, F. Dumur, J. Toufaily, T. Hamieh, T.-T. Bui, F. Goubard, B. Graff, D. Gigmes, J.P. Fouassier, J. Lalevée, Carbazole Derivatives with Thermally Activated Delayed Fluorescence Property as Photoinitiators/Photoredox Catalysts for LED 3D Printing Technology, Macromolecules. 50 (2017) 4913–4926. https://doi.org/10.1021/acs.macromol.7b01114.
[107] A. Al Mousawi, P. Garra, F. Dumur, T.-T. Bui, F. Goubard, J. Toufaily, T. Hamieh, B. Graff, D. Gigmes, J.P. Fouassier, J. Lalevée, Novel Carbazole Skeleton-Based Photoinitiators for LED Polymerization and LED Projector 3D Printing, Molecules. 22 (2017) 2143. https://doi.org/10.3390/molecules22122143.
[108] A.A. Mousawi, A. Arar, M. Ibrahim-Ouali, S. Duval, F. Dumur, P. Garra, J. Toufaily, T. Hamieh, B. Graff, D. Gigmes, J.-P. Fouassier, J. Lalevée, Carbazole-based compounds as photoinitiators for free radical and cationic polymerization upon near visible light illumination, Photochem. Photobiol. Sci. 17 (2018) 578–585. https://doi.org/10.1039/C7PP00400A.
[109] M. Abdallah, D. Magaldi, A. Hijazi, B. Graff, F. Dumur, J.-P. Fouassier, T.-T. Bui, F. Goubard, J. Lalevée, Development of new high-performance visible light photoinitiators based on carbazole scaffold and their applications in 3d printing and photocomposite synthesis, Journal of Polymer Science Part A: Polymer Chemistry. 57 (2019) 2081–2092. https://doi.org/10.1002/pola.29471.
[110] F. Dumur, Recent advances on carbazole-based photoinitiators of polymerization, European Polymer Journal. 125 (2020) 109503. https://doi.org/10.1016/j.eurpolymj.2020.109503.
[111] S. Liu, B. Graff, P. Xiao, F. Dumur, J. Lalevée, Nitro-Carbazole Based Oxime Esters as Dual Photo/Thermal Initiators for 3D Printing and Composite Preparation, Macromolecular Rapid Communications. 42 (2021) 2100207. https://doi.org/10.1002/marc.202100207.

[112] F. Hammoud, A. Hijazi, S. Duval, J. Lalevée, F. Dumur, 5,12-Dihydroindolo[3,2-a]carbazole: A promising scaffold for the design of visible light photoinitiators of polymerization, European Polymer Journal. 162 (2022) 110880. https://doi.org/10.1016/j.eurpolymj.2021.110880.
[113] S. Liu, N. Giacoletto, M. Schmitt, M. Nechab, B. Graff, F. Morlet-Savary, P. Xiao, F. Dumur, J. Lalevée, Effect of Decarboxylation on the Photoinitiation Behavior of Nitrocarbazole-Based Oxime Esters, Macromolecules. (2022). https://doi.org/10.1021/acs.macromol.2c00294.
[114] F. Hammoud, A. Hijazi, M. Ibrahim-Ouali, J. Lalevée, F. Dumur, Chemical engineering around the 5,12-dihydroindolo[3,2-a]carbazole scaffold : Fine tuning of the optical properties of visible light photoinitiators of polymerization, European Polymer Journal. (2022) 111218. https://doi.org/10.1016/j.eurpolymj.2022.111218.
[115] A. Al Mousawi, P. Garra, X. Sallenave, F. Dumur, J. Toufaily, T. Hamieh, B. Graff, D. Gigmes, J.P. Fouassier, J. Lalevée, π-Conjugated Dithienophosphole Derivatives as High Performance Photoinitiators for 3D Printing Resins, Macromolecules. 51 (2018) 1811–1821. https://doi.org/10.1021/acs.macromol.8b00044.
[116] F. Dumur, D. Gigmes, J.-P. Fouassier, J. Lalevée, Organic Electronics: An El Dorado in the Quest of New Photocatalysts for Polymerization Reactions, Acc. Chem. Res. 49 (2016) 1980–1989. https://doi.org/10.1021/acs.accounts.6b00227.
[117] M. Abdallah, H. Le, A. Hijazi, M. Schmitt, B. Graff, F. Dumur, T.-T. Bui, F. Goubard, J.-P. Fouassier, J. Lalevée, Acridone derivatives as high performance visible light photoinitiators for cationic and radical photosensitive resins for 3D printing technology and for low migration photopolymer property, Polymer. 159 (2018) 47–58. https://doi.org/10.1016/j.polymer.2018.11.021.
[118] J. Zhang, F. Dumur, M. Bouzrati, P. Xiao, C. Dietlin, F. Morlet-Savary, B. Graff, D. Gigmes, J.P. Fouassier, J. Lalevée, Novel panchromatic photopolymerizable matrices: N,N′-dibutylquinacridone as an efficient and versatile photoinitiator, Journal of Polymer Science Part A: Polymer Chemistry. 53 (2015) 1719–1727. https://doi.org/10.1002/pola.27615.
[119] F. Dumur, Recent Advances on Anthracene-based Photoinitiators of Polymerization, European Polymer Journal. (2022) 111139. https://doi.org/10.1016/j.eurpolymj.2022.111139.
[120] M.-A. Tehfe, F. Dumur, P. Xiao, J. Zhang, B. Graff, F. Morlet-Savary, D. Gigmes, J.-P. Fouassier, J. Lalevée, Photoinitiators based on a phenazine scaffold: High performance systems upon near-UV or visible LED (385, 395 and 405 nm) irradiations, Polymer. 55 (2014) 2285–2293. https://doi.org/10.1016/j.polymer.2014.04.005.
[121] J. Zhang, J. Lalevée, J. Zhao, B. Graff, M.H. Stenzel, P. Xiao, Dihydroxyanthraquinone derivatives: natural dyes as blue-light-sensitive versatile photoinitiators of photopolymerization, Polym. Chem. 7 (2016) 7316–7324. https://doi.org/10.1039/C6PY01550F.
[122] P. Garra, D. Brunel, G. Noirbent, B. Graff, F. Morlet-Savary, C. Dietlin, V.F. Sidorkin, F. Dumur, D. Duché, D. Gigmes, J.-P. Fouassier, J. Lalevée, Ferrocene-based (photo)redox polymerization under long wavelengths, Polym. Chem. 10 (2019) 1431–1441. https://doi.org/10.1039/C9PY00059C.
[123] S. Telitel, F. Dumur, D. Campolo, J. Poly, D. Gigmes, J.P. Fouassier, J. Lalevée, Iron complexes as potential photocatalysts for controlled radical photopolymerizations: A

tool for modifications and patterning of surfaces, Journal of Polymer Science Part A: Polymer Chemistry. 54 (2016) 702–713. https://doi.org/10.1002/pola.27896.
[124] J. Zhang, D. Campolo, F. Dumur, P. Xiao, J.P. Fouassier, D. Gigmes, J. Lalevée, Iron complexes as photoinitiators for radical and cationic polymerization through photoredox catalysis processes, Journal of Polymer Science Part A: Polymer Chemistry. 53 (2015) 42–49. https://doi.org/10.1002/pola.27435.
[125] J. Zhang, D. Campolo, F. Dumur, P. Xiao, J.P. Fouassier, D. Gigmes, J. Lalevée, Visible-light-sensitive photoredox catalysis by iron complexes: Applications in cationic and radical polymerization reactions, Journal of Polymer Science Part A: Polymer Chemistry. 54 (2016) 2247–2253. https://doi.org/10.1002/pola.28098.
[126] J. Zhang, D. Campolo, F. Dumur, P. Xiao, J.P. Fouassier, D. Gigmes, J. Lalevée, Iron Complexes in Visible-Light-Sensitive Photoredox Catalysis: Effect of Ligands on Their Photoinitiation Efficiencies, ChemCatChem. 8 (2016) 2227–2233. https://doi.org/10.1002/cctc.201600320.
[127] F. Dumur, Recent advances on ferrocene-based photoinitiating systems, European Polymer Journal. 147 (2021) 110328. https://doi.org/10.1016/j.eurpolymj.2021.110328.
[128] F. Dumur, Recent advances on iron-based photoinitiators of polymerization, European Polymer Journal. 139 (2020) 110026. https://doi.org/10.1016/j.eurpolymj.2020.110026.
[129] H. Mokbel, F. Dumur, J. Lalevée, On demand NIR activated photopolyaddition reactions, Polym. Chem. 11 (2020) 4250–4259. https://doi.org/10.1039/D0PY00639D.
[130] H. Mokbel, B. Graff, F. Dumur, J. Lalevée, NIR Sensitizer Operating under Long Wavelength (1064 nm) for Free Radical Photopolymerization Processes, Macromolecular Rapid Communications. 41 (2020) 2000289. https://doi.org/10.1002/marc.202000289.
[131] V. Launay, F. Dumur, D. Gigmes, J. Lalevée, Near-infrared light for polymer re-shaping and re-processing applications, Journal of Polymer Science. 59 (2021) 2193–2200. https://doi.org/10.1002/pol.20210450.
[132] A. Caron, G. Noirbent, D. Gigmes, F. Dumur, J. Lalevée, Near-Infrared PhotoInitiating Systems: Photothermal versus Triplet–Triplet Annihilation-Based Upconversion Polymerization, Macromolecular Rapid Communications. 42 (2021) 2100047. https://doi.org/10.1002/marc.202100047.
[133] A.-H. Bonardi, F. Bonardi, F. Morlet-Savary, C. Dietlin, G. Noirbent, T.M. Grant, J.-P. Fouassier, F. Dumur, B.H. Lessard, D. Gigmes, J. Lalevée, Photoinduced Thermal Polymerization Reactions, Macromolecules. 51 (2018) 8808–8820. https://doi.org/10.1021/acs.macromol.8b01741.
[134] V. Launay, F. Dumur, L. Pieuchot, J. Lalevée, Safe near infrared light for fast polymers surface sterilization using organic heaters, Mater. Chem. Front. (2022). https://doi.org/10.1039/D1QM01609A.
[135] M. Ghali, M. Benltifa, C. Brahmi, L. Elbassi, F. Dumur, C. Simonnet-Jégat, L. Bousselmi, J. Lalevée, LED and solar photodecomposition of erythrosine B and rose Bengal using H3PMo12O40/polymer photocatalyst, European Polymer Journal. 159 (2021) 110743. https://doi.org/10.1016/j.eurpolymj.2021.110743.
[136] C. Brahmi, M. Benltifa, M. Ghali, F. Dumur, C. Simonnet-Jégat, M. Valérie, F. Morlet-Savary, L. Bousselmi, J. Lalevée, Performance improvement of the photocatalytic process for the degradation of pharmaceutical compounds using new POM/polymer photocatalysts, Journal of Environmental Chemical Engineering. 9 (2021) 106015. https://doi.org/10.1016/j.jece.2021.106015.

[137] P. Xiao, F. Dumur, J. Zhang, J.P. Fouassier, D. Gigmes, J. Lalevée, Copper Complexes in Radical Photoinitiating Systems: Applications to Free Radical and Cationic Polymerization upon Visible LEDs, Macromolecules. 47 (2014) 3837–3844. https://doi.org/10.1021/ma5006793.
[138] P. Xiao, F. Dumur, J. Zhang, D. Gigmes, J.P. Fouassier, J. Lalevée, Copper complexes: the effect of ligands on their photoinitiation efficiencies in radical polymerization reactions under visible light, Polym. Chem. 5 (2014) 6350–6357. https://doi.org/10.1039/C4PY00925H.
[139] P. Xiao, J. Zhang, D. Campolo, F. Dumur, D. Gigmes, J.P. Fouassier, J. Lalevée, Copper and iron complexes as visible-light-sensitive photoinitiators of polymerization, Journal of Polymer Science Part A: Polymer Chemistry. 53 (2015) 2673–2684. https://doi.org/10.1002/pola.27762.
[140] P. Garra, M. Carré, F. Dumur, F. Morlet-Savary, C. Dietlin, D. Gigmes, J.-P. Fouassier, J. Lalevée, Copper-Based (Photo)redox Initiating Systems as Highly Efficient Systems for Interpenetrating Polymer Network Preparation, Macromolecules. 51 (2018) 679–688. https://doi.org/10.1021/acs.macromol.7b02491.
[141] P. Garra, F. Dumur, F. Morlet-Savary, C. Dietlin, D. Gigmes, J.P. Fouassier, J. Lalevée, Mechanosynthesis of a Copper complex for redox initiating systems with a unique near infrared light activation, Journal of Polymer Science Part A: Polymer Chemistry. 55 (2017) 3646–3655. https://doi.org/10.1002/pola.28750.
[142] P. Garra, F. Dumur, A.A. Mousawi, B. Graff, D. Gigmes, F. Morlet-Savary, C. Dietlin, J.P. Fouassier, J. Lalevée, Mechanosynthesized copper(I) complex based initiating systems for redox polymerization: towards upgraded oxidizing and reducing agents, Polym. Chem. 8 (2017) 5884–5896. https://doi.org/10.1039/C7PY01244F.
[143] H. Mokbel, D. Anderson, R. Plenderleith, C. Dietlin, F. Morlet-Savary, F. Dumur, D. Gigmes, J.-P. Fouassier, J. Lalevée, Copper photoredox catalyst "G1": a new high performance photoinitiator for near-UV and visible LEDs, Polym. Chem. 8 (2017) 5580–5592. https://doi.org/10.1039/C7PY01016H.
[144] H. Mokbel, D. Anderson, R. Plenderleith, C. Dietlin, F. Morlet-Savary, F. Dumur, D. Gigmes, J.P. Fouassier, J. Lalevée, Simultaneous initiation of radical and cationic polymerization reactions using the "G1" copper complex as photoredox catalyst: Applications of free radical/cationic hybrid photopolymerization in the composites and 3D printing fields, Progress in Organic Coatings. 132 (2019) 50–61. https://doi.org/10.1016/j.porgcoat.2019.02.044.
[145] A.A. Mousawi, A. Kermagoret, D.-L. Versace, J. Toufaily, T. Hamieh, B. Graff, F. Dumur, D. Gigmes, J.P. Fouassier, J. Lalevée, Copper photoredox catalysts for polymerization upon near UV or visible light: structure/reactivity/efficiency relationships and use in LED projector 3D printing resins, Polym. Chem. 8 (2017) 568–580. https://doi.org/10.1039/C6PY01958G.
[146] A. Mau, G. Noirbent, C. Dietlin, B. Graff, D. Gigmes, F. Dumur, J. Lalevée, Panchromatic Copper Complexes for Visible Light Photopolymerization, Photochem. 1 (2021). https://doi.org/10.3390/photochem1020010.
[147] A. Mau, C. Dietlin, F. Dumur, J. Lalevée, Concomitant initiation of radical and cationic polymerisations using new copper complexes as photoinitiators: Synthesis and characterisation of acrylate/epoxy interpenetrated polymer networks, European Polymer Journal. 152 (2021) 110457. https://doi.org/10.1016/j.eurpolymj.2021.110457.

[148] P. Garra, F. Dumur, D. Gigmes, A. Al Mousawi, F. Morlet-Savary, C. Dietlin, J.P. Fouassier, J. Lalevée, Copper (Photo)redox Catalyst for Radical Photopolymerization in Shadowed Areas and Access to Thick and Filled Samples, Macromolecules. 50 (2017) 3761–3771. https://doi.org/10.1021/acs.macromol.7b00622.
[149] P. Garra, F. Dumur, F. Morlet-Savary, C. Dietlin, J.P. Fouassier, J. Lalevée, A New Highly Efficient Amine-Free and Peroxide-Free Redox System for Free Radical Polymerization under Air with Possible Light Activation, Macromolecules. 49 (2016) 6296–6309. https://doi.org/10.1021/acs.macromol.6b01615.
[150] P. Garra, A. Kermagoret, A.A. Mousawi, F. Dumur, D. Gigmes, F. Morlet-Savary, C. Dietlin, J.P. Fouassier, J. Lalevée, New copper(I) complex based initiating systems in redox polymerization and comparison with the amine/benzoyl peroxide reference, Polym. Chem. 8 (2017) 4088–4097. https://doi.org/10.1039/C7PY00726D.
[151] G. Noirbent, F. Dumur, Recent Advances on Copper Complexes as Visible Light Photoinitiators and (Photo) Redox Initiators of Polymerization, Catalysts. 10 (2020). https://doi.org/10.3390/catal10090953.
[152] T. Borjigin, G. Noirbent, D. Gigmes, P. Xiao, F. Dumur, J. Lalevée, The new LED-Sensitive photoinitiators of Polymerization: Copper complexes in free radical and cationic photoinitiating systems and application in 3D printing, European Polymer Journal. 162 (2022) 110885. https://doi.org/10.1016/j.eurpolymj.2021.110885.
[153] J. Zhang, P. Xiao, F. Dumur, C. Guo, W. Hong, Y. Li, D. Gigmes, B. Graff, J.-P. Fouassier, J. Lalevée, Polymeric Photoinitiators: A New Search toward High Performance Visible Light Photoinitiating Systems, Macromolecular Chemistry and Physics. 217 (2016) 2145–2153. https://doi.org/10.1002/macp.201600260.
[154] M.-A. Tehfe, F. Dumur, P. Xiao, B. Graff, F. Morlet-Savary, J.-P. Fouassier, D. Gigmes, J. Lalevée, New chromone based photoinitiators for polymerization reactions under visible light, Polym. Chem. 4 (2013) 4234–4244. https://doi.org/10.1039/C3PY00536D.
[155] J. You, H. Fu, D. Zhao, T. Hu, J. Nie, T. Wang, Flavonol dyes with different substituents in photopolymerization, Journal of Photochemistry and Photobiology A: Chemistry. 386 (2020) 112097. https://doi.org/10.1016/j.jphotochem.2019.112097.
[156] A. Al Mousawi, P. Garra, M. Schmitt, J. Toufaily, T. Hamieh, B. Graff, J.P. Fouassier, F. Dumur, J. Lalevée, 3-Hydroxyflavone and N-Phenylglycine in High Performance Photoinitiating Systems for 3D Printing and Photocomposites Synthesis, Macromolecules. 51 (2018) 4633–4641. https://doi.org/10.1021/acs.macromol.8b00979.
[157] P. Xiao, F. Dumur, M. Frigoli, B. Graff, F. Morlet-Savary, G. Wantz, H. Bock, J.P. Fouassier, D. Gigmes, J. Lalevée, Perylene derivatives as photoinitiators in blue light sensitive cationic or radical curable films and panchromatic thiol-ene polymerizable films, European Polymer Journal. 53 (2014) 215–222. https://doi.org/10.1016/j.eurpolymj.2014.01.024.
[158] P. Xiao, F. Dumur, B. Graff, D. Gigmes, J.P. Fouassier, J. Lalevée, Red-Light-Induced Cationic Photopolymerization: Perylene Derivatives as Efficient Photoinitiators, Macromolecular Rapid Communications. 34 (2013) 1452–1458. https://doi.org/10.1002/marc.201300383.
[159] F. Dumur, Recent advances on perylene-based photoinitiators of polymerization, European Polymer Journal. 159 (2021) 110734. https://doi.org/10.1016/j.eurpolymj.2021.110734.
[160] M.-A. Tehfe, F. Dumur, B. Graff, D. Gigmes, J.-P. Fouassier, J. Lalevée, Green-Light-Induced Cationic Ring Opening Polymerization Reactions: Perylene-3,4:9,10-

bis(Dicarboximide) as Efficient Photosensitizers, Macromolecular Chemistry and Physics. 214 (2013) 1052–1060. https://doi.org/10.1002/macp.201200728.
[161] H. Chen, G. Noirbent, K. Sun, D. Brunel, D. Gigmes, F. Morlet-Savary, Y. Zhang, S. Liu, P. Xiao, F. Dumur, J. Lalevée, Photoinitiators derived from natural product scaffolds: monochalcones in three-component photoinitiating systems and their applications in 3D printing, Polym. Chem. 11 (2020) 4647–4659. https://doi.org/10.1039/D0PY00568A.
[162] L. Tang, J. Nie, X. Zhu, A high performance phenyl-free LED photoinitiator for cationic or hybrid photopolymerization and its application in LED cationic 3D printing, Polym. Chem. 11 (2020) 2855–2863. https://doi.org/10.1039/D0PY00142B.
[163] Y. Xu, G. Noirbent, D. Brunel, Z. Ding, D. Gigmes, B. Graff, P. Xiao, F. Dumur, J. Lalevée, Allyloxy ketones as efficient photoinitiators with high migration stability in free radical polymerization and 3D printing, Dyes and Pigments. 185 (2021) 108900. https://doi.org/10.1016/j.dyepig.2020.108900.
[164] Y. Xu, Z. Ding, H. Zhu, B. Graff, S. Knopf, P. Xiao, F. Dumur, J. Lalevée, Design of ketone derivatives as highly efficient photoinitiators for free radical and cationic photopolymerizations and application in 3D printing of composites, Journal of Polymer Science. 58 (2020) 3432–3445. https://doi.org/10.1002/pol.20200658.
[165] H. Chen, G. Noirbent, S. Liu, D. Brunel, B. Graff, D. Gigmes, Y. Zhang, K. Sun, F. Morlet-Savary, P. Xiao, F. Dumur, J. Lalevée, Bis-chalcone derivatives derived from natural products as near-UV/visible light sensitive photoinitiators for 3D/4D printing, Mater. Chem. Front. 5 (2021) 901–916. https://doi.org/10.1039/D0QM00755B.
[166] S. Liu, Y. Zhang, K. Sun, B. Graff, P. Xiao, F. Dumur, J. Lalevée, Design of photoinitiating systems based on the chalcone-anthracene scaffold for LED cationic photopolymerization and application in 3D printing, European Polymer Journal. 147 (2021) 110300. https://doi.org/10.1016/j.eurpolymj.2021.110300.
[167] N. Giacoletto, F. Dumur, Recent Advances in bis-Chalcone-Based Photoinitiators of Polymerization: From Mechanistic Investigations to Applications, Molecules. 26 (2021) 3192. https://doi.org/10.3390/molecules26113192.
[168] M. Ibrahim-Ouali, F. Dumur, Recent Advances on Chalcone-based Photoinitiators of Polymerization, European Polymer Journal. (2021) 110688. https://doi.org/10.1016/j.eurpolymj.2021.110688.
[169] H. Chen, G. Noirbent, S. Liu, Y. Zhang, K. Sun, F. Morlet-Savary, D. Gigmes, P. Xiao, F. Dumur, J. Lalevée, In situ generation of Ag nanoparticles during photopolymerization by using newly developed dyes-based three-component photoinitiating systems and the related 3D printing applications and their shape change behavior, Journal of Polymer Science. 59 (2021) 843–859. https://doi.org/10.1002/pol.20210154.
[170] H. Chen, M. Vahdati, P. Xiao, F. Dumur, J. Lalevée, Water-Soluble Visible Light Sensitive Photoinitiating System Based on Charge Transfer Complexes for the 3D Printing of Hydrogels, Polymers. 13 (2021). https://doi.org/10.3390/polym13183195.
[171] M.-A. Tehfe, F. Dumur, P. Xiao, M. Delgove, B. Graff, J.-P. Fouassier, D. Gigmes, J. Lalevée, Chalcone derivatives as highly versatile photoinitiators for radical, cationic, thiol–ene and IPN polymerization reactions upon exposure to visible light, Polym. Chem. 5 (2014) 382–390. https://doi.org/10.1039/C3PY00922J.
[172] K. Sun, Y. Xu, F. Dumur, F. Morlet-Savary, H. Chen, C. Dietlin, B. Graff, J. Lalevée, P. Xiao, In silico rational design by molecular modeling of new ketones as photoinitiators

in three-component photoinitiating systems: application in 3D printing, Polym. Chem. 11 (2020) 2230–2242. https://doi.org/10.1039/C9PY01874C.
[173] H. Chen, C. Regeard, H. Salmi, F. Morlet-Savary, N. Giacoletto, M. Nechab, P. Xiao, F. Dumur, J. Lalevée, Interpenetrating polymer network hydrogels using natural based dyes initiating systems: antibacterial activity and 3D/4D performance, European Polymer Journal. (2022) 111042. https://doi.org/10.1016/j.eurpolymj.2022.111042.
[174] J. Lalevée, F. Dumur, M.-A. Tehfe, A. Zein-Fakih, D. Gigmes, F. Morlet-Savary, B. Graff, J.-P. Fouassier, Dye photosensitized cationic ring-opening polymerization: Search for new dye skeletons, Polymer. 53 (2012) 4947–4954. https://doi.org/10.1016/j.polymer.2012.08.067.
[175] J. Li, X. Zhang, S. Ali, M.Y. Akram, J. Nie, X. Zhu, The effect of polyethylene glycoldiacrylate complexation on type II photoinitiator and promotion for visible light initiation system, Journal of Photochemistry and Photobiology A: Chemistry. 384 (2019) 112037. https://doi.org/10.1016/j.jphotochem.2019.112037.
[176] J. Li, S. Li, Y. Li, R. Li, J. Nie, X. Zhu, In situ monitoring of photopolymerization by photoinitiator with luminescence characteristics, Journal of Photochemistry and Photobiology A: Chemistry. 389 (2020) 112225. https://doi.org/10.1016/j.jphotochem.2019.112225.
[177] J. Li, Y. Hao, M. Zhong, L. Tang, J. Nie, X. Zhu, Synthesis of furan derivative as LED light photoinitiator: One-pot, low usage, photobleaching for light color 3D printing, Dyes and Pigments. 165 (2019) 467–473. https://doi.org/10.1016/j.dyepig.2019.03.011.
[178] Y. Xu, G. Noirbent, D. Brunel, Z. Ding, D. Gigmes, B. Graff, P. Xiao, F. Dumur, J. Lalevée, Novel ketone derivative-based photoinitiating systems for free radical polymerization under mild conditions and 3D printing, Polym. Chem. 11 (2020) 5767–5777. https://doi.org/10.1039/D0PY00990C.
[179] A.-H. Bonardi, S. Zahouily, C. Dietlin, B. Graff, F. Morlet-Savary, M. Ibrahim-Ouali, D. Gigmes, N. Hoffmann, F. Dumur, J. Lalevée, New 1,8-Naphthalimide Derivatives as Photoinitiators for Free-Radical Polymerization Upon Visible Light, Catalysts. 9 (2019) 637. https://doi.org/10.3390/catal9080637.
[180] J. Zhang, N. Zivic, F. Dumur, P. Xiao, B. Graff, J.P. Fouassier, D. Gigmes, J. Lalevée, Naphthalimide-Tertiary Amine Derivatives as Blue-Light-Sensitive Photoinitiators, ChemPhotoChem. 2 (2018) 481–489. https://doi.org/10.1002/cptc.201800006.
[181] P. Xiao, F. Dumur, J. Zhang, B. Graff, D. Gigmes, J.P. Fouassier, J. Lalevée, Naphthalimide Derivatives: Substituent Effects on the Photoinitiating Ability in Polymerizations under Near UV, Purple, White and Blue LEDs (385, 395, 405, 455, or 470 nm), Macromolecular Chemistry and Physics. 216 (2015) 1782–1790. https://doi.org/10.1002/macp.201500150.
[182] P. Xiao, F. Dumur, J. Zhang, B. Graff, D. Gigmes, J.P. Fouassier, J. Lalevée, Naphthalimide-phthalimide derivative based photoinitiating systems for polymerization reactions under blue lights, Journal of Polymer Science Part A: Polymer Chemistry. 53 (2015) 665–674. https://doi.org/10.1002/pola.27490.
[183] J. Zhang, N. Zivic, F. Dumur, P. Xiao, B. Graff, D. Gigmes, J.P. Fouassier, J. Lalevée, A benzophenone-naphthalimide derivative as versatile photoinitiator of polymerization under near UV and visible lights, Journal of Polymer Science Part A: Polymer Chemistry. 53 (2015) 445–451. https://doi.org/10.1002/pola.27451.

[184] J. Zhang, N. Zivic, F. Dumur, P. Xiao, B. Graff, J.P. Fouassier, D. Gigmes, J. Lalevée, N-[2-(Dimethylamino)ethyl]-1,8-naphthalimide derivatives as photoinitiators under LEDs, Polym. Chem. 9 (2018) 994–1003. https://doi.org/10.1039/C8PY00055G.
[185] J. Zhang, F. Dumur, P. Xiao, B. Graff, D. Bardelang, D. Gigmes, J.P. Fouassier, J. Lalevée, Structure Design of Naphthalimide Derivatives: Toward Versatile Photoinitiators for Near-UV/Visible LEDs, 3D Printing, and Water-Soluble Photoinitiating Systems, Macromolecules. 48 (2015) 2054–2063. https://doi.org/10.1021/acs.macromol.5b00201.
[186] J. Zhang, N. Zivic, F. Dumur, P. Xiao, B. Graff, J.P. Fouassier, D. Gigmes, J. Lalevée, UV-violet-blue LED induced polymerizations: Specific photoinitiating systems at 365, 385, 395 and 405 nm, Polymer. 55 (2014) 6641–6648. https://doi.org/10.1016/j.polymer.2014.11.002.
[187] P. Xiao, F. Dumur, B. Graff, D. Gigmes, J.P. Fouassier, J. Lalevée, Blue Light Sensitive Dyes for Various Photopolymerization Reactions: Naphthalimide and Naphthalic Anhydride Derivatives., Macromolecules. 47 (2014) 601–608. https://doi.org/10.1021/ma402376x.
[188] P. Xiao, F. Dumur, M. Frigoli, M.-A. Tehfe, B. Graff, J.P. Fouassier, D. Gigmes, J. Lalevée, Naphthalimide based methacrylated photoinitiators in radical and cationic photopolymerization under visible light, Polym. Chem. 4 (2013) 5440–5448. https://doi.org/10.1039/C3PY00766A.
[189] G. Noirbent, F. Dumur, Recent advances on naphthalic anhydrides and 1,8-naphthalimide-based photoinitiators of polymerization, European Polymer Journal. 132 (2020) 109702. https://doi.org/10.1016/j.eurpolymj.2020.109702.
[190] M. Rahal, H. Mokbel, B. Graff, V. Pertici, D. Gigmes, J. Toufaily, T. Hamieh, F. Dumur, J. Lalevée, Naphthalimide-Based Dyes as Photoinitiators under Visible Light Irradiation and their Applications: Photocomposite Synthesis, 3D printing and Polymerization in Water, ChemPhotoChem. 5 (2021) 476–490. https://doi.org/10.1002/cptc.202000306.
[191] M. Rahal, B. Graff, J. Toufaily, T. Hamieh, M. Ibrahim-Ouali, F. Dumur, J. Lalevée, Naphthyl-Naphthalimides as High-Performance Visible Light Photoinitiators for 3D Printing and Photocomposites Synthesis, Catalysts. 11 (2021). https://doi.org/10.3390/catal11111269.
[192] N. Zivic, J. Zhang, D. Bardelang, F. Dumur, P. Xiao, T. Jet, D.-L. Versace, C. Dietlin, F. Morlet-Savary, B. Graff, J.P. Fouassier, D. Gigmes, J. Lalevée, Novel naphthalimide–amine based photoinitiators operating under violet and blue LEDs and usable for various polymerization reactions and synthesis of hydrogels, Polym. Chem. 7 (2015) 418–429. https://doi.org/10.1039/C5PY01617G.
[193] P. Xiao, F. Dumur, B. Graff, F. Morlet-Savary, D. Gigmes, J.P. Fouassier, J. Lalevée, Design of High Performance Photoinitiators at 385–405 nm: Search around the Naphthalene Scaffold, Macromolecules. 47 (2014) 973–978. https://doi.org/10.1021/ma402622v.
[194] P. Xiao, F. Dumur, J. Zhang, B. Graff, D. Gigmes, J.P. Fouassier, J. Lalevée, Amino and nitro substituted 2-amino-1H-benzo[de]isoquinoline-1,3(2H)-diones: as versatile photoinitiators of polymerization from violet-blue LED absorption to a panchromatic behavior, Polym. Chem. 6 (2015) 1171–1179. https://doi.org/10.1039/C4PY01409J.
[195] M.-A. Tehfe, F. Dumur, B. Graff, J.-L. Clément, D. Gigmes, F. Morlet-Savary, J.-P. Fouassier, J. Lalevée, New Cleavable Photoinitiator Architecture with Huge Molar

Extinction Coefficients for Polymerization in the 340–450 nm Range., Macromolecules. 46 (2013) 736–746. https://doi.org/10.1021/ma3024359.
[196] C. Brahmi, M. Benltifa, C. Vaulot, L. Michelin, F. Dumur, A. Airoudj, F. Morlet-Savary, B. Raveau, L. Bousselmi, J. Lalevée, New hybrid perovskites/polymer composites for the photodegradation of organic dyes, European Polymer Journal. 157 (2021) 110641. https://doi.org/10.1016/j.eurpolymj.2021.110641.
[197] H. Mokbel, F. Dumur, B. Raveau, F. Morlet-Savary, C. Simonnet-Jégat, D. Gigmes, J. Toufaily, T. Hamieh, J.P. Fouassier, J. Lalevée, Perovskites as new radical photoinitiators for radical and cationic polymerizations, Tetrahedron. 72 (2016) 7686–7690. https://doi.org/10.1016/j.tet.2016.03.057.
[198] M.-A. Tehfe, A. Zein-Fakih, J. Lalevée, F. Dumur, D. Gigmes, B. Graff, F. Morlet-Savary, T. Hamieh, J.-P. Fouassier, New pyridinium salts as versatile compounds for dye sensitized photopolymerization, European Polymer Journal. 49 (2013) 567–574. https://doi.org/10.1016/j.eurpolymj.2012.10.010.
[199] P. Xiao, M. Frigoli, F. Dumur, B. Graff, D. Gigmes, J.P. Fouassier, J. Lalevée, Julolidine or Fluorenone Based Push–Pull Dyes for Polymerization upon Soft Polychromatic Visible Light or Green Light., Macromolecules. 47 (2014) 106–112. https://doi.org/10.1021/ma402196p.
[200] H. Mokbel, F. Dumur, B. Graff, C.R. Mayer, D. Gigmes, J. Toufaily, T. Hamieh, J.-P. Fouassier, J. Lalevée, Michler's Ketone as an Interesting Scaffold for the Design of High-Performance Dyes in Photoinitiating Systems Upon Visible Light, Macromolecular Chemistry and Physics. 215 (2014) 783–790. https://doi.org/10.1002/macp.201300779.
[201] M.-A. Tehfe, F. Dumur, B. Graff, F. Morlet-Savary, J.-P. Fouassier, D. Gigmes, J. Lalevée, New Push–Pull Dyes Derived from Michler's Ketone For Polymerization Reactions Upon Visible Lights., Macromolecules. 46 (2013) 3761–3770. https://doi.org/10.1021/ma400766z.
[202] H. Mokbel, F. Dumur, C.R. Mayer, F. Morlet-Savary, B. Graff, D. Gigmes, J. Toufaily, T. Hamieh, J.-P. Fouassier, J. Lalevée, End capped polyenic structures as visible light sensitive photoinitiators for polymerization of vinylethers, Dyes and Pigments. 105 (2014) 121–129. https://doi.org/10.1016/j.dyepig.2014.02.002.
[203] S. Telitel, F. Dumur, T. Kavalli, B. Graff, F. Morlet-Savary, D. Gigmes, J.-P. Fouassier, J. Lalevée, The 1,3-bis(dicyanomethylidene)indane skeleton as a (photo) initiator in thermal ring opening polymerization at RT and radical or cationic photopolymerization, RSC Adv. 4 (2014) 15930–15936. https://doi.org/10.1039/C3RA42819B.
[204] P. Xiao, F. Dumur, B. Graff, F. Morlet-Savary, L. Vidal, D. Gigmes, J.P. Fouassier, J. Lalevée, Structural Effects in the Indanedione Skeleton for the Design of Low Intensity 300–500 nm Light Sensitive Initiators., Macromolecules. 47 (2014) 26–34. https://doi.org/10.1021/ma402149g.
[205] K. Sun, S. Liu, C. Pigot, D. Brunel, B. Graff, M. Nechab, D. Gigmes, F. Morlet-Savary, Y. Zhang, P. Xiao, F. Dumur, J. Lalevée, Novel Push–Pull Dyes Derived from 1H-cyclopenta[b]naphthalene-1,3(2H)-dione as Versatile Photoinitiators for Photopolymerization and Their Related Applications: 3D Printing and Fabrication of Photocomposites, Catalysts. 10 (2020) 1196. https://doi.org/10.3390/catal10101196.
[206] K. Sun, S. Liu, H. Chen, F. Morlet-Savary, B. Graff, C. Pigot, M. Nechab, P. Xiao, F. Dumur, J. Lalevée, N-ethyl carbazole-1-allylidene-based push-pull dyes as efficient

light harvesting photoinitiators for sunlight induced polymerization, European Polymer Journal. 147 (2021) 110331. https://doi.org/10.1016/j.eurpolymj.2021.110331.
[207] M.-A. Tehfe, F. Dumur, B. Graff, F. Morlet-Savary, D. Gigmes, J.-P. Fouassier, J. Lalevée, Push–pull (thio)barbituric acid derivatives in dye photosensitized radical and cationic polymerization reactions under 457/473 nm laser beams or blue LEDs, Polym. Chem. 4 (2013) 3866–3875. https://doi.org/10.1039/C3PY00372H.
[208] K. Sun, H. Chen, Y. Zhang, F. Morlet-Savary, B. Graff, P. Xiao, F. Dumur, J. Lalevée, High-performance sunlight induced polymerization using novel push-pull dyes with high light absorption properties, European Polymer Journal. 151 (2021) 110410. https://doi.org/10.1016/j.eurpolymj.2021.110410.
[209] H. Mokbel, F. Dumur, S. Telitel, L. Vidal, P. Xiao, D.-L. Versace, M.-A. Tehfe, F. Morlet-Savary, B. Graff, J.-P. Fouassier, D. Gigmes, J. Toufaily, T. Hamieh, J. Lalevée, Photoinitiating systems of polymerization and in situ incorporation of metal nanoparticles into polymer matrices upon exposure to visible light: push–pull malonate and malononitrile based dyes, Polym. Chem. 4 (2013) 5679–5687. https://doi.org/10.1039/C3PY00846K.
[210] S. Helmy, S. Oh, F.A. Leibfarth, C.J. Hawker, J. Read de Alaniz, Design and Synthesis of Donor–Acceptor Stenhouse Adducts: A Visible Light Photoswitch Derived from Furfural, J. Org. Chem. 79 (2014) 11316–11329. https://doi.org/10.1021/jo502206g.
[211] K. Sun, C. Pigot, Y. Zhang, T. Borjigin, F. Morlet-Savary, B. Graff, M. Nechab, P. Xiao, F. Dumur, J. Lalevée, Sunlight Induced Polymerization Photoinitiated by Novel Push–Pull Dyes: Indane-1,3-Dione, 1H-Cyclopenta[b]Naphthalene-1,3(2H)-Dione and 4-Dimethoxyphenyl-1-Allylidene Derivatives, Macromolecular Chemistry and Physics. n/a (2022) 2100439. https://doi.org/10.1002/macp.202100439.
[212] F. Dumur, Recent Advances on Visible Light Thiophene-based Photoinitiators of Polymerization, European Polymer Journal. (2022) 111120. https://doi.org/10.1016/j.eurpolymj.2022.111120.
[213] F. Dumur, Recent advances on visible light Triphenylamine-based photoinitiators of polymerization, European Polymer Journal. 166 (2022) 111036. https://doi.org/10.1016/j.eurpolymj.2022.111036.
[214] N. Karaca, N. Ocal, N. Arsu, S. Jockusch, Thioxanthone-benzothiophenes as photoinitiator for free radical polymerization, Journal of Photochemistry and Photobiology A: Chemistry. 331 (2016) 22–28. https://doi.org/10.1016/j.jphotochem.2016.01.017.
[215] D.K. Balta, N. Cetiner, G. Temel, Z. Turgut, N. Arsu, An annelated thioxanthone as a new Type II initiator, Journal of Photochemistry and Photobiology A: Chemistry. 199 (2008) 316–321. https://doi.org/10.1016/j.jphotochem.2008.06.008.
[216] D.K. Balta, G. Temel, G. Goksu, N. Ocal, N. Arsu, Thioxanthone–Diphenyl Anthracene: Visible Light Photoinitiator, Macromolecules. 45 (2012) 119–125. https://doi.org/10.1021/ma202168m.
[217] S. Dadashi-Silab, C. Aydogan, Y. Yagci, Shining a light on an adaptable photoinitiator: advances in photopolymerizations initiated by thioxanthones, Polym. Chem. 6 (2015) 6595–6615. https://doi.org/10.1039/C5PY01004G.
[218] T.N. Eren, N. Yasar, V. Aviyente, F. Morlet-Savary, B. Graff, J.P. Fouassier, J. Lalevee, D. Avci, Photophysical and Photochemical Studies of Novel Thioxanthone-Functionalized Methacrylates through LED Excitation, Macromolecular Chemistry and Physics. 217 (2016) 1501–1512. https://doi.org/10.1002/macp.201600051.

[219] J. Qiu, J. Wei, Thioxanthone photoinitiator containing polymerizable N-aromatic maleimide for photopolymerization, J Polym Res. 21 (2014) 559. https://doi.org/10.1007/s10965-014-0559-4.
[220] H. Tar, D. Sevinc Esen, M. Aydin, C. Ley, N. Arsu, X. Allonas, Panchromatic Type II Photoinitiator for Free Radical Polymerization Based on Thioxanthone Derivative, Macromolecules. 46 (2013) 3266–3272. https://doi.org/10.1021/ma302641d.
[221] Q. Wu, X. Wang, Y. Xiong, J. Yang, H. Tang, Thioxanthone based one-component polymerizable visible light photoinitiator for free radical polymerization, RSC Adv. 6 (2016) 66098–66107. https://doi.org/10.1039/C6RA15349F.
[222] Q. Wu, K. Tang, Y. Xiong, X. Wang, J. Yang, H. Tang, High-Performance and Low Migration One-Component Thioxanthone Visible Light Photoinitiators, Macromolecular Chemistry and Physics. 218 (2017) 1600484. https://doi.org/10.1002/macp.201600484.
[223] X. Wu, M. Jin, J.-P. Malval, D. Wan, H. Pu, Visible light-emitting diode-sensitive thioxanthone derivatives used in versatile photoinitiating systems for photopolymerizations, Journal of Polymer Science Part A: Polymer Chemistry. 55 (2017) 4037–4045. https://doi.org/10.1002/pola.28871.
[224] J. Lalevée, M.-A. Tehfe, F. Dumur, D. Gigmes, B. Graff, F. Morlet-Savary, J.-P. Fouassier, Light-Harvesting Organic Photoinitiators of Polymerization, Macromolecular Rapid Communications. 34 (2013) 239–245. https://doi.org/10.1002/marc.201200578.
[225] D.S. Esen, F. Karasu, N. Arsu, The investigation of photoinitiated polymerization of multifunctional acrylates with TX-BT by Photo-DSC and RT-FTIR, Progress in Organic Coatings. 70 (2011) 102–107. https://doi.org/10.1016/j.porgcoat.2010.10.010.
[226] J. Lalevée, N. Blanchard, M.A. Tehfe, C. Fries, F. Morlet-Savary, D. Gigmes, J.P. Fouassier, New thioxanthone and xanthone photoinitiators based on silyl radical chemistry, Polym. Chem. 2 (2011) 1077–1084. https://doi.org/10.1039/C0PY00392A.
[227] M.-A. Tehfe, F. Dumur, E. Contal, B. Graff, D. Gigmes, J.-P. Fouassier, J. Lalevée, Novel Highly Efficient Organophotocatalysts: Truxene–Acridine-1,8-diones as Photoinitiators of Polymerization, Macromolecular Chemistry and Physics. 214 (2013) 2189–2201. https://doi.org/10.1002/macp.201300362.
[228] P. Xiao, F. Dumur, M.-A. Tehfe, B. Graff, D. Gigmes, J.P. Fouassier, J. Lalevée, Difunctional acridinediones as photoinitiators of polymerization under UV and visible lights: Structural effects, Polymer. 54 (2013) 3458–3466. https://doi.org/10.1016/j.polymer.2013.04.055.
[229] P. Xiao, F. Dumur, M.-A. Tehfe, B. Graff, D. Gigmes, J.P. Fouassier, J. Lalevée, Acridinediones: Effect of Substituents on Their Photoinitiating Abilities in Radical and Cationic Photopolymerization, Macromolecular Chemistry and Physics. 214 (2013) 2276–2282. https://doi.org/10.1002/macp.201300363.
[230] S.C. Rasmussen, S.J. Evenson, Dithieno[3,2-b:2′,3′-d]pyrrole-based materials: Synthesis and application to organic electronics, Progress in Polymer Science. 38 (2013) 1773–1804. https://doi.org/10.1016/j.progpolymsci.2013.04.004.
[231] X. Zou, S. Cui, J. Li, X. Wei, M. Zheng, Diketopyrrolopyrrole Based Organic Semiconductor Materials for Field-Effect Transistors, Frontiers in Chemistry. 9 (2021). https://www.frontiersin.org/article/10.3389/fchem.2021.671294.
[232] C. Bulumulla, R. Gunawardhana, P.L. Gamage, J.T. Miller, R.N. Kularatne, M.C. Biewer, M.C. Stefan, Pyrrole-Containing Semiconducting Materials: Synthesis and

Applications in Organic Photovoltaics and Organic Field-Effect Transistors, ACS Appl. Mater. Interfaces. 12 (2020) 32209–32232. https://doi.org/10.1021/acsami.0c07161.
[233] T.T. Do, M. Stephen, K.L. Chan, S. Manzhos, P.L. Burn, P. Sonar, Pyrrolo[3,2-b]pyrrole-1,4-dione (IsoDPP) End Capped with Napthalimide or Phthalimide: Novel Small Molecular Acceptors for Organic Solar Cells, Molecules. 25 (2020). https://doi.org/10.3390/molecules25204700.
[234] S.S.M. Fernandes, M.C.R. Castro, D. Ivanou, A. Mendes, M.M.M. Raposo, Push-Pull Heterocyclic Dyes Based on Pyrrole and Thiophene: Synthesis and Evaluation of Their Optical, Redox and Photovoltaic Properties, Coatings. 12 (2022) 34. https://doi.org/10.3390/coatings12010034.
[235] P. Gautam, C.P. Yu, G. Zhang, V.E. Hillier, J.M.W. Chan, Pulling with the Pentafluorosulfanyl Acceptor in Push–Pull Dyes, J. Org. Chem. 82 (2017) 11008–11020. https://doi.org/10.1021/acs.joc.7b01972.
[236] X. Ma, R. Liang, F. Yang, Z. Zhao, A. Zhang, N. Song, Q. Zhou, J. Zhang, Synthesis and properties of novel second-order NLO chromophores containing pyrrole as an auxiliary electron donor, J. Mater. Chem. 18 (2008) 1756–1764. https://doi.org/10.1039/B720023D.
[237] A. Facchetti, A. Abbotto, L. Beverina, M.E. van der Boom, P. Dutta, G. Evmenenko, T.J. Marks, G.A. Pagani, Azinium−(π-Bridge)−Pyrrole NLO-Phores: Influence of Heterocycle Acceptors on Chromophoric and Self-Assembled Thin-Film Properties, Chem. Mater. 14 (2002) 4996–5005. https://doi.org/10.1021/cm0205635.
[238] Q. Li, C. Lu, J. Zhu, E. Fu, C. Zhong, S. Li, Y. Cui, J. Qin, Z. Li, Nonlinear Optical Chromophores with Pyrrole Moieties as the Conjugated Bridge: Enhanced NLO Effects and Interesting Optical Behavior, J. Phys. Chem. B. 112 (2008) 4545–4551. https://doi.org/10.1021/jp0768322.
[239] M.C.R. Castro, A.M.C. Fonseca, M. Belsley, M.M.M. Raposo, Highly efficient and thermally stable NLO organic materials based on pyrrole and thiophene heterocycles, in: M.F. Costa (Ed.), Braga, Portugal, 2011: p. 80012U. https://doi.org/10.1117/12.892205.
[240] P. Camurlu, Polypyrrole derivatives for electrochromic applications, RSC Adv. 4 (2014) 55832–55845. https://doi.org/10.1039/C4RA11827H.
[241] T. Jarosz, P. Ledwon, Electrochemically Produced Copolymers of Pyrrole and Its Derivatives: A Plentitude of Material Properties Using "Simple" Heterocyclic Co-Monomers, Materials. 14 (2021) 281. https://doi.org/10.3390/ma14020281.
[242] M. Czichy, H. Zhylitskaya, P. Zassowski, M. Navakouski, P. Chulkin, P. Janasik, M. Lapkowski, M. Stępień, Electrochemical Polymerization of Pyrrole–Perimidine Hybrids: Low-Band-Gap Materials with High n-Doping Activity, J. Phys. Chem. C. 124 (2020) 14350–14362. https://doi.org/10.1021/acs.jpcc.0c03002.
[243] J.A. Balam-Villarreal, B.J. López-Mayorga, D. Gallardo-Rosas, R.A. Toscano, M.P. Carreón-Castro, V.A. Basiuk, F. Cortés-Guzmán, J.G. López-Cortés, M.C. Ortega-Alfaro, π-Extended push–pull azo-pyrrole photoswitches: synthesis, solvatochromism and optical band gaps, Org. Biomol. Chem. 18 (2020) 1657–1670. https://doi.org/10.1039/C9OB02410G.
[244] J.-Y. Park, S.-Y. Gwon, N.-S. Yoon, Y.-A. Son, S.-H. Kim, Isophorone and pyrrole based push-pull system dye: Design, preparation and spectral switching on pH/fluoride ion, Fibers Polym. 12 (2011) 692. https://doi.org/10.1007/s12221-011-0692-1.

[245] H. Li, L. Yang, R. Tang, Y. Hou, Y. Yang, H. Wang, H. Han, J. Qin, Q. Li, Z. Li, Organic dyes incorporating N-functionalized pyrrole as conjugated bridge for dye-sensitized solar cells: Convenient synthesis, additional withdrawing group on the π-bridge and the suppressed aggregation, Dyes and Pigments. 99 (2013) 863–870. https://doi.org/10.1016/j.dyepig.2013.05.030.
[246] B. Sekaran, Y. Jang, R. Misra, F. D'Souza, Push–Pull Porphyrins via β-Pyrrole Functionalization: Evidence of Excited State Events Leading to High-Potential Charge-Separated States, Chemistry – A European Journal. 25 (2019) 12991–13001. https://doi.org/10.1002/chem.201902286.
[247] N. Danchev, A. Bijev, D. Yaneva, S. Vladimirova, I. Nikolova, Synthesis, Acute Toxicity, and Analgesic Activity of New Derivatives of Pyrrole, Archiv Der Pharmazie. 339 (2006) 670–674. https://doi.org/10.1002/ardp.200600116.
[248] B.-C. Ivan, F. Dumitrascu, A.I. Anghel, R.V. Ancuceanu, S. Shova, D. Dumitrescu, C. Draghici, O.T. Olaru, G.M. Nitulescu, M. Dinu, S.-F. Barbuceanu, Synthesis and Toxicity Evaluation of New Pyrroles Obtained by the Reaction of Activated Alkynes with 1-Methyl-3-(cyanomethyl)benzimidazolium Bromide, Molecules. 26 (2021) 6435. https://doi.org/10.3390/molecules26216435.
[249] F. Yang, N.G. Nickols, B.C. Li, J.O. Szablowski, S.R. Hamilton, J.L. Meier, C.-M. Wang, P.B. Dervan, Animal Toxicity of Hairpin Pyrrole-Imidazole Polyamides Varies with the Turn Unit, J. Med. Chem. 56 (2013) 7449–7457. https://doi.org/10.1021/jm401100s.
[250] R.E. Sigler, M.A. Dominick, E.J. Mcguire, Subacute Toxicity of a Halogenated Pyrrole Hydroxymethylglutaryl-Coenzyme A Reductase Inhibitor in Wistar Rats, Toxicol Pathol. 20 (1992) 595–602. https://doi.org/10.1177/019262339202000406.
[251] Y. Morita, K. Takagi, M. Fukuchi-Mizutani, K. Ishiguro, Y. Tanaka, E. Nitasaka, M. Nakayama, N. Saito, T. Kagami, A. Hoshino, S. Iida, A chalcone isomerase-like protein enhances flavonoid production and flower pigmentation, The Plant Journal. 78 (2014) 294–304. https://doi.org/10.1111/tpj.12469.
[252] Ramya Kuber Banoth, A. Thatikonda, A Review on Natural Chalcones : An Update, International Journal Of Pharmaceutical Sciences And Research. 11 (2020) 546–555.
[253] Z. Rozmer, P. Perjési, Naturally occurring chalcones and their biological activities, Phytochem Rev. 15 (2016) 87–120. https://doi.org/10.1007/s11101-014-9387-8.
[254] H. Ghouila, N. Meksi, W. Haddar, M.F. Mhenni, H.B. Jannet, Extraction, identification and dyeing studies of Isosalipurposide, a natural chalcone dye from Acacia cyanophylla flowers on wool, Industrial Crops and Products. 35 (2012) 31–36. https://doi.org/10.1016/j.indcrop.2011.05.026.
[255] M.A. Lago, A.R.-B. de Quirós, R. Sendón, J. Bustos, M.T. Nieto, P. Paseiro, Photoinitiators: a food safety review, Food Additives & Contaminants: Part A. 32 (2015) 779–798. https://doi.org/10.1080/19440049.2015.1014866.
[256] H. Wang, J. Wei, X. Jiang, J. Yin, Novel chemical-bonded polymerizable sulfur-containing photoinitiators comprising the structure of planar N-phenylmaleimide and benzophenone for photopolymerization, Polymer. 47 (2006) 4967–4975. https://doi.org/10.1016/j.polymer.2006.04.027.
[257] Z. Osváth, T. Tóth, B. Iván, Synthesis, characterization, LCST-type behavior and unprecedented heating-cooling hysteresis of poly(N-isopropylacrylamide-co-3-(trimethoxysilyl)propyl methacrylate) copolymers, Polymer. 108 (2017) 395–399. https://doi.org/10.1016/j.polymer.2016.12.002.

[258] X. Huang, X. Wang, Y. Zhao, Study on a series of water-soluble photoinitiators for fabrication of 3D hydrogels by two-photon polymerization, Dyes and Pigments. 141 (2017) 413–419. https://doi.org/10.1016/j.dyepig.2017.02.040.
[259] X. Wu, J. Malval, D. Wan, M. Jin, D-π-A-type aryl dialkylsulfonium salts as one-component versatile photoinitiators under UV/visible LEDs irradiation, Dyes and Pigments. 132 (2016) 128–135. https://doi.org/10.1016/j.dyepig.2016.04.004.
[260] T. Xue, Y. Li, L. Tang, R. Tang, J. Nie, X. Zhu, Pyrrole-based enone dyes as radical photointiator under 405/460 nm LED lamp: The effect of ketone structure, Dyes and Pigments. 191 (2021) 109372. https://doi.org/10.1016/j.dyepig.2021.109372.
[261] T. Xue, L. Tang, R. Tang, Y. Li, J. Nie, X. Zhu, Color evolution of a pyrrole-based enone dye in radical photopolymerization formulations, Dyes and Pigments. 188 (2021) 109212. https://doi.org/10.1016/j.dyepig.2021.109212.
[262] J. Li, H. Lu, H. Zheng, X. Zhou, J. Nie, X. Zhu, Thermally activated pyrrole chalcone free radical photoinitiator with excellent stability to sunlight, European Polymer Journal. 162 (2022) 110884. https://doi.org/10.1016/j.eurpolymj.2021.110884.
[263] J.H. Lee, R.K. Prud'homme, I.A. Aksay, Cure depth in photopolymerization: Experiments and theory, Journal of Materials Research. 16 (2001) 3536–3544. https://doi.org/10.1557/JMR.2001.0485.
[264] T.F. Zhou, X.Y. Ma, W.X. Han, X.P. Guo, R.Q. Gu, L.J. Yu, J. Li, Y.M. Zhao, T. Wang, D–D–A dyes with phenothiazine–carbazole/triphenylamine as double donors in photopolymerization under 455 nm and 532 nm laser beams11Electronic supplementary information (ESI) available: Detailed synthesis of all dyes and associated spectra. See DOI: 10.1039/c6py00918b, Polymer Chemistry. 7 (2016) 5039–5049. https://doi.org/10.1039/c6py00918b.
[265] T. Xue, B. Huang, Y. Li, X. Li, J. Nie, X. Zhu, Enone dyes as visible photoinitiator in radical polymerization: The influence of peripheral N-alkylated (hetero)aromatic amine group, Journal of Photochemistry and Photobiology A: Chemistry. 419 (2021) 113449. https://doi.org/10.1016/j.jphotochem.2021.113449.
[266] M. Christoff, V.G. Toscano, W.J. Baader, Influence of methoxy substitution on flavonoid photophysics: a steady state and laser flash photolysis study, Journal of Photochemistry and Photobiology A: Chemistry. 101 (1996) 11–20. https://doi.org/10.1016/S1010-6030(96)04422-X.
[267] P.J. Wagner, 1,5-Biradicals and five-membered rings generated by .delta.-hydrogen abstraction in photoexcited ketones, Acc. Chem. Res. 22 (1989) 83–91. https://doi.org/10.1021/ar00159a001.
[268] W.W. Bao, R. Li, Z.C. Dai, J. Tang, X. Shi, J.T. Geng, Z.F. Deng, J. Hua, Diketopyrrolopyrrole (DPP)-Based Materials and Its Applications: A Review, Frontiers in Chemistry. 8 (2020). https://doi.org/10.3389/fchem.2020.00679.
[269] M. Kaur, D.H. Choi, Diketopyrrolopyrrole: brilliant red pigment dye-based fluorescent probes and their applications, Chem. Soc. Rev. 44 (2015) 58–77. https://doi.org/10.1039/C4CS00248B.
[270] M. Grzybowski, D.T. Gryko, Diketopyrrolopyrroles: Synthesis, Reactivity, and Optical Properties, Advanced Optical Materials. 3 (2015) 280–320. https://doi.org/10.1002/adom.201400559.
[271] S. Ghosh, S. Shankar, D.S. Philips, A. Ajayaghosh, Diketopyrrolopyrrole-based functional supramolecular polymers: next-generation materials for optoelectronic

applications, Materials Today Chemistry. 16 (2020) 100242. https://doi.org/10.1016/j.mtchem.2020.100242.
[272] A. Iqbal, M. Jost, R. Kirchmayr, J. Pfenninger, A. Rochat, O. Wallquist, The synthesis and properties of 1,4-diketo-pyrrolo[3,4-C]pyrroles, Bulletin Des Sociétés Chimiques Belges. 97 (1988) 615–644. https://doi.org/10.1002/bscb.19880970804.
[273] Y. Li, P. Sonar, S.P. Singh, M.S. Soh, M. van Meurs, J. Tan, Annealing-Free High-Mobility Diketopyrrolopyrrole−Quaterthiophene Copolymer for Solution-Processed Organic Thin Film Transistors, J. Am. Chem. Soc. 133 (2011) 2198–2204. https://doi.org/10.1021/ja1085996.
[274] B. Sun, W. Hong, H. Aziz, N.M. Abukhdeir, Y. Li, Dramatically enhanced molecular ordering and charge transport of a DPP-based polymer assisted by oligomers through antiplasticization, J. Mater. Chem. C. 1 (2013) 4423–4426. https://doi.org/10.1039/C3TC30667D.
[275] L. Murphy, W. Hong, H. Aziz, Y. Li, Organic photovoltaics with thick active layers (~800nm) using a high mobility polymer donor, Solar Energy Materials and Solar Cells. 114 (2013) 71–81. https://doi.org/10.1016/j.solmat.2013.02.033.
[276] Y. Li, P. Sonar, L. Murphy, W. Hong, High mobility diketopyrrolopyrrole (DPP)-based organic semiconductor materials for organic thin film transistors and photovoltaics, Energy Environ. Sci. 6 (2013) 1684–1710. https://doi.org/10.1039/C3EE00015J.
[277] Y. Li, S.P. Singh, P. Sonar, A High Mobility P-Type DPP-Thieno[3,2-b]thiophene Copolymer for Organic Thin-Film Transistors, Advanced Materials. 22 (2010) 4862–4866. https://doi.org/10.1002/adma.201002313.
[278] Y. Li, P. Sonar, S.P. Singh, W. Zeng, M.S. Soh, 3,6-Di(furan-2-yl)pyrrolo[3,4-c]pyrrole-1,4(2H,5H)-dione and bithiophene copolymer with rather disordered chain orientation showing high mobility in organic thin film transistors, J. Mater. Chem. 21 (2011) 10829–10835. https://doi.org/10.1039/C1JM11290B.
[279] W. Hong, C. Guo, Y. Li, Y. Zheng, C. Huang, S. Lu, A. Facchetti, Synthesis and thin-film transistor performance of benzodipyrrolinone and bithiophene donor-acceptor copolymers, J. Mater. Chem. 22 (2012) 22282–22289. https://doi.org/10.1039/C2JM34867E.
[280] M. Bouzrati-Zerelli, N. Zivic, F. Dumur, D. Gigmes, B. Graff, J.P. Fouassier, J. Lalevée, New violet to yellow light sensitive diketo pyrrolo–pyrrole photoinitiators: high performance systems with unusual bleaching properties and solubility in water, Polym. Chem. 8 (2017) 2028–2040. https://doi.org/10.1039/C7PY00202E.
[281] C. Dietlin, T.T. Trinh, S. Schweizer, B. Graff, F. Morlet-Savary, P.-A. Noirot, J. Lalevée, New Phosphine Oxides as High Performance Near- UV Type I Photoinitiators of Radical Polymerization, Molecules. 25 (2020). https://doi.org/10.3390/molecules25071671.
[282] D. Nowak, J. Ortyl, I. Kamińska-Borek, K. Kukuła, M. Topa, R. Popielarz, Photopolymerization of hybrid monomers: Part I: Comparison of the performance of selected photoinitiators in cationic and free-radical polymerization of hybrid monomers, Polymer Testing. 64 (2017) 313–320. https://doi.org/10.1016/j.polymertesting.2017.10.020.
[283] V.V. Rocheva, A.V. Koroleva, A.G. Savelyev, K.V. Khaydukov, A.N. Generalova, A.V. Nechaev, A.E. Guller, V.A. Semchishen, B.N. Chichkov, E.V. Khaydukov, High-resolution 3D photopolymerization assisted by upconversion nanoparticles for rapid

prototyping applications, Sci Rep. 8 (2018) 3663–3663. https://doi.org/10.1038/s41598-018-21793-0.
[284] Y. Xu, Y. Chen, X. Liu, S. Xue, Radical Photopolymerization Using 1,4-Dihydropyrrolo[3,2-b]pyrrole Derivatives Prepared via One-Pot Synthesis, ACS Omega. 6 (2021) 20902–20911. https://doi.org/10.1021/acsomega.1c02338.
[285] A. Janiga, D.T. Gryko, 1,4-Dihydropyrrolo[3,2-b]pyrrole and Its π-Expanded Analogues, Chemistry – An Asian Journal. 9 (2014) 3036–3045. https://doi.org/10.1002/asia.201402367.
[286] Y. Ji, Z. Peng, B. Tong, J. Shi, J. Zhi, Y. Dong, Polymorphism-dependent aggregation-induced emission of pyrrolopyrrole-based derivative and its multi-stimuli response behaviors, Dyes and Pigments. 139 (2017) 664–671. https://doi.org/10.1016/j.dyepig.2016.12.061.
[287] B. Sadowski, K. Hassanein, B. Ventura, D.T. Gryko, Tetraphenylethylenepyrrolo[3,2-b]pyrrole Hybrids as Solid-State Emitters: The Role of Substitution Pattern, Org. Lett. 20 (2018) 3183–3186. https://doi.org/10.1021/acs.orglett.8b01011.
[288] H. Bürckstümmer, E.V. Tulyakova, M. Deppisch, M.R. Lenze, N.M. Kronenberg, M. Gsänger, M. Stolte, K. Meerholz, F. Würthner, Efficient Solution-Processed Bulk Heterojunction Solar Cells by Antiparallel Supramolecular Arrangement of Dipolar Donor–Acceptor Dyes, Angewandte Chemie International Edition. 50 (2011) 11628–11632. https://doi.org/10.1002/anie.201105133.
[289] R.K. Canjeevaram Balasubramanyam, R. Kumar, S.J. Ippolito, S.K. Bhargava, S.R. Periasamy, R. Narayan, P. Basak, Quadrupolar (A-π-D-π-A) Tetra-aryl 1,4-Dihydropyrrolo[3,2-b]pyrroles as Single Molecular Resistive Memory Devices: Substituent Triggered Amphoteric Redox Performance and Electrical Bistability, J. Phys. Chem. C. 120 (2016) 11313–11323. https://doi.org/10.1021/acs.jpcc.5b11509.
[290] R. Ballini, M. Petrini, Recent synthetic developments in the nitro to carbonyl conversion (Nef reaction), Tetrahedron. 60 (2004) 1017–1047. https://doi.org/10.1016/j.tet.2003.11.016.
[291] G. Stewart, Y. Jiao, E.J. Valente, P.P. Fu, T. Li, Z. Hu, H. Yu, Photochemical reaction of 9-nitro-substituted anthracene-like molecules 9-methyl-10-nitroanthracene and 12-methyl-7-nitrobenz[a]anthracene, Journal of Photochemistry and Photobiology A: Chemistry. 201 (2009) 39–44. https://doi.org/10.1016/j.jphotochem.2008.09.016.
[292] M.C. Morel, I. Alers, R. Arce, Photochemical degradation of 1,6- and 1,8-dinitropyrene in solution, Null. 26 (2006) 207–219. https://doi.org/10.1080/10406630600760576.
[293] R.K. Canjeevaram Balasubramanyam, A.E. Kandjani, C.J. Harrison, S.S.A. Abdul Haroon Rashid, Y.M. Sabri, S.K. Bhargava, R. Narayan, P. Basak, S.J. Ippolito, 1,4-Dihydropyrrolo[3,2-b]pyrroles as a Single Component Photoactive Layer: A New Paradigm for Broadband Detection, ACS Appl. Mater. Interfaces. 9 (2017) 27875–27882. https://doi.org/10.1021/acsami.7b08906.
[294] M.O. Senge, N.N. Sergeeva, K.J. Hale, Classic highlights in porphyrin and porphyrinoid total synthesis and biosynthesis, Chem. Soc. Rev. 50 (2021) 4730–4789. https://doi.org/10.1039/C7CS00719A.
[295] S. Hiroto, Y. Miyake, H. Shinokubo, Synthesis and Functionalization of Porphyrins through Organometallic Methodologies, Chem. Rev. 117 (2017) 2910–3043. https://doi.org/10.1021/acs.chemrev.6b00427.
[296] M. Biesaga, K. Pyrzyńska, M. Trojanowicz, Porphyrins in analytical chemistry. A review, Talanta. 51 (2000) 209–224. https://doi.org/10.1016/S0039-9140(99)00291-X.

[297] B.B. Wayland, G. Poszmik, S.L. Mukerjee, M. Fryd, Living Radical Polymerization of Acrylates by Organocobalt Porphyrin Complexes, J. Am. Chem. Soc. 116 (1994) 7943–7944. https://doi.org/10.1021/ja00096a080.
[298] Z. Lu, M. Fryd, B.B. Wayland, New Life for Living Radical Polymerization Mediated by Cobalt(II) Metalloradicals, Macromolecules. 37 (2004) 2686–2687. https://doi.org/10.1021/ma035924w.
[299] B.B. Wayland, C.-H. Peng, X. Fu, Z. Lu, M. Fryd, Degenerative Transfer and Reversible Termination Mechanisms for Living Radical Polymerizations Mediated by Cobalt Porphyrins, Macromolecules. 39 (2006) 8219–8222. https://doi.org/10.1021/ma061643n.
[300] S. Li, B. de Bruin, C.-H. Peng, M. Fryd, B.B. Wayland, Exchange of Organic Radicals with Organo-Cobalt Complexes Formed in the Living Radical Polymerization of Vinyl Acetate, J. Am. Chem. Soc. 130 (2008) 13373–13381. https://doi.org/10.1021/ja804010h.
[301] C.-H. Peng, S. Li, B.B. Wayland, Aspects of Living Radical Polymerization Mediated by Cobalt Porphyrin Complexes, Journal of the Chinese Chemical Society. 56 (2009) 219–233. https://doi.org/10.1002/jccs.200900032.
[302] C.-H. Peng, J. Scricco, S. Li, M. Fryd, B.B. Wayland, Organo-Cobalt Mediated Living Radical Polymerization of Vinyl Acetate, Macromolecules. 41 (2008) 2368–2373. https://doi.org/10.1021/ma702500b.
[303] Y. Zhao, M. Yu, X. Fu, Photo-cleavage of the cobalt–carbon bond: visible light-induced living radical polymerization mediated by organo-cobalt porphyrins, Chem. Commun. 49 (2013) 5186–5188. https://doi.org/10.1039/C3CC41466C.
[304] C.-S. Hsu, T.-Y. Yang, C.-H. Peng, Vinyl acetate living radical polymerization mediated by cobalt porphyrins: kinetic–mechanistic studies, Polym. Chem. 5 (2014) 3867–3875. https://doi.org/10.1039/C4PY00191E.
[305] Y. Zhao, M. Yu, S. Zhang, Y. Liu, X. Fu, Visible Light Induced Living/Controlled Radical Polymerization of Acrylates Catalyzed by Cobalt Porphyrins, Macromolecules. 47 (2014) 6238–6245. https://doi.org/10.1021/ma5014385.
[306] C.-H. Peng, M. Fryd, B.B. Wayland, Organocobalt Mediated Radical Polymerization of Acrylic Acid in Water, Macromolecules. 40 (2007) 6814–6819. https://doi.org/10.1021/ma070836n.
[307] D. Kim, J.W. Stansbury, A photo-oxidizable kinetic pathway of three-component photoinitiator systems containing porphrin dye (Zn-tpp), an electron donor and diphenyl iodonium salt, Journal of Polymer Science Part A: Polymer Chemistry. 47 (2009) 3131–3141. https://doi.org/10.1002/pola.23401.
[308] J. Yeow, S. Shanmugam, N. Corrigan, R.P. Kuchel, J. Xu, C. Boyer, A Polymerization-Induced Self-Assembly Approach to Nanoparticles Loaded with Singlet Oxygen Generators, Macromolecules. 49 (2016) 7277–7285. https://doi.org/10.1021/acs.macromol.6b01581.
[309] S. Shanmugam, J. Xu, C. Boyer, Exploiting Metalloporphyrins for Selective Living Radical Polymerization Tunable over Visible Wavelengths, J. Am. Chem. Soc. 137 (2015) 9174–9185. https://doi.org/10.1021/jacs.5b05274.
[310] S. Shanmugam, J. Xu, C. Boyer, Utilizing the electron transfer mechanism of chlorophyll a under light for controlled radical polymerization, Chem. Sci. 6 (2015) 1341–1349. https://doi.org/10.1039/C4SC03342F.
[311] M. da G.H. Vicente, K.M. Smith, Syntheses and Functionalizations of Porphyrin Macrocycles, Current Organic Synthesis. 11 (n.d.) 3–28.

[312] Y. Takeda, S. Takahara, Y. Kobayashi, H. Misawa, H. Sakuragi, K. Tokumaru, Isoporphyrins. Near-Infrared Dyes with Noticeable Photochemical and Redox Properties, Chemistry Letters. 19 (1990) 2103–2106. https://doi.org/10.1246/cl.1990.2103.
[313] M.L. Viger, W. Sheng, K. Doré, A.H. Alhasan, C.-J. Carling, J. Lux, C. de Gracia Lux, M. Grossman, R. Malinow, A. Almutairi, Near-Infrared-Induced Heating of Confined Water in Polymeric Particles for Efficient Payload Release, ACS Nano. 8 (2014) 4815–4826. https://doi.org/10.1021/nn500702g.
[314] J. Cao, J. Chi, J. Xia, Y. Zhang, S. Han, Y. Sun, Iodinated Cyanine Dyes for Fast Near-Infrared-Guided Deep Tissue Synergistic Phototherapy, ACS Appl. Mater. Interfaces. 11 (2019) 25720–25729. https://doi.org/10.1021/acsami.9b07694.
[315] T.-M. Liu, J. Conde, T. Lipiński, A. Bednarkiewicz, C.-C. Huang, Revisiting the classification of NIR-absorbing/emitting nanomaterials for in vivo bioapplications, NPG Asia Mater. 8 (2016) e295–e295. https://doi.org/10.1038/am.2016.106.
[316] D. Gigmes, P.-E. Dufils, D. Glé, D. Bertin, C. Lefay, Y. Guillaneuf, Intermolecular radical 1,2-addition of the BlocBuilder MA alkoxyamine onto activated olefins: a versatile tool for the synthesis of complex macromolecular architecture, Polym. Chem. 2 (2011) 1624–1631. https://doi.org/10.1039/C1PY00057H.
[317] C. Belon, X. Allonas, C. Croutxé-barghorn, J. Lalevée, Overcoming the oxygen inhibition in the photopolymerization of acrylates: A study of the beneficial effect of triphenylphosphine, Journal of Polymer Science Part A: Polymer Chemistry. 48 (2010) 2462–2469. https://doi.org/10.1002/pola.24017.
[318] S.C. Ligon, B. Husár, H. Wutzel, R. Holman, R. Liska, Strategies to Reduce Oxygen Inhibition in Photoinduced Polymerization, Chem. Rev. 114 (2014) 557–589. https://doi.org/10.1021/cr3005197.
[319] S.A. Buckler, Autoxidation of Trialkylphosphines, J. Am. Chem. Soc. 84 (1962) 3093–3097. https://doi.org/10.1021/ja00875a011.
[320] F. Bureš, Fundamental aspects of property tuning in push–pull molecules, RSC Adv. 4 (2014) 58826–58851. https://doi.org/10.1039/C4RA11264D.
[321] J. Kulhánek, F. Bureš, O. Pytela, T. Mikysek, J. Ludvík, A. Růžička, Push-pull molecules with a systematically extended π-conjugated system featuring 4,5-dicyanoimidazole, Dyes and Pigments. 85 (2010) 57–65. https://doi.org/10.1016/j.dyepig.2009.10.004.
[322] B. Diffey, U. Osterwalder, Labelled sunscreen SPFs may overestimate protection in natural sunlight, Photochem Photobiol Sci. 16 (2017) 1519–1523. https://doi.org/10.1039/c7pp00260b.
[323] J.P. Fouassier, X. Allonas, D. Burget, Photopolymerization reactions under visible lights: principle, mechanisms and examples of applications, Progress in Organic Coatings. 47 (2003) 16–36. https://doi.org/10.1016/S0300-9440(03)00011-0.
[324] M. Schmitt, Synthesis and testing of ZnO nanoparticles for photo-initiation: experimental observation of two different non-migration initiators for bulk polymerization, Nanoscale. 7 (2015) 9532–9544. https://doi.org/10.1039/C5NR00850F.
[325] M.L. Allegrezza, Z.M. DeMartini, A.J. Kloster, Z.A. Digby, D. Konkolewicz, Visible and sunlight driven RAFT photopolymerization accelerated by amines: kinetics and mechanism, Polym. Chem. 7 (2016) 6626–6636. https://doi.org/10.1039/C6PY01433J.
[326] J. Wang, M. Rivero, A. Muñoz Bonilla, J. Sanchez-Marcos, W. Xue, G. Chen, W. Zhang, X. Zhu, Natural RAFT Polymerization: Recyclable-Catalyst-Aided, Opened-to-Air, and

Sunlight-Photolyzed RAFT Polymerizations, ACS Macro Lett. 5 (2016) 1278–1282. https://doi.org/10.1021/acsmacrolett.6b00818.
[327] M. Ciftci, M.A. Tasdelen, Y. Yagci, Sunlight induced atom transfer radical polymerization by using dimanganese decacarbonyl, Polym. Chem. 5 (2014) 600–606. https://doi.org/10.1039/C3PY01009K.
[328] C. Decker, T. Bendaikha, Interpenetrating polymer networks. II. Sunlight-induced polymerization of multifunctional acrylates, Journal of Applied Polymer Science. 70 (1998) 2269–2282. https://doi.org/10.1002/(SICI)1097-4628(19981212)70:11<2269::AID-APP21>3.0.CO;2-D.
[329] C.O. Yanez, C.D. Andrade, K.D. Belfield, Characterization of novel sulfonium photoacid generators and their microwave-assisted synthesis, Chem. Commun. (2009) 827–829. https://doi.org/10.1039/B815831B.
[330] M. Jin, H. Xu, H. Hong, J.-P. Malval, Y. Zhang, A. Ren, D. Wan, H. Pu, Design of D–π–A type photoacid generators for high efficiency excitation at 405 nm and 800 nm, Chem. Commun. 49 (2013) 8480–8482. https://doi.org/10.1039/C3CC43018A.
[331] J.V. Crivello, M. Sangermano, Visible and long-wavelength photoinitiated cationic polymerization, Journal of Polymer Science Part A: Polymer Chemistry. 39 (2001) 343–356. https://doi.org/10.1002/1099-0518(20010201)39:3<343::AID-POLA1001>3.0.CO;2-J.
[332] S. Chen, X. Zhao, M. Jin, W. Huang, G. Ye, H. Pan, D. Wan, Effects of C3-aromatic heterocycles on 1,3,5-triaryl-2-pyrazoline sulfonium salt photoacid generators as light-emitting diode-sensitive cationic photoinitiators, Journal of Polymer Science. 59 (2021) 1899–1911. https://doi.org/10.1002/pol.20210333.
[333] F. Hammoud, N. Giacoletto, M. Nechab, B. Graff, A. Hijazi, F. Dumur, J. Lalevée, 5,12-Dialkyl-5,12-dihydroindolo[3,2-a]carbazole-Based Oxime-Esters for LED Photoinitiating Systems and Application on 3D Printing, Macromolecular Materials and Engineering. n/a (2022) 2200082. https://doi.org/10.1002/mame.202200082.
[334] Y. Ding, S. Jiang, Y. Gao, J. Nie, H. Du, F. Sun, Photochromic Polymers Based on Fluorophenyl Oxime Ester Photoinitiators as Photoswitchable Molecules, Macromolecules. 53 (2020) 5701–5710. https://doi.org/10.1021/acs.macromol.0c00198.
[335] X. Ma, R. Gu, L. Yu, W. Han, J. Li, X. Li, T. Wang, Conjugated phenothiazine oxime esters as free radical photoinitiators, Polym. Chem. 8 (2017) 6134–6142. https://doi.org/10.1039/C7PY00797C.
[336] F. Hammoud, Z.-H. Lee, B. Graff, A. Hijazi, J. Lalevée, Y.-C. Chen, Novel phenylamine-based oxime ester photoinitiators for LED-induced free radical, cationic, and hybrid polymerization, Journal of Polymer Science. 59 (2021) 1711–1723. https://doi.org/10.1002/pol.20210298.
[337] W. Qiu, J. Zhu, K. Dietliker, Z. Li, Polymerizable Oxime Esters: An Efficient Photoinitiator with Low Migration Ability for 3D Printing to Fabricate Luminescent Devices, ChemPhotoChem. 4 (2020) 5296–5303. https://doi.org/10.1002/cptc.202000146.